DESIGN OF AN ACTIVE SUSPENSION SYSTEM FOR FORWARDER CABIN

GIRISHKASTURI.L.H
QIWU WANG

KTH Industrial Engineering
and Management

Master of Science Thesis
Stockholm, Sweden 2012

DESIGN OF AN ACTIVE SUSPENSION SYSTEM FOR FORWARDER CABIN

Girishkasturi.L.H
Qiwu Wang

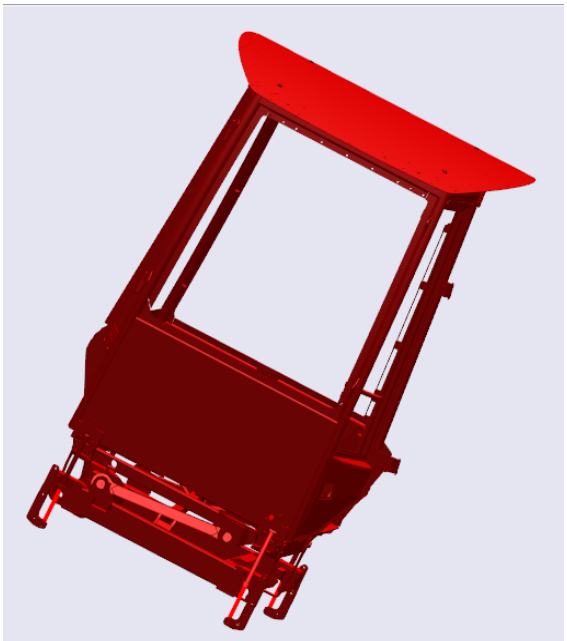

Master of Science Thesis MMK 2012:76 MDA 450
KTH Industrial Engineering and Management
Machine Design
SE-100 44 STOCKHOLM

KTH Industriell teknik och management

Examensarbete MMK 2012:76 MDA 450

DESIGN OF AN ACTIVE SUSPENSION SYSTEM FOR FORWARDER CABIN

Girishkasturi.L.H
Qiwu Wang

Godkänt	Examinator	Handledare
2012-09-21	Jan Wikander	Bengt O. Eriksson
	Uppdragsgivare	Kontaktperson
	Komatsu Forest	Erik Nilsson

Sammanfattning

En skotare är ett fordon som transporterar stockar ut från skogen till en större väg. Komatsu Forest AB har utvecklat en ny hytt upphängning till en av sina skotarmodeller. Den är baserad på passiva komponenter, fjädrar och dämpare. Komatsu vill undersöka möjligheterna till aktiv fjädring av det nya hytt konceptet. Syftet med detta arbete är att utveckla en simuleringsmodell med aktiv fjädring för det befintliga passiva upphängningssystem av skotarens kabin. Syftet är att minska hytt vibrationer inducerade från vägen i området 1-5 Hz.

Arbetet är uppdelat i ett mekaniskt och ett hydrauliskt delsystem där en kaskad kopplad reglerstruktur antas kunna användas. Det mekaniska delsystemet modelleras i programvaran Simulink som en SimMechanics model för att kunna simuleras. På grund av att hytt upphängningen har tre mekaniska frihetsgrader men det regleras med fyra ställdon uppstår ett problem som kallas för överaktuerat system. En kvadratisk programmering algoritm utvecklades för att på ett optimalt sätt fördela krafterna från de fyra ställdonen på de tre frihetsgraderna på hytten.

För de hydrauliska delsystemet, är matematiska modeller av olika detaljnivå utvecklade. Simuleringsresultaten av den härledda modellen jämförs sedan med SimHydraulics modellen och systemets egenskaper härleds. En hydraulisk kraft regulator är utvecklad för att uppnå det önskade målet från regleringen av mekaniken.

Från körningar i skogen finns det uppmätta vägdata, dessa matas in i den kompletta simulerings modellen med reglering och analyseras. Baserat på simuleringsresultat kan sedan sensorer och den hydrauliska utrustning såsom ventiler väljas för implementering på en prototypmaskin.

I denna avhandling har Girishkasturi.LH ansvarat för hydraulsystemets design och analys och Qiwu Wang ansvarat för den mekaniska system analysen och regler designen. Analysen av det kompletta systemet är gemensamt utfört.

KTH Industrial Engineering and Management

Master of Science Thesis MMK 2012:76 MDA 450

DESIGN OF AN ACTIVE SUSPENSION SYSTEM FOR FORWARDER CABIN

Girishkasturi.L.H
Qiwu Wang

Approved	Examiner	Supervisor
2012-09-21	Jan Wikander	Bengt O. Eriksson
	Commissioner	Contact person
	Komatsu Forest	Erik Nilsson

Abstract

A forwarder is a forestry vehicle that carries logs from forest to a roadside landing. Komatsu Forest AB developed a new passive multi-DOF cabin suspension of a forwarder, and an attempt of active suspension control based on their mechanical solution is desired. The purpose of this thesis is to develop a simulation model of active suspension for an existing passive suspension system of the forwarder cabin, in order to reduce the vibration between 1-5 Hz within the given cylinder stroke limitation.

This thesis is modularized into mechanical and hydraulic subsystems and a cascaded control structure is adopted. For the mechanical subsystems, the system model is developed and analyzed based on mechanics theory, and then a SimMechanics model is derived for detailed simulation. Due to the property of over-actuated system, a quadratic programming algorithm is developed to optimally allocate control efforts. Then the control design of roll, pitch and heave is analyzed. According to the desired frequency response the controllers are designed with different control strategies. For the hydraulic subsystems, mathematic models of different detailed level are developed. The simulation results of the derived model are compared with the SimHydraulics model and the system properties are deduced. Also an internal mode force controller is developed to achieve the desired goal of force reference tracking.

Then the measured vibration data obtained from Skogforsk is fed into the integrated system and analyzed. Based on the simulation result, the sensors and hydraulic equipment are selected for the real-time implementation.

In this thesis, Girishkasturi.L.H is responsible for the hydraulic system design and analysis and Qiwu Wang is responsible for the mechanical system analysis and control design. The integrated system analysis is a joint work.

FOREWORD

We would like to thank all the people who have helped us during this thesis.

Thanks to Bengt O. Eriksson for your great guidance and help during this thesis, your valuable experience and suggestions kept thesis on the right track, and we have learnt a lot from the discussion with you.
Thanks to Jan Wikander, Björn Löfgren, Erik Nilsson, Joakim Johansson, Peter Assarsson, Petrus Jönsson, Bo Stångberg for your help during the whole thesis. You have answered us so many questions and gave us great support for this thesis.

Besides, we would like to thank all the people who have helped us during our master study, it is a wonderful experience studying and working with you.

Girishkasturi.L.H

Qiwu Wang

Stockholm, September 2012

NOMENCLATURE

$X_{\max}$, Y_{max}	The maximum movement of upper frame in x, y direction (m)
$l_{long\ rod}$, $l_{short\ rod}$	The length of long connecting rod and short connecting rods (m)
$\theta_{cylinder\ max}$, $\phi_{cylinder\ max}$	The maximum angular movement of cylinders caused by x and y movement (m)
$L_{cylinder}$	The distance between the spherical joint on cylinders and the one on the housing (m)
l_{length}, l_{width}	The length and width of upper frame (m)
ϕ_e^u, θ_e^u	Roll and pitch of upper frame in earth frame of reference (rad)
r_b^u, p_b^u	Rotation velocity of roll and pitch of upper frame in body-fixed frame of reference (rad/s)
ϕ_e^l, θ_e^l	Roll and pitch of lower frame in earth frame of reference (rad)
r_b^l, p_b^l	Rotational velocity of pitch and roll of lower frame in body-fixed frame (rad/s)
$\phi_\delta, \theta_\delta$	Angular difference between upper and lower frame (rad)
z_e,	Displacement vector of upper frame in earth frame of reference pointing upward (m)
z_b	Displacement vector of upper frame in body-fixed frame pointing upward(m)
v_{ez}	Velocity vector in earth frame pointing upward (m/s)
v_{bz}	Velocity vector in body-fixed frame pointing upward (m/s)
$E = [z_e\ \ \phi_e^u, \theta_e^u]^T$	Displacement vector matrix of upper frame in earth frame
$V = [v_{bz}\ r_b^u, p_b^u\ ]^T$	Velocity vector matrix of upper frame in body-fixed frame
T	Transition matrix from body-fixed frame to earth frame
z_1, z_2, z_3, z_4	Displacement of four cylinders (m)
M_B	Inertia matrix of upper frame WRT body-fixed frame
k_1	Rotational spring constant of rubber bushings (rad/s)
l_{l1}	Distance between cylinder1 to center of gravity along x axle (m)
l_{l2}	Distance between cylinder3 to center of gravity along x axle (m)
l_{w1}	Distance between cylinder1 to center of gravity along y axle (m)
l_{w2}	Distance between cylinder2 to center of gravity along y axle (m)
$F_{c1}, F_{c2}, F_{c3}, F_{c4}$	Force provided by cyliner1, cyliner2, cyliner3 and cyliner4 (N)
U_z, U_p, U_r	Input from cylinders WRT z_b, roll and pitch in earth frame
Q_A, Q_B	Flow through port A and B of cylinder in $m3/s$
P_s, P_t	Supply and tank pressure Pa
P_A, P_B	Pressure in chamber A and B
C_D	Coefficient of discharge

K_{va}, K_{vb}	Valve flow coefficients
x_v, x_{vmax}	Spool displacementm, Maximum spool displacement m
V_{A0}, A_A	Initial volume in m^3, Area in $m^2$of cylinder chamber A
V_{B0}, A_B	Initial volume in m^3, Area in $m^2$of cylinder chamber B
$x_{cyl}, \dot{x}_{cyl}$	Cylinder position in m, velocity in m^2/s
f_f, f_e	Friction force, External load force in N
K	Proportional valve gain
ω_v	Cut-off frequency of proportional valve
U, U_{max}	Input voltage, Maximum input voltage in V
t	Proportional valve time constant
C_L	Coefficient of leakage in valve $m^3/s\sqrt{Pa}$
P_L, F_L	Load pressure in Pa, Load Force in N
Q_C	Leakage flow in valve $m3/s$

TABLE OF CONTENTS

1 INTRODUCTION

1.1 Background and Problem Description

A forwarder is a forestry vehicle that carries logs from forest to a roadside landing. From the definition it could be inferred that it works in a harsh environment. The forwarder does not move in a flat plane and might induce significant vibration to the operator, which leads to severe health issues. The vibration isolation ability of a forwarder is evaluated by the level of acceleration which operators are exposed to. In 2002 the European council adopted directives 2002/44/EC which applies the principles of the Framework Directive to risks arising from hand-arm vibration (HAV) and whole-body vibration (WBV), setting minimum requirements for the prevention of vibration-related health issues. The Vibration Directive established agreed levels of exposure above which employers must take certain actions to control risks, and in setting the daily exposure limits [1].

Three categories of suspension system have been applied in industry: passive suspension, semi-active suspension, and active suspension. The active suspensions are characterized by a requirement that at least a portion of suspension force generation is provided through active power sources such as compressors, hydraulic pumps [2]. This kind of character gives active suspension greater capability to reduce the vibration but also more power consumption.

Komatsu Forest AB developed a new passive multi-degree-of freedom cabin suspension, but an attempt of active suspension control based on their mechanical solution is also desired. With the active suspension system the vibration should be significantly reduced and the cost should be kept low.

1.2 Purpose

The purpose of the project is to develop a simulation model of active suspension for an existing passive suspension system of the forwarder cabin, in order to reduce health related issues of operators abiding by the EU directives. The requirement given by Komatsu is that reducing the vibration between $1-5\ Hz$ within the given cylinder stroke limitation. The overall goal of this thesis is to develop a three degree-of-freedom active suspension control system and analyze the system performance and deduce the system requirements for real time implementation. The process includes the following tasks

1. Model the overall system and simulate it in different levels of detail;
2. Develop methods to design the controllers which can actively isolate the vibration from the ground;
3. Simulate the closed-loop system analyze system behaviors;
4. Hardware selection for real-time implementation based on simulation results.

1.3 Method

This thesis is modularized into mechanical and hydraulic subsystems. The mathematic model of mechanical system is analyzed based on mechanics theory, then a SimMechanics model is derived for detailed simulation; the basic theory of hydraulic is used to analyze the system and the simulations are carried out with Simulink and SimHydraulics.

For the control design, the cascaded control structure is selected in this work. The hydraulic system comprises of PID controller to provide desired force; for mechanical system standard PID/ PD controllers is designed to reduce the vibration of mechanical system.

In the end the Simulink model of hydraulic system and SimMechanics model are merged together to simulate the overall system.

1.4 System description

The simple representation of mechanical design of the suspension system is as shown in Figure 1.1.

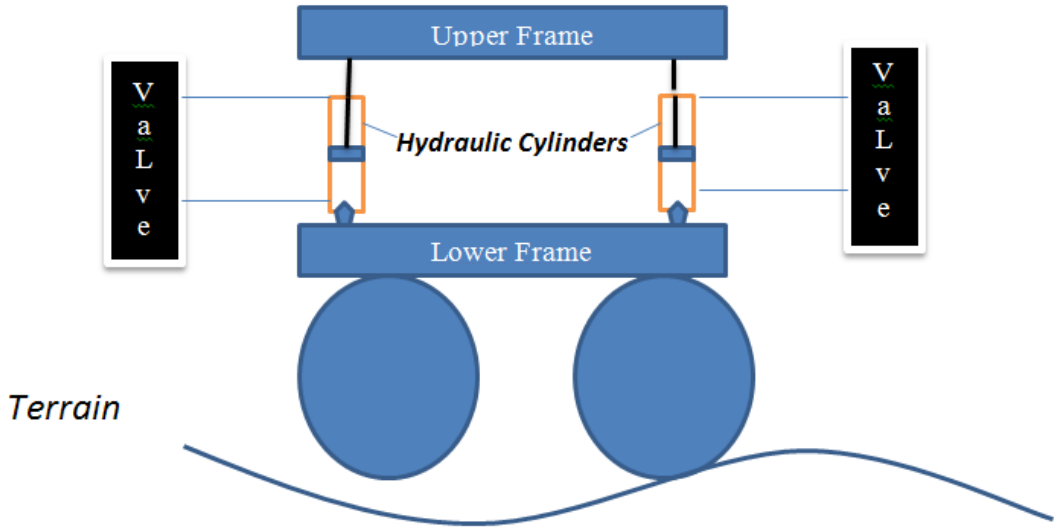

Figure 1.1 Simplified suspension system structure

When the valve is closed, the upper frame and lower frame of the system, connected by the cylinder, will not have any relative motion between them. Due to the absence of relative motion, when the vehicle moves in a terrain, the upper frame is induced with the same vibration as that of the lower frame. Hence in order for the suspension to be active, the cylinders should be able to actuate the upper frame either to follow the motion or to maintain an equilibrium position. But when the valve is open, the pressure on the actuation port of the cylinder increases and hence moves the upper frame in that direction. For the cylinder to be actuated, it should be provided with some reference input signal which results in an output force from the cylinder. Here is when the requirement to separate the system in to two control modules arises: inner loop control and outer loop control.

The main task of the outer loop controller is to generate reference force signals for the cylinders in order to attenuate the vibration from ground. Especially when the amplitude of force induced on the lower frame is high, the outer loop controller comes in to major action.

The inner loop controller's task is to generate a force equivalent to the reference force in order to supress the effect of shock induced force at a faster rate. The inner loop controller will also be able to handle the effect of reaction force induced on upper frame due low amplitude vibrations as there is pressurised fluid inside the cylinder chamber.

1.4.1 Mechanical system

The suspension system consists of an upper frame, a lower frame, two lateral connecting rods, one longitudinal connecting rod, 6 rubber bushings and 4 hydraulic cylinders. The upper frame will be connected with the forwarder cabin, and the lower frame will be connected with the chassis. In the Figure 1.2, it could be seen that the upper frame and lower frame are connected by the connecting rods, and the rubber bushings are placed at the joints between them. The four

hydraulic cylinders are placed at the four corners of the frames, connecting upper and lower frame with spherical constraints which gives them three rotational DOF.

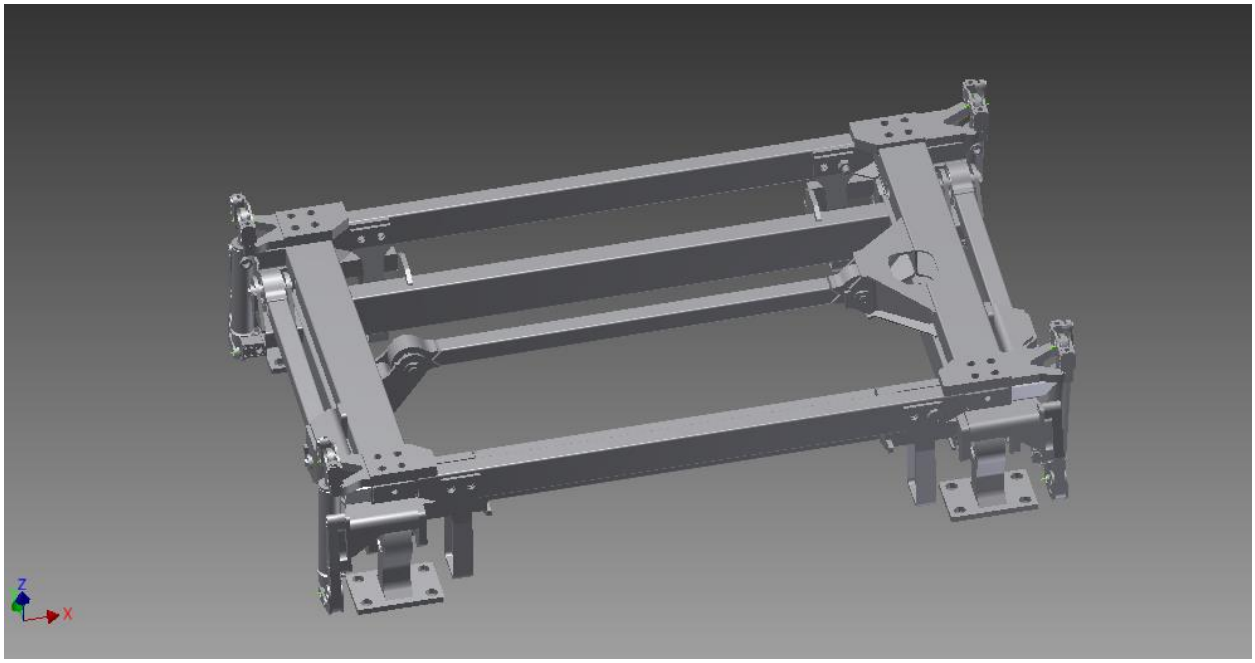

Figure 1.2 The passive suspension system designed by Komatsu

In this suspension system, the vibration coming from the ground will be transferred from chassis to the lower frame, so the goal of the active suspension system is to isolate the vibration between the lower frame and the upper frame.

It could be seen that the kinematic of upper frame is constrained by the rods and rubber bushings. The connecting rods eliminate the longitudinal and lateral movement as well as the yaw movement; and the elasticity of rubber bushings gives the degree of freedom in pitch, roll and heave. Therefore in this thesis focus is given to reduce the vibration of roll, pitch and heave motion. Moreover the maximum stroke of cylinder is ± 100 mm, which limits the movement of the upper frame. The detailed dynamic and kinematic analysis will be given in Chapter 3.

1.4.2 Hydraulic system

In general a fluid system comprises of a hydraulic pump, relief valve, proportional valve and an actuator. These systems are used in a wide range of applications for their ease of controllability. The other major advantages include high power-to-weight ratio, capability of being stalled, fast response and acceleration and long service life.

The main components considered for hydraulic system are, asymmetric cylinder, 4/3 proportional valve, a tank and a constant pressure source. A schematic of the hydraulic system is as seen below in Figure 1.3.

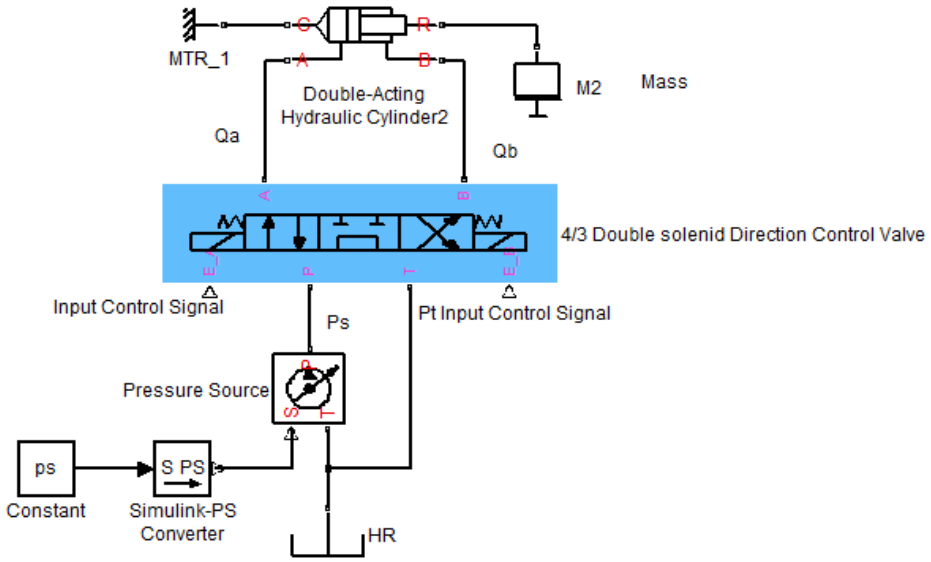

Figure 1.3 The basic Hydraulic Circuit

The Cylinder used in this thesis is a double acting cylinder of 200 mm stroke with an inbuilt position sensor. Directional control valves are one of the most fundamental parts in hydraulic circuitry. They allow fluid to distribute the flow to different paths from one or more sources. There are different types of valves based on the functionality, geometry, spool landing and the actuation type. Zero lapped valves as in Figure 1.1 are recommended in this application, where a tautest control is required.

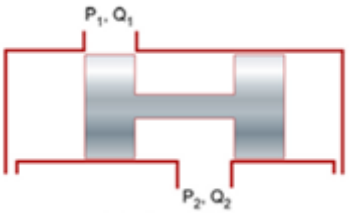

Figure 1.4 Zero lapped valve

1.4.3 Overall Control Architecture

Generally speaking there are two ways to achieve this platform control: controlling the motion of cylinders, where certain cylinder's position corresponds to certain platform altitude, or directly control the altitude of the platform. In this work, the second method is adopted since the suspension system is an over-actuated. The system has four inputs and three outputs (DOFs), this means the system cannot be modeled properly with displacement and velocity of the four cylinders as state variables; besides the altitude (roll and pitch) are more interested than the displacement of cylinders in the control design. The general control architecture is shown in the figure below.

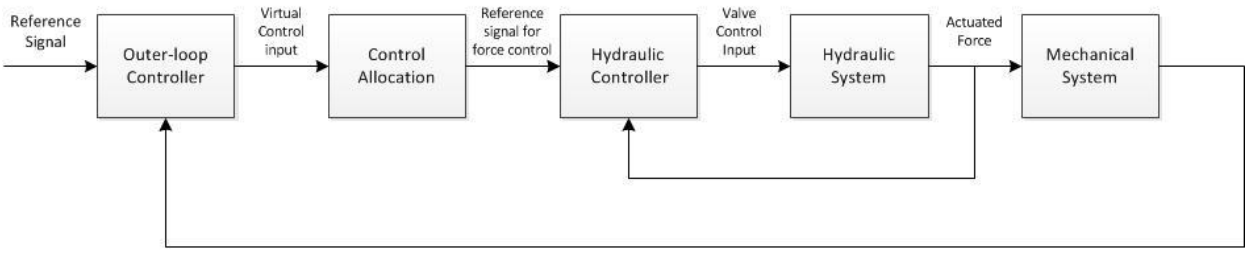

Figure 1.5 Overall control architecture

The control system has a cascaded structure which consists of three parts: outer-loop controller, control allocation module and the hydraulic (inner-loop) controller. The outer-loop controller, feedbacks the angular and heave movement and computes the "virtual control inputs" which are the net torques and net force to control roll, pitch and heave movement; the control allocation module will calculate the desired forces from hydraulic cylinders to achieve the required "virtual control inputs" (net forces and net torques); then the hydraulic controller will control the solenoid valve to actuate the cylinder.

1.5 Delimitation

In this thesis the following delimitation are defined

1. Mobile vehicles use Load sensing pump as the power source but in this work, modeling and simulations are performed assuming the power source to be a constant pressure pump.
2. All kinematic properties introduced by longitudinal and lateral movement (Figure 1.) are ignored
3. The hydraulic cylinders are assumed to be perpendicular to the lower frame.
4. Due to the elimination of yaw movement, Coriolis force is ignored.
5. The friction and complex dynamic of rubber bushings are ignored

Please note that, although these effects are ignored, some of their influences are still analyzed in this report for the further design.

1.6 Structure of thesis

The entire thesis report is divided into nine chapters. Chapter One introduces the background, purpose, goal, methods and finally gives a short description and overall system architecture of this thesis work. Chapter Two presents the theoretical reference frame that is necessary for the performed research, design or product development. In chapter Three the kinematics and dynamics of the mechanical system is analyzed and modeled. Chapter Four introduces the design method of outer loop controller. Chapter Five explains the mathematical modeling, simulation and control development for the inner loop system. In chapter six the measured vibration data obtained from Skogforsk is fed in to the integrated system and analyzed. Chapter Seven and Eight explains the sensor and hydraulic equipment selection for real-time implementation. Chapter Nine concludes the final outcome of this thesis.

In this work, Girishkasturi.L.H is responsible for the hydraulic system design and analysis and Qiwu Wang is responsible for the mechanical system analysis and control design. The integrated system analysis is a joint work.

2. FRAME OF REFERENCE

This chapter presents the theoretical reference frame that is necessary for the performed research, design or product development.

2.1 Suspension System of Forwarders

The suspension system, which isolates vibration from road suffice, plays an important role in ride comfort. Normal suspension systems consist of springs, shock absorbers and linkages that connect their upper components to lower components. Suspension system can be categorized into passive, semi-active and active suspension system.
Although suspension system is one of the most important components of vehicles, most forest machines were not equipped with suspension system until recent years. Suspension system of forwarders could be divided into different levels such as primary suspension system (front and rear axle suspension system) and secondary suspension system (cab suspension and seat suspension) [5]. According to the new legislation, vibration exposure may not exceed the limit value. If the limit value is exceeded, the employer shall take immediate measures to reduce the vibration exposure.

	Action value	Limit value
Hand and arm vibrations	$2.5\ \mathrm{m/s^2}$	$5.0\ \mathrm{m/s^2}$
Whole-body vibrations	$0.5\ \mathrm{m/s^2}$	$1.1\ \mathrm{m/s^2}$

Table 2.1 Legislation on vibration of forest machines

Active suspension is an automotive technology which uses actuators, e.g. hydraulic cylinders, in order to control the movement of suspension. Comparing to passive suspension and semi-active suspension system, active suspension could achieve better damping characteristics and improve ride comfort.

2.2 Hydraulics

The Hydraulic fluid acts a medium to transfer force from the pump to the end effector and they can be of different types e.g., mineral oils, biodegradable oils and water based oils. Few technical properties that describe these fluids include density, viscosity and bulk modulus.

Density:
The density ϱ, of a fluid is defined as: “mass per unit volume” (Welty et al., 1984). In general for engineering problem, the manufactures provide the specific gravity i.e. the ratio of actual density of fluid to the density of water at standard temperature for it to make the calibration relative.

$$\varrho = \mathrm{m/V}$$

Viscosity:
Viscosity is the measure of fluids resistance to deformation when subjected to a shearing force (Welty et al., 1984). Generally two types of viscosity are provided in the data sheet: dynamic viscosity (μ) and kinematic viscosity (ν). Dynamic viscosity is a measure of the internal resistance and kinematic viscosity is the ratio of absolute or dynamic viscosity to density – a quantity in which no force is involved and knowledge on this is absolutely necessary to design a hydraulic system.

Bulk modulus:
Bulk modulus (β) is a measure of the compressibility of a fluid. The basic definition of fluid bulk modulus is the fractional reduction in fluid volume corresponding to unit increase of applied pressure (McCloy and Martin, 1973).

$$\beta = -V * (\frac{\partial P}{\partial V})$$

2.3 Hydraulic Control

The hydraulic system consists of a hydraulic pump, valve and an actuator that helps in achieving the desired action of vibration control. The control signal given over the valve determines the motion of the actuator. The amount of fluid flowing from the valve in to the cylinder determines the force at the output. The pressure of the supply fluid from the pump would determine the reaction rate of the system. When it comes to controlling the position of actuators, the output from the sensor is taken as the feedback and corresponding control signal is generated by the controller. The generated control signal triggers the valve opening. The valve could be solenoid actuated or pneumatic depending on the space and cost constraints.

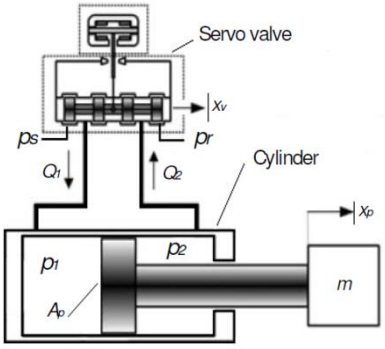

Figure 2.1 Hydraulic Valve, Cylinder assembly

2.4 Cascade control

A cascade control structure is constructed by two (or more) control loops in a cascade structure, in which one controller's output set the reference of the other one. The controller generate reference signal is called primary or outer loop controller. The controller receiving the set point is called the secondary or inner loop controller. The secondary controller has fastest response and calculates control signals according to the reference from primary or intermediate controller; however the primary or intermediate controller, unlike single loop controllers, computes reference for the inner loop instead of generating a control signal for the actuators.

As a rule of thumb the inner-loop controller should be at least 3 times faster than the outer-loop controller to attenuate disturbances and compensate nonlinearity of inner loop.

2.5 Sensitivity function and complementary sensitivity function

A closed-loop control system should has proper capability to attenuate the external disturbances. Load disturbances are typically dominated in low frequencies area. Take the cruise control system in an automobile as example, the disturbances are the gravity forces caused by changes of the slope of the road [2]. In control theory, the capability of disturbance attenuation of a control system is characterized by the sensitivity function S. Correspondingly the capability of handling

the measurement noise and model uncertainties is characterized by the complementary sensitivity function T.

A block diagram of closed-loop system is shown in Figure 2.2. The block G represent the process, and F_r and F_y represent the feedforward and feedback controller respectively. The signal $w_u$is the input disturbance and w is the output disturbance, in this application this disturbance could be interpreted as the (angular) displacement of upper frame caused by the uneven ground.

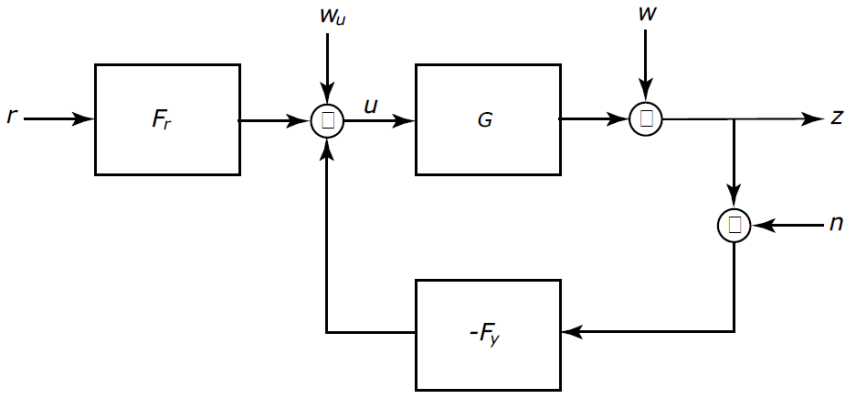

Figure 2.2 Block diagram of closed-loop system

The sensitivity function S represents the response from output disturbance w to the output z; and the complementary sensitivity function T represents the response from measurement noise n and model uncertainty to the output z. These functions are calculated below

$$S = G_{w\to z} = \frac{1}{1+GF_y} \qquad T = G_{n\to z} = \frac{GF_y}{1+GF_y}$$

If $F_y = F_r$, the complementary sensitivity function T is exactly same as the closed-loop system response. It could be seen that these functions have the property of

$$S + T = 1$$

which implies that the capability of disturbance attenuation and handling model uncertainty cannot be both high at a certain frequency. Actually the sensitivity function S has a "high-pass" property, sensitivity function T has a "low-pass" property, which implies the system is more capable to reduce the disturbance in low frequency domain and can handle model uncertainty better in high frequency domain. With a faster controller, the closed loop system is able to handle higher frequency disturbance, but also require a more accuracy model.

2.6 Over-actuated system and quadratic programming algorithm

The Over-actuated system, which usually exists in aircraft and robotics applications, equips more control input than output due to the actuator performance constraint or requirement of redundancy. In order to achieve the desired performance, control efforts need to be allocated to each actuator. In some case the control allocation need to consider the actuator dynamic interaction, but in most cases it can be treated statically with mathematical programming algorithm [3]. The general control structure can be modulated as below, the outer controller compute a virtual control input, e.g. a net force or net torque, and then control allocation module will distribute the real control effort in an optimized way.

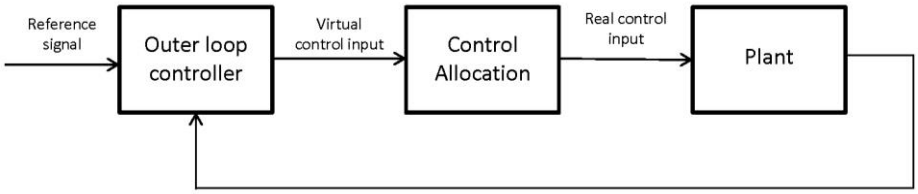

Figure 2.3 Over-actuated system control module

A linearly constrained optimization problem with a quadratic objective function is called a quadratic program (QP). The general quadratic program can be written as

$$\text{Minimize } f(x) = cx + \frac{1}{2}x^T Qx$$

$$\text{Subject to } Ax \leq b \text{ and } x \geq 0$$

Where c is an n-dimensional row vector describing the coefficients of the linear terms in the objective function; and Q is an $(n \times n)$ symmetric matrix describing the coefficients of the quadratic terms. [4].

3 MODELLING OF MECHANICAL SYSTEM

In this chapter a Newton-Euler model is derived based on kinematic and dynamic analysis. In the beginning some approximations are made in order to simplify the mathematic model, and two kinds of reference frame are introduced. Then kinematic properties of system are analyzed in both frames of reference. Based on the kinematic analysis, a dynamic model is derived and feedback linearization method is discussed for this application. Last not least the simulation files are created based on related analysis.

3.1 Approximations and Assumptions

According to the previous analysis, the upper frame have three significant DOF movement, pitch, roll, and heave, as well as three DOF which are longitudinal movement, lateral movement, and yaw movement. These movements are so small that they should not be considered as control variables; however the longitudinal and lateral movements will have some effects on the behavior of system. Besides some other physical phenomenon, e.g. Coriolis force, will give small effect to the system. In this work these effects are estimated and analyzed for the further design. Generally speaking four major approximations are made in order to simplify the mathematic model:

1) All kinematic properties introduced by longitudinal and lateral movement are ignored

The longitudinal and lateral relative movements between upper and lower frames are almost eliminated by the mechanical system, but small motions still could be generated by the rotation of connecting rods. The maximum stroke of each cylinder is ± 100, and the maximum pitch and roll angle between frames are $\pm 6°$ and $\pm 12°$, so the maximum movement can be roughly estimated as below

$$X_{\max} = (1 - \cos 6°) * l_{long\ rod} = 6.2286mm \tag{3.1}$$

$$Y_{max} = (1 - \cos 12°) * l_{short\ rod} = 14.6411\ mm \tag{3.2}$$

where $l_{long\ rod}$, $l_{short\ rod}$ are the length of long connecting rod and short connecting rods. The calculation above shows that the movement in x and y are very small, thus the related kinematic can be ignored.

2) The hydraulic cylinders are assumed to be perpendicular to the lower frame.

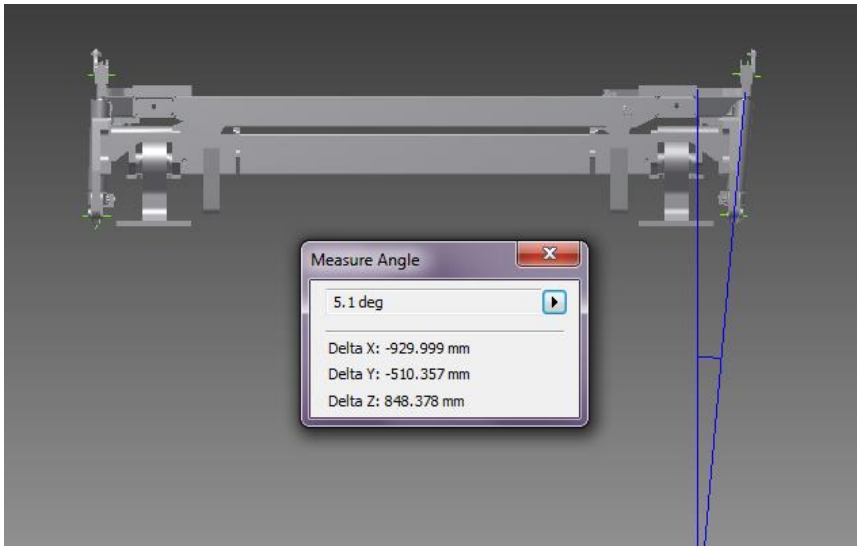

Figure 3.1 Inclination between upper frame and cylinders

As mentioned in Figure 1.2 the cylinders have spherical constraints with upper and lower frame, which gives them three extra rotational DOF. In the initial condition (the pistons are at the bottom position) the hydraulic cylinders are not perpendicular to the lower frame (Figure 3.1), also when the upper frame has linear or rotation movement with regard to the lower frame, the angle between the cylinder and upper frame changes. The maximum angular movement of cylinders introduced by the rotation of upper frame is taken as an example and roughly estimated below.

$$roll_{cyl\_max} = \arcsin[(1-\cos 12°) * \frac{l_{width}}{2L_{cylinder}}] = 2.555° \tag{3.3}$$

$$pitch_{cyl\_max} = \arcsin[(1-\cos 6°) * \frac{l_{length}}{2L_{cylinder}}] = 1.1689° \tag{3.4}$$

The calculation in (3.3) and (3.4) shows that the rotation of these cylinders could be very small. If these angular movements of cylinders were taken into consideration, it would dramatically increase the complexity of dynamic and kinematic analysis since the center of rotation is not constant anymore. Thanks to the considerate machine design these angles are so small that could be ignored. Furthermore, it could be estimated that when all the cylinders at the center position of their strokes, they are almost perpendicular to the lower frame. So the hydraulic cylinders could be assumed to be perpendicular to the lower frame in this case. This also means the yaw movement could also be ignored.

3) Since the yaw movement is not taken into consideration, the Coriolis force is also ignored;
4) The horizontal displacement of upper frame gives extra tension of rubber bushings, which is also ignored.

According to these assumptions, a time-invariant model will be delivered in which complexity is significantly reduced. However the designer should keep these model approximations in mind and handle them in control design.

3.2 Selection of frame of reference

A good selection of frame of reference can simplify calculation. In order to describe the kinematics and dynamics of upper frame, two reference frames are defined: The earth frame of reference (E-frame) and the body-fixed frame of reference (B-frame).

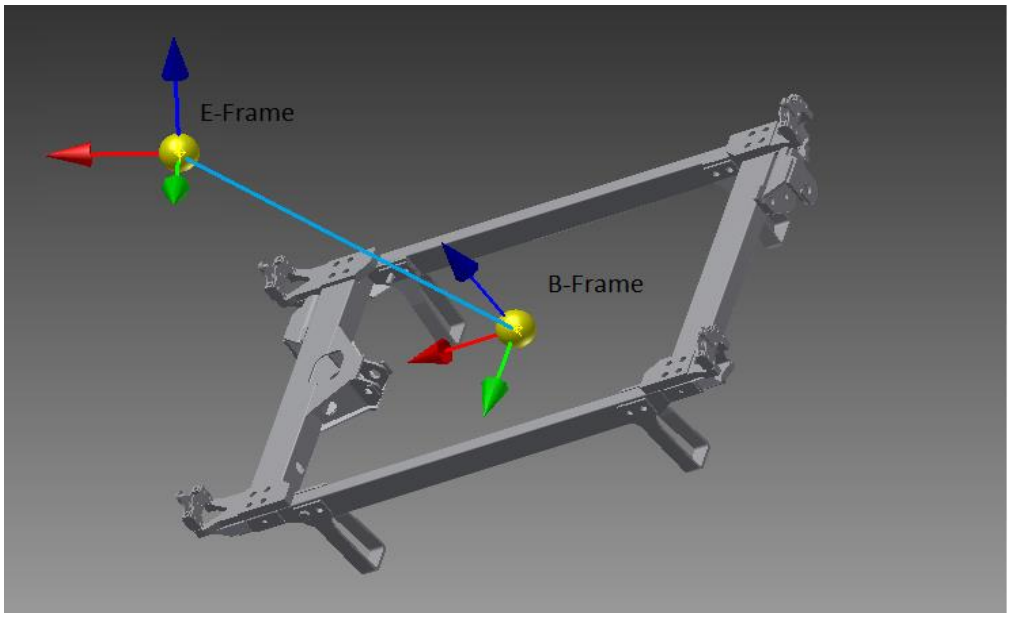

Figure 3.2 Frame of references

Figure 3.2 shows the setup of these two frames of reference. The earth frame of reference is a "static", inertial frame of reference, and effects of vibration should be estimated in this reference frame. The body-fixed frame is a coordinate system fixed on the upper frame (or the passenger cabin), the reason to select this B-frame is that the inputs of the upper frame, net forces and net torques, are easier to be calculated in this frame of reference.

For the convenience of creating the SimMechanics simulation, the directions of coordinates are selected according to the given CAD file. The earth frame of reference is defined as: the origin of frame is the gravity centre of upper frame, z_e have the opposite direction of the gravity, the xy plane of E-frame is perpendicular to z_e; x_e points towards to the opposite direction of movement of the forwarder, and y_e point towards to the left side of the forwarder which is perpendicular to x_e. It could be seen that the frame of reference is orthogonal. The body-fix frame is defined as: origin O_b is at the centre of gravity of upper frame; x_b is parallel to the long side and pointing backward; y_b is parallel to short side of frame and point to the left of x_b; z_b is orthogonal to the xy plane and towards to the upside. It could be seen in the figure these two frames of reference are both right-hand coordinates.

3.4 Kinematics analysis

In this case there are two ways to analyze the system kinematics: map the movement of upper frame from B-frame to E-frame, or directly use the displacement of hydraulic cylinders and Euler angle of lower frame to get information of upper frame in E-frame. In this thesis both of these methods are analyzed.

3.4.1 Transformation from the body-fix frame to the earth frame

The rotation of upper frame is defined by the orientation of body-fixed frame with regard to the earth frame of reference. The Euler angles, roll and pitch, are denoted as ϕ and θ respectively. Since most of body-fixed rotational information directly from sensors is angular velocity, the transfer matrix is defined to convert angular velocities to E-frame. The angular velocity of roll and pitch on upper frame are represented as r and p respectively. The equations below shows the kinematics of three DOF of the upper frame

$$\dot{E} = TV \tag{3.5}$$

$$E = [z_e \ \ \phi_e^u \ \ \theta_e^u]^T \tag{3.6}$$

$$V = [v_{bz} \ r_e^u \ p_e^u]^T \tag{3.7}$$

In which $\dot{E}$ is the velocity vector of upper frame with respect to E-frame, V is the velocity vector with respect to B-frame, and matrix T (shows in equation 3.7) is the transfer matrix from the body-fixed frame to the earth frame.

The projection from z_b to z_e is

$$z_e = z_b cos\phi_e^u cos\theta_e^u \tag{3.8}$$

The transfer matrix can be determined by resolving the Euler velocities into the body-fixed frame as shown in equations (3.7)

$$\begin{bmatrix} \dot{z_e} \\ \dot{\phi_e^u} \\ \dot{\theta_e^u} \end{bmatrix} = \begin{bmatrix} cos\phi_e^u cos\theta_e^u & 0 & 0 \\ 0 & 1 & sin\phi_e^u tan\theta_e^u \\ 0 & 0 & cos\phi_e^u \end{bmatrix} \begin{bmatrix} v_{bz} \\ r_b^u \\ p_b^u \end{bmatrix} \tag{3.9}$$

3.4.2 Convert from displacement of hydraulic cylinders and to the earth frame

The displacements of the four cylinders are defined as z_1, z_2, z_3 and z_4, which z_1 and z_2 are the front cylinders and z_3 and z_4 are the rear cylinders. Since the upper frame could be considered as a rigid body, these variables have the property of

$$z_1 - z_2 = z_3 - z_4 \tag{3.10}$$

$$z_1 - z_3 = z_2 - z_4 \tag{3.11}$$

After including the angular displacement of lower frame, the pitch and roll angle is given by

$$\phi_e^u = acrsin\frac{z_2 - z_1}{l_{width}} + \phi_e^l \tag{3.12}$$

$$\theta_e^u = \text{acrsin}\frac{z_3 - z_1}{l_{length}} + \theta_e^l \tag{3.13}$$

$$z_b = (z_1 + z_2 + z_3 + z_4)/4 \tag{3.14}$$

where the l_{length} and l_{width} are the length and width of upper frame, ϕ_e^l and θ_e^l are the Euler angle of roll and pitch of lower frame.

For the kinematics analysis it could be seen that both methods are straightforward, however in the coming dynamics analysis, the first method which based on the B-frame is used, because:

- There are four cylinders but three DOF of upper frame can only introduce three groups of dynamic equations, this means the dynamics of four cylinders cannot be modeled properly;
- Velocity measurement is available in body-fixed frame;
- Inertia matrix of upper frame is time-invariant;

3.5 Selection of state variables

In this case, the most important states are angular displacement of pitch and roll, as well as the displacement in heave direction. In order to estimate the capability of disturbance attenuation, the angular displacement in earth reference frame must be selected. Also angular velocities are interested, since the related information in in body-fixed frame of reference can be obtained from gyroscope, so r_b^u, p_b^u are selected as state variables; For the heave movement, since it is difficult to find accurate sensors to directly measure the position in E-frame, the z_b and v_{bz} in B-frame are selected. Besides the deflection of suspension is also very important, so the angular difference between upper and lower frame, ϕ_δ and θ_δ respectively, are also selected in this case. To sum up the state variable x is

$$x^T = [z_b\ v_{bz}\ \phi_e^u\ r_b^u\ \theta_e^u\ p_b^u\ \phi_\delta\ \theta_\delta] \tag{3.15}$$

3.6 Dynamics analysis

According to Newton laws, the dynamics of upper frame is calculated below

$$M_B = \begin{bmatrix} m & 0 & 0 \\ 0 & I_{xx} & I_{xy} \\ 0 & I_{yx} & I_{yy} \end{bmatrix},\ F_B = \begin{bmatrix} F_z^B & \tau_{roll} & \tau_{pitch} \end{bmatrix}^T \tag{3.16}$$

$$F_B = M_B \dot{V} \tag{3.17}$$

The matrix M_B is part of the inertia matrix which only involves the selected state variables. And F_z^B is the net force imposed in heave motion, and τ_{roll} and τ_{pitch} are the net torques imposed in roll and pitch motion. The main forces and torque implied on the upper frame are forces from cylinders, gravity, and rubber bushings.

1. Cylinder force U_A and the gravity

$$U_A = \begin{bmatrix} U_z \\ U_\phi \\ U_\theta \end{bmatrix} = \begin{bmatrix} F_{c1} + F_{c2} + F_{c3} + F_{c4} \\ \left((F_{c2} + F_{c4}) * l_{w2} - (F_{c1} + F_{c3}) * l_{w1}\right) * cos\phi_\delta cos\theta_\delta \\ \left((F_{c1} + F_{c2}) * l_{l1} - (F_{c3} + F_{c4}) * l_{l2}\right) * cos\phi_\delta cos\theta_\delta \end{bmatrix} \tag{3.18}$$

The input matrix U_A is calculated in body-fixed frame. In the matrix above F_{c1} and F_{c2} are the forces generated from front cylinders, F_{c3} and F_{c4} are the rear cylinders; l_{l1} is the distance from the joints of front cylinders to the gravity centre of upper frame; l_{l2} is the distance from the joints of rear cylinders to the gravity centre of upper frame; l_{w1} is the distance from the joints of left side cylinders to the centre of gravity; l_{w2} is the distance from the joints of right side cylinders to the centre of gravity.

Besides the impact given by the gravity could be modelled as

$$G_B(z) = -mg * cos\phi_e^l cos\theta_e^l \tag{3.19}$$

Please notice that there are nonlinear components in the equation (3.16) and (3.17). These additional nonlinearities in U_A actually play a role of feedback linearization in the control system design. If these trigonometric elements are not considerate as elements of control input U_A, then they should exist along the state variables in the differential equation groups, especially for the pitch and roll which are nonlinearly coupled with ϕ_δ and θ_δ. Indeed, there are some arguments querying the robustness of feedback linearization. However it could be seen that these trigonometric elements are introduced by the kinematic and geometry properties of system, besides they are not frequency dependent. This means that the uncertainty of these nonlinearities is quite small. Also feedback linearization is good to guarantee the global stability of a nonlinear system, especially when the angle ϕ_e^l and θ_e^l became large. So in this case it is suitable to use feedback linearization to cancel the nonlinearity.

However this feedback linearization method also has a disadvantage of making the elements of equation (3.16) and (3.17) angular-dependable due to the trigonometric elements. If these trigonometric elements are not exist (3.16) and (3.17) the right part of equation is totally static, which means the control allocation module (detailed introduced in Chapter Four) could use a static distribution coefficients rather than calculate them on-the-fly. The later analysis shows these on-line calculation load might be large. In order to overcome this disadvantage a simplified algorithm is developed which considerably reduced the computation load. However if the computation load is still very problematic in real-time implementation, this feedback linearization is not suitable anymore. Consequentially these trigonometric elements should be removed from equation (3.16) and (3.17). However some other control strategy, e.g. gain scheduling, should be adopt to handle the nonlinearities to guarantee the global stability of system.

2. Rubber bushings

An ideal Rubber bushing has six degree of freedom: three from radial load, one from torsional load, and two from conical load (see the figure below). However for the rubber bushings used by the passive suspension system, their spring constant for radial load are so high that the related

DOF could be ignored. There are many researches about detailed modeling the rubber bushings, but in this work they are modeled as 3-dimensional springs and dampers. Figure 3.3 shows the load distribution and kinematics of rubber bushing.

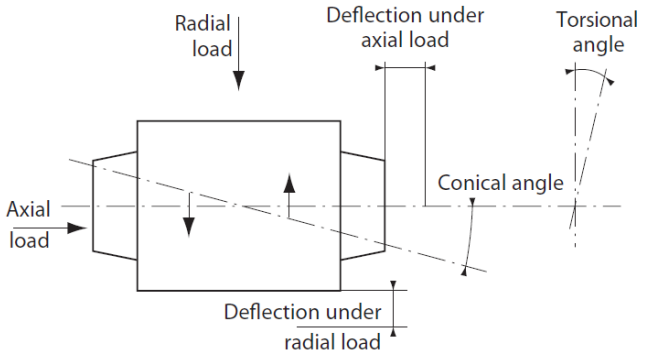

Figure 3.3 Rubber bushing (Mecmove AB, 2012)

There are six rubber bushings in passive suspension system, but only their overall influence on the system is interested. The torque generated by rubber bushings could be summarized by

$$T_\phi = -d_1 r_\delta - k_1 \phi_\delta \tag{3.20}$$

$$T_\theta = -d_2 p_\delta - k_2 \theta_\delta \tag{3.21}$$

In which

$$r_\delta = r_b^u - r_b^l,\ \phi_\delta = \phi_e^u - \phi_e^l \tag{3.22}$$

$$p_\delta = p_b^u - p_b^l,\ \theta_\delta = \theta_e^u - \theta_e^l \tag{3.23}$$

which d_1, k_1, d_2, k_2 are the damping ratio and spring coefficient on roll and pitch movement. In practice, due to the complexity of system, these parameters should be identified by data acquisition rather than theoretical calculation (especially the damping ratios which don't have any specification on the datasheet). But in order to simulate the related dynamic property a rough calculation is made below.

At first the torsional torque is not considered in this case. In the CAD drawing of the rubber bushings it is specified that the spring coefficient of torsional rotation is $20Nm/°$, this mean if torsional angle is large it could generate a torque much larger than the static friction. Then the surface between shaft and rubber bushing will slide rather than twist the rubber in the bushing. Due to this assumption, in the white box model, the torque generated by the torsional rotation is ignored, but the controller should be robust enough to handle model uncertainty. Also according to the specification of bushings, the spring coefficient of conical rotation is

$$K_{conical} = 24Nm/° = 1375.1\ Nm/rad \tag{3.24}$$

It could be roughly estimated that

$$k_1 = \frac{K_{conical}}{2} = 687.55\ Nm/rad \tag{3.25}$$

$$k_2 = K_{conical} = 1375.1\ Nm/rad \tag{3.26}$$

For the damping ratio some random value are tried

$$D_{conical} = 1\ Nm/° = 57.3\ Nm/rad^2 \tag{3.27}$$

$$d_1 = 28.65\ Nm/rad^2 \tag{3.28}$$

$$d_2 = 57.3\ Nm/rad^2 \tag{3.29}$$

3.7 Nonlinear model

In the mathematic model, the motion of lower frame will be considered as disturbance which are represented by W_ϕ and $W_\theta$and According to the previous analysis, a nonlinear model of system could be delivered

$$\begin{bmatrix} \dot{v}_{bz} \\ \dot{z_B} \\ \dot{r_b^u} \\ \dot{\phi_e^u} \\ \dot{p_b^u} \\ \dot{\theta_e^u} \\ \dot{\phi}_\delta \\ \dot{\theta}_\delta \end{bmatrix} = \begin{bmatrix} G_B/m\ +\ U_z/m \\ v_{bz} \\ -I_1U_\theta + I_2U_\phi\ +\ I_2T_\phi - I_1T_\theta \\ r_b^u + p_b^u sin\phi_e^u tan\theta_e^u \\ -I_4U_\phi + I_3U_\theta + I_3T_\theta - I_4T_\phi \\ p_b^u cos\phi_e^u \\ r_b^u - W_\phi \\ p_b^u - W_\theta \end{bmatrix} \tag{3.30}$$

$$I_1 = \frac{I_{xy}}{I_{xx}I_{yy} - I_{yx}I_{xy}}, I_2 = \frac{I_{yy}}{I_{xx}I_{yy} - I_{yx}I_{xy}}, I_3 = \frac{I_{xx}}{I_{xx}I_{yy} - I_{yx}I_{xy}}, I_4 = \frac{I_{yx}}{I_{xx}I_{yy} - I_{yx}I_{xy}}$$

3.8 Simplified and linearized model

From the data provided by Komatsu it could be seen that the value of I_1 and I_4 is small, this means that this multiple-input-multiple-output system is slightly coupled. In order to simplify the control design a linearized and decouple model is delivered.

$$\begin{bmatrix} \dot{v}_{bz} \\ \dot{z_B} \\ \dot{r_b^u} \\ \dot{\phi_e^u} \\ \dot{p_b^u} \\ \dot{\theta_e^u} \\ \dot{\phi}_\delta \\ \dot{\theta}_\delta \end{bmatrix} = \begin{bmatrix} -g\ +\ U_z/m \\ v_{bz} \\ I_2U_\phi\ +\ I_2T_\phi \\ r_b^u \\ I_3U_\theta + I_3T_\theta \\ p_b^u \\ r_b^u - W_\phi \\ p_b^u - W_\theta \end{bmatrix} \tag{3.31}$$

3.9 Model of the system including the cabin

Generally speaking the major structure of the model including the cabin is similar to the one without the cabin. However there are certain additional factors will influence the system dynamics. The main causes of these factors are the height and weight of cabin. In the case of excluding the cabin, the gravity centre of upper frame almost has the same height of joints of hydraulic cylinders, also its weight is relatively small, and therefore some effect could be ignored. However the cabin has a very heavy weight and its centre of gravity is about half meter higher than the joints of hydraulic cylinders. So the influence of centrifugal force and torque generated by the inclination of cabin cannot be ignored anymore.

1. Centrifugal force

$$F_{centrifugal} = mr_b^{u2} h_{cab} + mp_b^{u2} h_{cab} \quad (3.32)$$

h_{cab} is the height of gravity centre of cabin.

2. Torque generated by the inclination of cabin

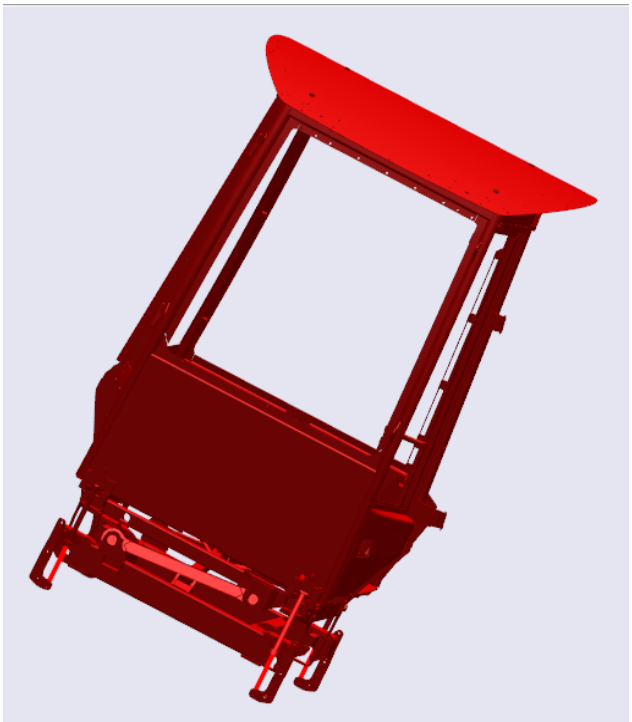

Figure 3.4 The suspension system including the passenger cabin

Since there is an inclination of cabin, the gravity will apply a torque on the cabin and component force towards to the direction of x_B and y_B. Correspondingly the connecting rods between the upper frame and lower frame will generate a reaction force. However in most cases connecting rods is not parallel to the upper frame, so the vertical force component will aggravate the torque applied by the gravity. Since the dynamic of connecting rods is not interested in this application, the related effect will be represented as

$$T_{\phi rod} = coef_{rod} sin\phi_e^u \quad (3.33)$$

$$T_{\theta rod} = coef_{rod} sin\theta_e^u \quad (3.34)$$

The value of $coef_{rod}$ could be estimated by experiments. So the torque generated by the inclination of cabin is calculated below

$$T_{\phi cab} = mgh_{cab} sin\phi_e^u + T_{\phi rod} \quad (3.35)$$

$$T_{\theta cab} = mgh_{cab} sin\theta_e^u + cT_{\theta rod} \quad (3.36)$$

Please noticed that these influence introduced by the cabin increase system coupling and nonlinearity. In order to simplify the control design, these effects are also cancelled with feedback linearization instead of including into dynamic model.

3.10 Simulation of mechanical system

Based on previous mechanical system analysis, simulation files need to be developed to simulate the system dynamics. Two kinds of simulation files are developed according to different requirements on simulation details. First a linear Simulink model is developed according to theoretical analysis; then a SimMechanics model is created based on the information in the CAD file. In both model disturbances from lower frame are imposed to test the systems capability of reducing vibration.

3.10.1 Simulink model

Based on the system dynamic analysis, a Simulink model is developed to simulate the behaviour of closed-loop system. For hydraulic system, if the valve is closed then the upper frame should have the same motion as lower frame. So in this simulation the acceleration of lower frame is fed into the upper frame as disturbance, which represent the upper frame will follow the motion of upper frame if there's no action from the valve. In Figure 3.5 the angular position of upper frame and lower frame are totally overlapped, which indicate this simulation method reflect the correct property of hydraulic system.

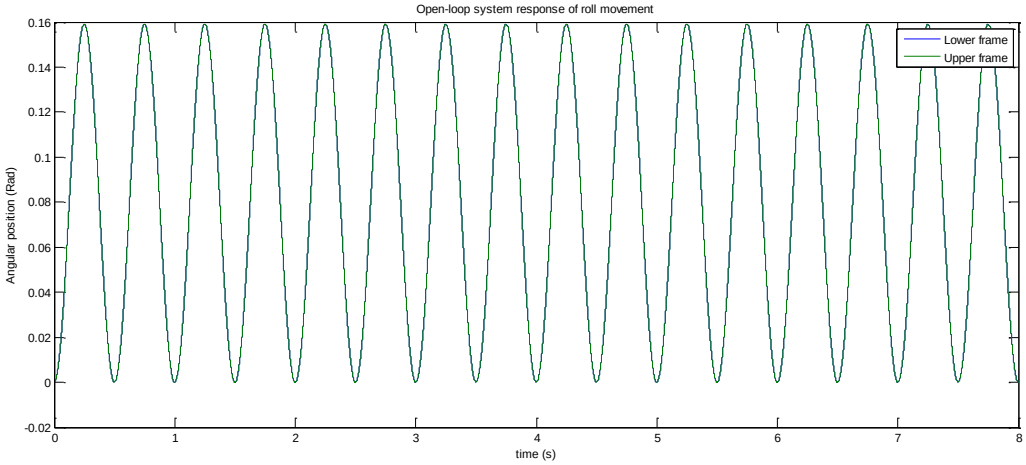

Figure 3.5 Open-loop system response of roll movement of Simulink model

3.10.2 SimMechanics model

The SimMechanics model are able to simulated detailed system properties of the suspension system; besides its another advantage is that, as stated before, the model can be automatically generated by some CAD software, and the "SimMechanics Link" function in Creo Elements is used in this work. In the CAD file of Creo Elements, some constraints are predefined. The rubber bushings and the joints on hydraulic cylinder are considered as point alignments; and the surfaces between hydraulic cylinders and pistons are defined as mates. Then a rough SimMechanics model will be generated, and its mass properties should be modified according to the steel density ($7.85\ g/cm^3$ in this case).

Another adjustment need to make is the joints of rubber bushings. These constrains in the auto-generated file are "Spherical" which cannot connect with springs and dampers. In this case spherical blocks are replaced by gimbal blocks which give three rotational DOF.

One important issue about SimMechanics model needs to be noticed is about the joint actuators. Generally speaking the motion generation of joint actuators needs three inputs: position, velocity and acceleration. But in this simulation file the hydraulic cylinders are only considered as ideal force inputs, this means the motion of roll and pitch are almost isolated from lower frame. In order to simulate the hydraulic property stated before, some modification need to be made here. It is found that if only position and veocity signal is given to the lower frame, the motion of upper frame is almost same as the lower frame. So in this case the only position and veocity signal are connected with the joint actuator between lower frame and ground. Furthermore in order to avoid accumulation error, the rotation matrix output from body sensor is select to observe the angular position in earth frame.
Figure 3.6 shows the system response when the valve is closed. It could be seen that the upper frame almost follow the motion of lower frame except a little drift. And Figure 3.7 shows the heave motion of the open-loop system which also correctly reflects the property of hydraulic

system. Please notice that the verification of a certain DOF (e.g. roll movement) is based on the stabilization of other degree of freedom.

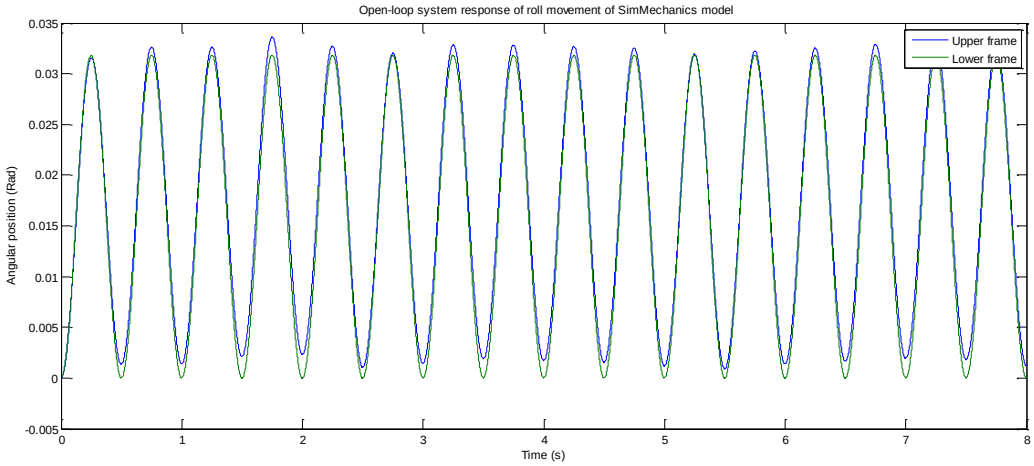

Figure 3.6 Open-loop system response of roll movement of SimMechanics model

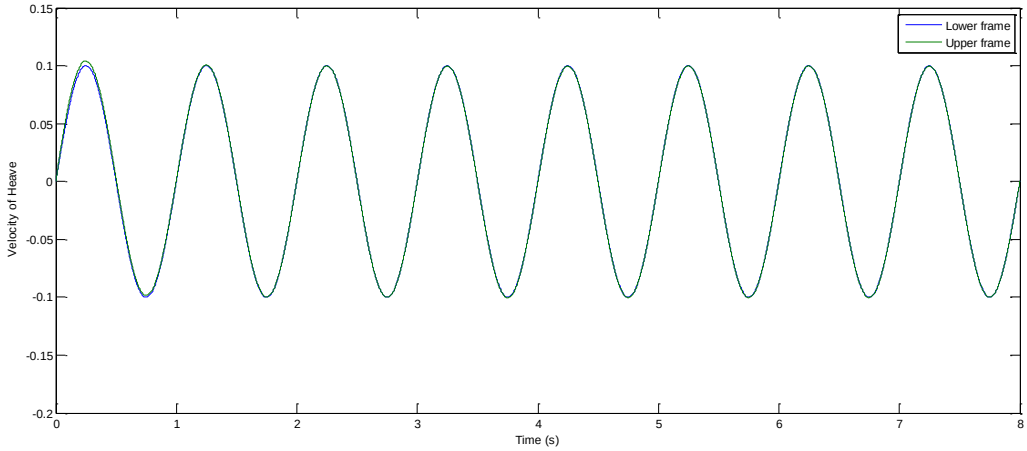

Figure 3.7 Open-loop system response of heave movement of SimMechanics model

3.10.3 Comparison of SimMechanics model and Simulink model

The figures below show the comparison of the Simulink and SimMechanics simulation. The inputs of the verification cases are 0.5 Hz, 1 Hz, 2 Hz and 3 Hz respectively. The amplitude of input for roll and pitch are 15 Nm and the input for the heave motion is 10 N. These frequency areas are chosen because they are interested in the further control design. Generally speaking, the result of Simulink fit the detailed SimMechanics simulation.

The figure 3.8 and figure 3.9 shows the comparison of roll and pitch motion in the two different models. With input of 0.5 Hz and 1 Hz, the angular position outputs are almost the same, which indicate high similarity of the two models. With input of 2 Hz and 3 Hz, there exist certain drift between the output of two model, however the amplitude and phase are quite similar, so Simulink model is accurate enough to represent the property of system.

For the model verification of heave motion, an adjustment is made here. Due to the effect of gravity, the cylinder can easily exceed its stroke limitation with sine wave input. So in both models the effect of gravity is compensated. In Figure 3.10, it could be seen that with 0.5 Hz input, there is a low frequency model error of the Simulink model. This is because in the low frequency domain, the gain of the system is large. When the amplitude of heave displacement is big, the torsion of rubber bushing caused by heave movement cannot be ignored. However,

except the low frequency component, the amplitude and phase of the fluctuation around $0.5Hz$ are quite similar.

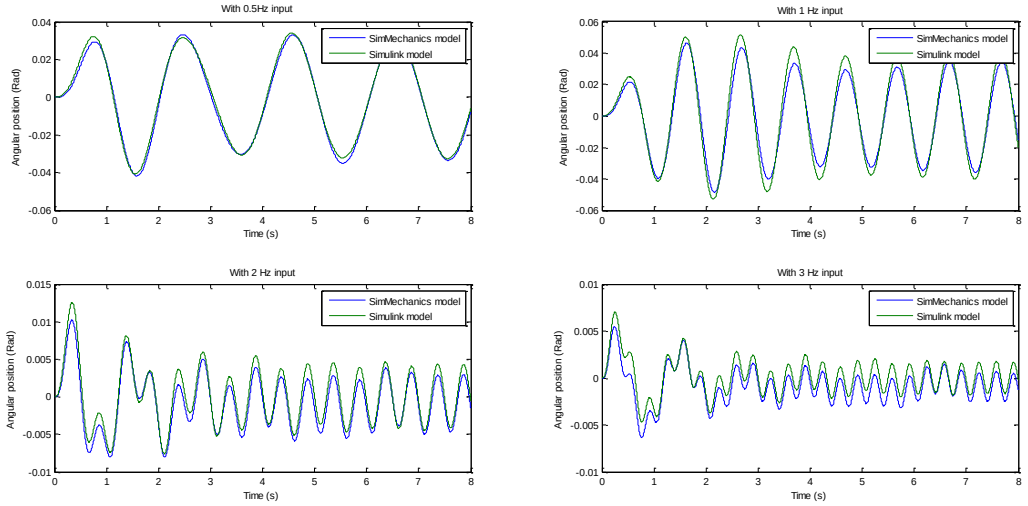

Figure 3.8 Comparison of Simulink and SimMechanics model of roll movement

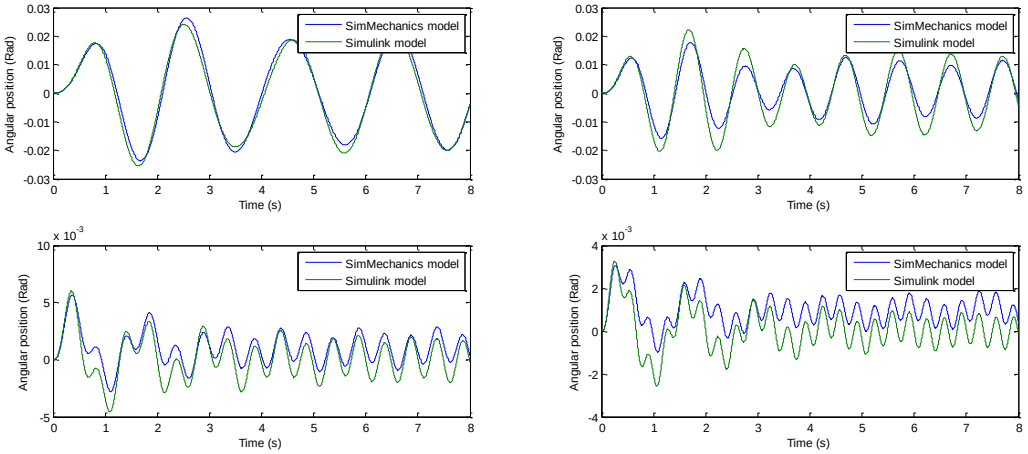

Figure 3.9 Comparison of Simulink and SimMechanics model of pitch movement

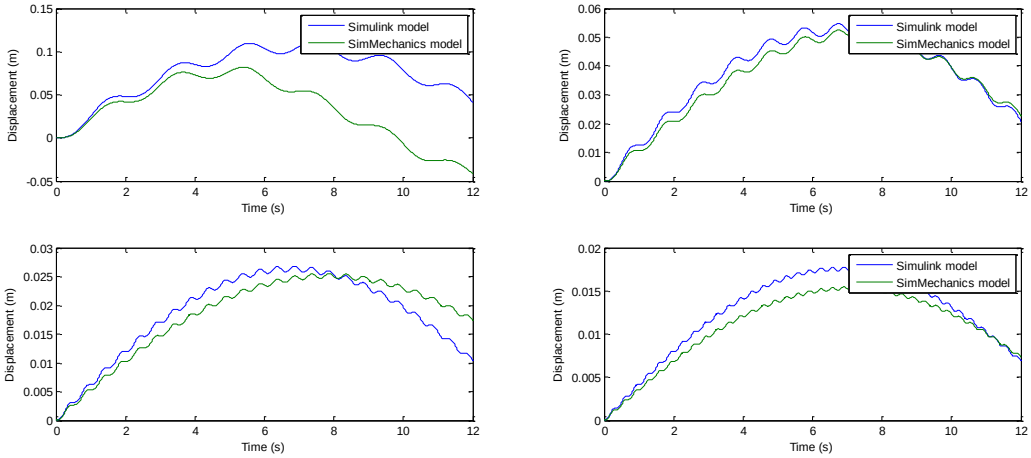

Figure 3.10 Comparison of Simulink and SimMechanics model of heave movement

4. CONTROL DESIGN OF MECHANICAL SYSTEM

This chapter introduces the method of control design of mechanical system. At beginning a quadratic programming algorithm is developed to optimally allocate control efforts for the over-actuated system. Then the control design of roll and pitch for mechanical system is analyzed, based on the desired frequency response the controllers are designed with two different control strategies. In the end, the controller for heave motion is discussed separately.

4.1 Control allocation of over-actuated system

As stated before, the suspension system is an over-actuated system which has three outputs and four inputs, in order to make the control system work optimally, an algorithm should be developed to allocate the control efforts. The relationship between cylinder forces and inputs to upper frame (Equation 3.18) could be reformulated into Equation 4.1. The matrix $\mathrm{A_{eq}}$ is calculated based on the kinematic and dynamic analysis, representing the relationship between the cylinder forces and the net torques and forces imposed on the upper frame; B_{eq} indicating the desired control efforts which are calculated by the outer-loop controller, and vector x is desired force from each cylinder.

$$\mathrm{A_{eq}}x = B_{eq} \tag{4.1}$$

in which

$$x = [\,\mathrm{F_{c1}} \quad \mathrm{F_{c2}} \quad \mathrm{F_{c3}} \quad \mathrm{F_{c4}}]^T$$

$$\mathrm{A_{eq}} = \begin{bmatrix} a_{11} & a_{12} & a_{13} & a_{14} \\ a_{21} & a_{22} & a_{23} & a_{24} \\ a_{31} & a_{32} & a_{33} & a_{34} \end{bmatrix}$$

$$B_{eq} = \begin{bmatrix} U_z & U_\phi & U_\theta \end{bmatrix}^T$$

In the equations 4.1, the input matrix $\mathrm{A_{eq}}$ has three rows and four columns, which means for a certain desired B_{eq} there are infinite combinations of $\mathrm{F_{c1}}, \mathrm{F_{c2}}, \mathrm{F_{c3}}, \mathrm{F_{c4}}$. So the objective of the control allocation module is to calculate the optimal solution which requires least energy from the hydraulic system to achieve certain net torque and net forces, and the objective function is defined as below.

$$J = \mathrm{F_{c1}^2} + \mathrm{F_{c2}^2} + \mathrm{F_{c3}^2} + \mathrm{F_{c4}^2} \tag{4.2}$$

In this case, the Equation 3.18 gives the elements of $\mathrm{A_{eq}}$ equalities of

$$a_{11} = a_{12} = a_{13} = a_{14} = 1$$

$$a_{21} = a_{23} = -l_{w1}\cos\phi_\delta\cos\theta_\delta\,,\ a_{22} = a_{24} = l_{w2}\cos\phi_\delta\cos\theta_\delta \tag{4.3}$$

$$a_{31} = a_{32} = \mathrm{l_{l1}}\cos\phi_\delta\cos\theta_\delta\,,\ a_{33} = a_{34} = -\mathrm{l_{l2}}\cos\phi_\delta\cos\theta_\delta$$

4.1.1 A standard solution

In the reference a standard solution is given. Quadratic programming problem

$$\min \mathrm{u^T W u}$$

$$\mathrm{s.t.\ v = Bu} \tag{4.4}$$

is solved by

$$\mathrm{u = WB^T(BWB)^{-1}v} \tag{4.5}$$

where W is a symmetric positive definite weighting matrix, $B \in R^{k\times m}$ is a factorization of B_u , named as control effectiveness matrix, i.e. $B_u = B_v B$.[7]

4.1.2 A simplified algorithm

The method stated above provides a universal solution of control allocation for over-actuated systems. But it could be seen that the solution requires seven matrix operations and one of them is matrix inverse operation. For a normal microcontroller these 4×4 matrix operations will occupy lots of computation load which causes large time delay. However in this special implementation, the equality relationship (4.3) among the elements of A_{eq} gives an opportunity to simplify the algorithm.

This simplification method utilized the concept of "line" in n-dimensional hyperspace. A one-dimension subspace could be interpreted as a line in n-dimensional hyperspace. In this case A_{eq} is a 3×4 matrix with the rank of 3, which means $A_{eq}$is a one-dimension subspace of R^4, so it could be considered as a line in 4-dimensional space. Accordingly, the problem of minimizing the objective J can be formulated as "finding the point p, on the line l defined by A_{eq}, which has the closest distance to the origin". And the point p turns out to be the intersection of the line l and a line which across the origin and perpendicular to l.

It can be proved that the direction vector of the line l defined by A_{eq} is

$$D = (d_1, d_2, d_3, d_4)^T \tag{4.6}$$

where

$$d_1 = \begin{vmatrix} a_{12} & a_{13} & a_{14} \\ a_{22} & a_{23} & a_{24} \\ a_{32} & a_{33} & a_{34} \end{vmatrix}, d_2 = -\begin{vmatrix} a_{11} & a_{13} & a_{14} \\ a_{21} & a_{23} & a_{24} \\ a_{31} & a_{33} & a_{34} \end{vmatrix}$$

$$d_3 = \begin{vmatrix} a_{11} & a_{12} & a_{14} \\ a_{21} & a_{22} & a_{24} \\ a_{31} & a_{32} & a_{34} \end{vmatrix}, d_4 = -\begin{vmatrix} a_{11} & a_{12} & a_{13} \\ a_{21} & a_{22} & a_{23} \\ a_{31} & a_{32} & a_{33} \end{vmatrix}$$

So the desired point p can be determined by equations

$$\begin{aligned} d_1 F_{c1} + d_2 F_{c2} + d_3 F_{c3} + d_4 F_{c4} &= 0 \\ a_{11} F_{c1} + a_{12} F_{c2} + a_{13} F_{c3} + a_{14} F_{c4} &= U_z \\ a_{21} F_{c1} + a_{22} F_{c2} + a_{23} F_{c3} + a_{24} F_{c4} &= U_\phi \\ a_{31} F_{c1} + a_{32} F_{c2} + a_{33} F_{c3} + a_{34} F_{c4} &= U_\theta \end{aligned} \tag{4.7}$$

When substitute $a_{11}, a_{12} \ldots a_{34}$ in to d_1, d_2, d_3, d_4, due to equality of (4.3), the direction vector has the property equality of (4.8)

$$d_1 = d_4 = -d_2 = -d_3 = a_{11}a_{21}a_{33} - a_{11}a_{22}a_{33} + a_{31}a_{13}a_{22} - a_{31}a_{21}a_{13} \tag{4.8}$$

And the previous equations became

$$\begin{aligned} F_{c1} - F_{c2} - F_{c3} + F_{c4} &= 0 \\ a_{11} F_{c1} + a_{12} F_{c2} + a_{13} F_{c3} + a_{14} F_{c4} &= U_z \\ a_{21} F_{c1} + a_{22} F_{c2} + a_{23} F_{c3} + a_{24} F_{c4} &= U_\phi \\ a_{31} F_{c1} + a_{32} F_{c2} + a_{33} F_{c3} + a_{34} F_{c4} &= U_\theta \end{aligned}$$

So the optimal solution can be achieved by

$$x_{qp} = A_1^{-1} B_1 \tag{4.9}$$

where

$$A_1 = \begin{bmatrix} 1 & -1 & -1 & 1 \\ a_{11} & a_{12} & a_{13} & a_{14} \\ a_{21} & a_{22} & a_{23} & a_{24} \\ a_{31} & a_{32} & a_{33} & a_{34} \end{bmatrix}, B_1 = \begin{bmatrix} 0 \; U_z \; U_\phi \; U_\theta \end{bmatrix}^T$$

4.1.3 Algorithm comparison and implementation issue

The equations above gives a mathematical proof of the improved algorithm, then a small test is made to test its performance. In this case the algorithm above is compared with MATLAB function "quadprog". The MATLAB function "quadprog" is the standard function to solve the universal quadratic programming problem; unfortunately its computation load is so large that is not suitable to be implemented in any real-time system. In this test B_{eq} is created by some random sinusoidal wave and the output is optimized output vector x. The figure below shows the comparison of these two algorithms, it could be seen that these two 4-dimensional signals are totally overlapped, this means the simplified algorithm has the same calculation results as the standard MATLAB function. So based on previous mathematic proof and the real-time test, the functionality of the simplified algorithm is verified.

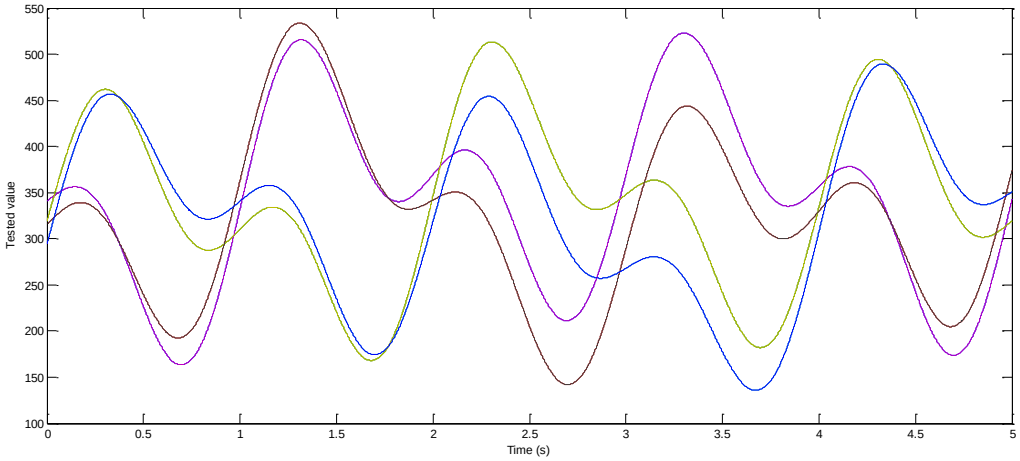

Figure 4.1 Comparison of new algorithm with MATLAB standard function

Even though the algorithm is already simplified, attentions should also be paid to the computation load and time delay. Since the dSPACE will be utilized in control prototype, the C code is auto generated by MATLAB. However the function of matrix inversion has more than one hundred lines of code where involve several loops of iterations and the variables are defined as float. But the microcontroller provided by Komatsu is fix-point based, so the computation time of the matrix inversion might be long.

In order to reduce the computation load, the inverse of matrix could be pre-calculated with symbols, due to the equality of (4.3), the complexity of pre-calculated coefficients is much less than a normal matrix. Then during the real-time computation the microcontroller just need to calculate the values of these coefficients with fixed point data type.

The matrix inverse pre-calculation based on symbols is showed in the equations below,

$$A_1^{-1} = \begin{pmatrix} \frac{1}{4} & -\frac{c_2}{4c_1} & c_6 & c_7 \\ -\frac{1}{4} & \frac{c_3}{4c_1} & -c_6 & c_7 \\ -\frac{1}{4} & \frac{c_4}{4c_1} & c_6 & -c_7 \\ \frac{1}{4} & \frac{c_5}{4c_1} & -c_6 & -c_7 \end{pmatrix} \tag{4.10}$$

And the optimized forces could be calculated as

$$\begin{aligned} \mathrm{F_{c1}} &= -\frac{c_2}{4c_1} U_z - c_6 U_\phi + c_7 U_\theta \\ \mathrm{F_{c2}} &= \frac{c_3}{4c_1} U_z + c_6 U_\phi + c_7 U_\theta \\ \mathrm{F_{c3}} &= \frac{c_4}{4c_1} U_z + c_6 U_\phi - c_7 U_\theta \\ \mathrm{F_{c4}} &= \frac{c_5}{4c_1} U_z + c_6 U_\phi - c_7 U_\theta \end{aligned} \tag{4.11}$$

in which

$$\begin{aligned} c_1 &= -a_{21}\, a_{32} + a_{22}\, a32 - a31\, a22 + a31\, a21 \\ c_2 &= a21\, a32 - 3\, a22\, a32 + a31\, a22 + a31\, a21 \\ c_3 &= -3\, a21\, a32 + a22\, a32 + a31\, a22 + a31\, a21 \\ c_4 &= a22\, a32 - 3\, a31\, a22 + a21\, a32 + a31\, a21 \\ c_5 &= -a22\, a32 + 3\, a31\, a21 - a21\, a32 - a31\, a22 \end{aligned}$$

$$c_6 = \frac{1}{2\,(-a22 + a21)}\,,\; c_7 = \frac{1}{2\,(-a32 + a31)}$$

4.2 Roll and Pitch controller

This part of thesis introduces the design process of outer-loop controller which regulates the roll and pitch movement of mechanical system. Since cascaded control structure is adopted in this work, the outer-loop control design is based on the assumption that inner-loop can provide the desired control input. In the beginning, the controller is designed based on the system without the cabin; when the control design is finished and tuned, the system including the cabin will be analyzed, and the previous control method will be adjusted according to the additional dynamic property of cabin.

4.2.1 General introduction and ideal response analysis

As stated before the main trade off of the active suspension system is the ride comfort and suspension deflection. Since the off-road vehicles works in very bumpy ground, the stroke of cylinders should be used efficiently. In order to optimize the control design the ideal frequency response is developed here.

For the low-frequency area which below 1 Hz, the amplitude of road fluctuation is very large, it could be intuitively explained as large slope or ramp. According to the system requirement, this frequency area is not interested also vibration reduction will occupy large portion of cylinder stroke, so the gain of system should be close to one, which means the motion cabin should

follow the ground fluctuation. Due to the same reason the phase lag, which cause suspension deflection but won't reduce any vibration, should be also minimized.

The system gain between 1 Hz and 3 Hz should be as small as possible since it is the most interested frequency area. Besides the amplitude of vibration is relatively small thus the side-effect of phase lag is not large and stroke of cylinder will be used efficiently. So within this area the controller should reduce the vibration significantly.

The frequency area between 3 Hz and 5 Hz is also important. But due to the limitation of the dynamic of hydraulic system, the outer-loop controller, which should at least 5 times slower than the hydraulic controller, is not fast enough to handle the frequency domain larger than 3 Hz (Chapter 2.5). So the gain of this area will be close to one. Since the controller is not able to reduce the vibration in this area, any phase lag in this frequency area is waste of energy and cylinder stroke, so the phase lag should also be minimized.

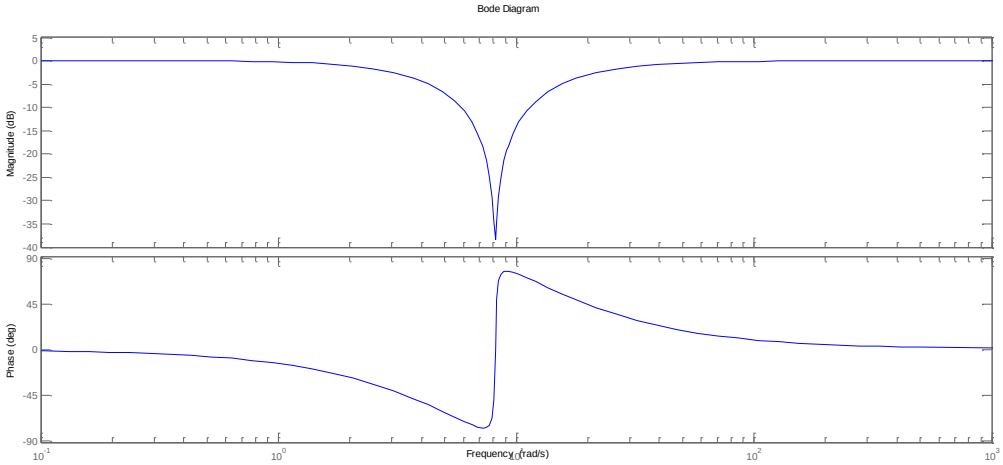

Figure 4.2 Ideal frequency response from disturbance to the motion of upper frame

According to previous analysis the ideal frequency response is given in the Figure 4.2. The Bode diagram above shows the general idea of required response from disturbance of ground to the motion of upper frame. So the controller should modify the system dynamic property according to this frequency response. Please notice that the order of actual closed-loop system response will be high and this figure, which created based on a second order system, only shows a general idea of it.

In this work several control strategy are developed and their performances is compared and analyzed. At first, based on the system without cabin, a control system consists of an outer-loop controller which stabilizing upper frame, and four cylinder stroke feedback controllers which limit cylinder stroke in low frequency area are developed. Then based on the model including the cabin, an outer-loop controller and a state feedback of angular difference, which has similar function of the stroke feedback, are designed to achieve satisfactory performance.

4.2.2 Control design based on the system without cabin

The Figure 4.3 shows the control strategy of the suspension system without the passenger cabin. This control strategy consists of an outer-loop controller and four cylinder stroke feedback controllers. The outer-loop controller will stabilize upper frame and attenuate the disturbance in the "interested" frequency area, and its reference signal is the "slow and large motion" of the vibration; while the four cylinder stroke feedback controllers, which reference signal is the center position of the stroke, will limit cylinder stroke in the low, "not interested" frequency domain.

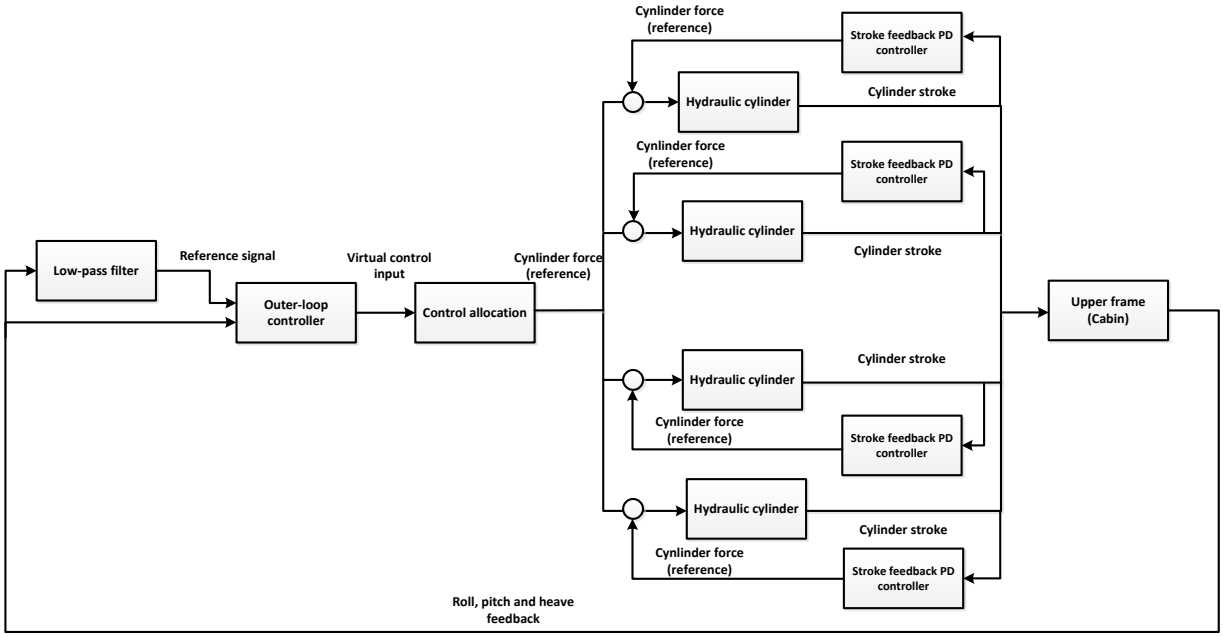

Figure 4.3 control strategy of system without cabin

As discussed in the previous chapter the coupling between roll and pitch are quite small so they can be handled as two single-DOF controller. Here the roll controller is taken as an example. First the Outer-loop sPID controller to reduce the disturbance for the upper frame is derived based on part of the model

$$\dot{\phi_e^u} = r_b^u \tag{4.12}$$

$$\dot{r_b^u} = I_2 U_\phi \tag{4.13}$$

In this case the transfer function is

$$G_{roll} = \frac{0.03782}{s^2} \tag{4.14}$$

In this model the torque generated by rubber bushings is considered as unmodeled dynamic. The input of this single DOF subsystem is the net torque and the output is the roll angle. The bandwidth of the outer-loop controller is constrained by the inner-loop controller. According to the rule of thumb of cascaded control strategy, the outer-loop controller should be at least 5 times slower than the inner-loop controller. In this work, the bandwidth of inner-loop controller is around $15\,Hz$ (detailed introduced in Chapter 5), so the bandwidth of outer-loop controller should be around $15\ \mathrm{rad/s}$. Also its input for step response should be smooth enough for the inner loop controller to provide; besides system's overshoot should be less than 5% which indicate a well damped system. Last not least the output disturbance should be as small as possible. Considering the rising time and the computation load of control allocation module, the sampling time is selected as 0.02s and the Euler backward method is adopted to discretize the controller. The dynamic property of discretized closed-loop system is shown in the table below

Rise time	0.1 second
Settling time	1.7 second
Overshoot	3.91 %
Peak	1.04
Gain margin	17.4 at 65.9
Phase margin	68 at 13.1
Closed-loop stability	stable

Table 4.1 Index of PID controller for roll movement

For some regular controller designs, the performance of reference following have highest priority during the design process, however in this case the sensitivity function, which indicate the capability of vibration attenuation, is more important. So the frequency response of sensitivity function is showed in the figure below. It could be seen that the system have significant capability to reduce the vibration at the frequency area below 1.5 Hz.

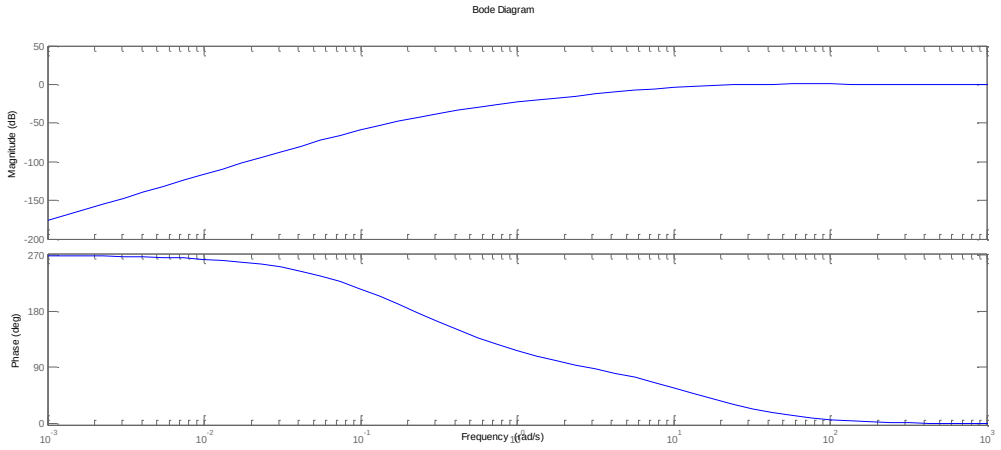

Figure 4.4 Sensitivity function of the closed-loop system of roll movement

The controller which stabilized pitch movement could also be delivered following the same method and discretized with same sampling period of 0.02s, the dynamic property of closed-loop system is shown is the table below

Rise time	0.1 second
Settling time	1.6 second
Overshoot	2.87 %
Peak	1.03
Gain margin	18.4 at 65
Phase margin	70 at 11.8
Closed-loop stability	Stable

Table 4.2 Index of PID controller for pitch movement

In order to use the stroke of suspension more efficiently, the reference signal of this outer-loop controller is set as the low frequency motion of the lower frame; this means that the upper frame should follow the slow and large fluctuation of ground. In this case the measurement of lower frame is connected with upper frame with a first-order low-pass filter between them. The

bandwidth of this filter should be small enough to filter out the high frequency components, but the phase lag should not be large in order to guarantee the suspension won't waste much stroke for slow vibration.

The functionality of this outer-loop PID controller is to stabilize the roll and pitch of upper frame and reduce the vibration. But in the low frequency domain the suspension deflection will be high which will use most of the stroke of hydraulic cylinder. So this controller could guarantee the stability of system and the attenuation of the vibration, but stroke of cylinder is not efficiently used.

In order to give some constraint on the suspension deflection four stroke feedback PD controllers are implemented at each cylinder (Figure 4.3), these controllers use the feedback of cylinder position and generate force towards to the center of the stroke, and the reference of these controllers are the center position of the hydraulic cylinders. This idea comes from some passive suspension designs which use mechanical springs and dampers to guarantee the road holding of vehicle. The advantages of designing a stroke feedback PD controller, "digital spring and damper", is that the feedback is totally linear which reduce the system complexity and it is easier to tune the parameters.

In this design one of the important goals is to use as less cylinder stroke as possible in very low frequency domain, this means the bandwidth of the PD controller should be larger than 0.5 Hz so the stroke of the cylinder will follow the potential reference, the center position of cylinder, in this frequency area. However since the system is over-actuated, it is impossible to derive the model of cylinders which include the dynamic the upper frame, the value of P and D are manually chosen by experiences which give satisfactory performance. At the same time a low-pass filter on the D part is implemented which make this controller would affect the high frequency property too much.

The figure below shows the system response of roll movement with input to lower frame at $0.5\,Hz$, $2Hz$ and $3\,Hz$. It could be seen that around $2\,Hz$ the suspension has the best performance of disturbance attenuation, when it comes to $0.5\,Hz$ the motion of upper frame will almost follow the movement of lower frame; due to the bandwidth limitation the vibration could not be significantly reduced in high frequency domain.

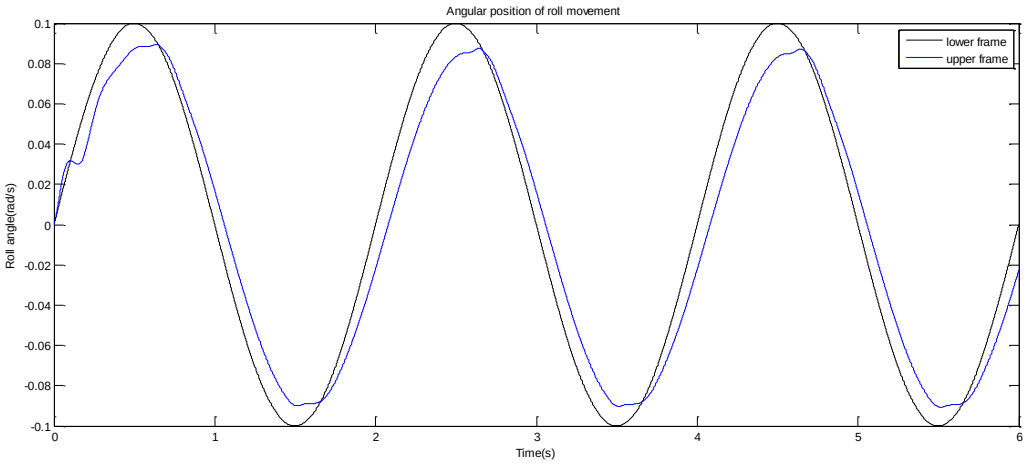

Figure 4.5 Response of roll movement at 0.5 Hz

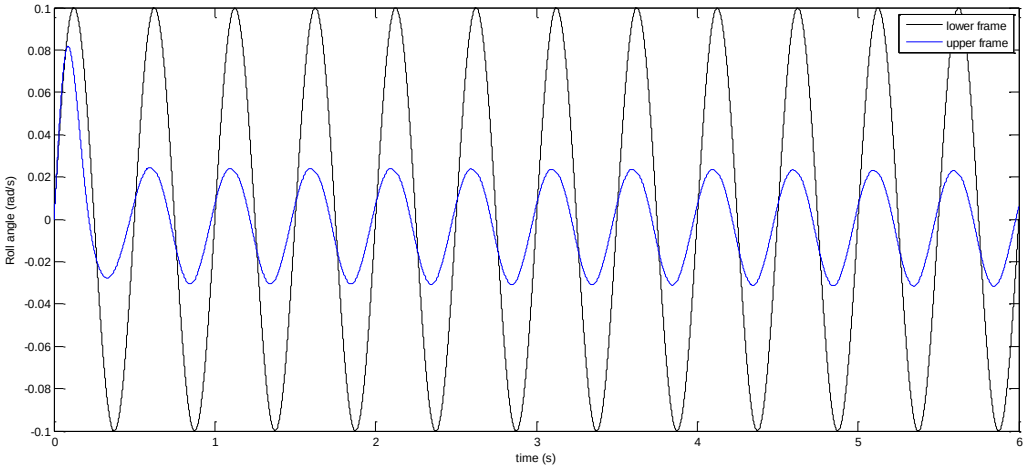

Figure 4.6 Response of roll movement at 2 Hz

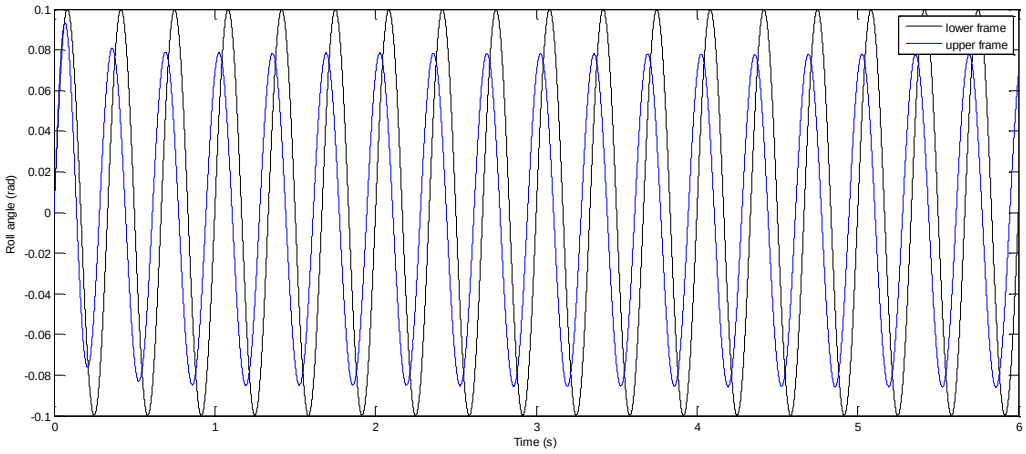

Figure 4.7 Response of roll movement at 3 Hz

This method is more suitable for the system without the cabin. However when it comes to the system including the passenger cabin this method is not suitable anymore due to the power efficiency issue. The effect of these stroke feedback controllers actually is giving feedback of the angular differences. In another word, any cylinder force directly imposed on the upper frame could be interpreted as a net force and net torques (Equation 3.18). For this over-actuated system, the forces generated by these cylinder stroke feedback controller will influence the system in the form of net forces and net torque; however these force don't go through the control allocation module which optimize the square sum of the forces (see Figure 4.3). This means to achieve same control effect this form of control system consume more force than the one which all the desired net torque and net force are optimally allocated. So in the later discussion, this problem is solved by another method implemented on the system including the cabin.

4.2.3 Control design based on the system including the passenger cabin

The control design of the system including the cabin is similar to the previous case. Similar to the previous case an outer-loop PID controller is designed to stabilize the upper frame, and the sampling time is also 0.02s; nevertheless a feedback of the angular difference between upper and lower frame is introduced in this case (Figure 4.8). The design method and performance requirement of the outer-loop controller is same as the case without cabin. However instead of give direct constraint to the stroke of cylinder, the angular difference feedback is designed to have the same functionality. In another word, the angular difference feedback should give the

same net torque as previous stroke feedback imposed on the passenger cabin. So in this case all the control efforts are allocated by the quadratic programming algorithm which optimizes the power consumption.

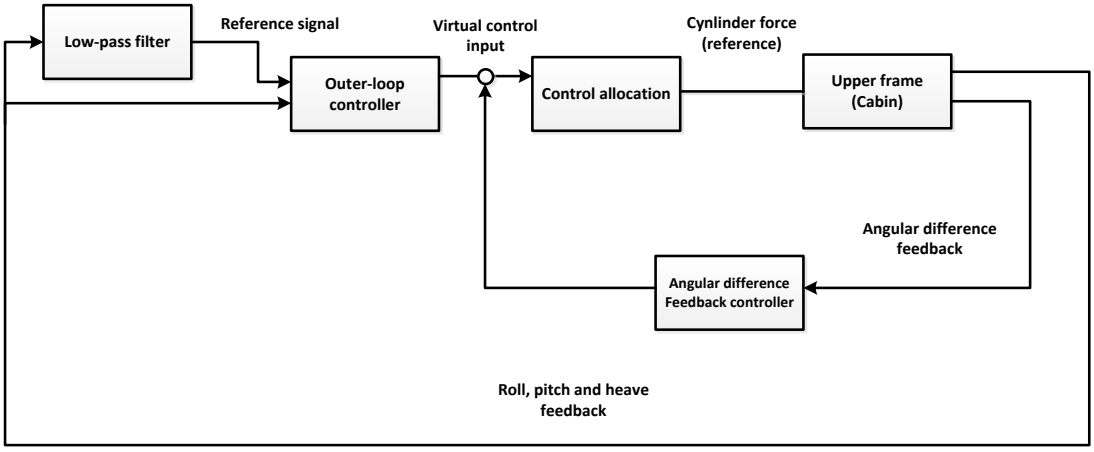

Figure 4.8 control strategy of system including the passenger cabin

In order to follow the slow motion of lower frame, the reference signal for the PID controller is also generated from the measurement of lower frame connected with a low-pass filter. Same as previous case, the filter should filter out the high frequency components and preserve the low frequency component. It could be estimated that a filter with smaller bandwidth will introduce phase lag at lower frequency domain; but a larger bandwidth will decrease the capability of vibration attenuation of higher frequency. So in this case the low-pass filter is tuned such that the system has small phase lag between 0.1 Hz to 1 Hz, as well as has acceptable response at higher frequency area.

The figure below shows the frequency response at 0.5 Hz, 2Hz and 3 Hz. It could be seen that the system with the cabin has similar property as previous case, except a larger gain at 2Hz. The reason is that the controller is designed conservatively considering the extremely heavy cabin. Even all control efforts are optimized allocated, the force required from hydraulic cylinders are still very high. It could be estimated that when pressure is high, the control precision and fastness will lost. In the simulation a more aggressive controller does show better performance but in practice it will be problematic and is not recommended here.

The design of pitch controller follows exactly method and procedure, which lead to the same frequency response.

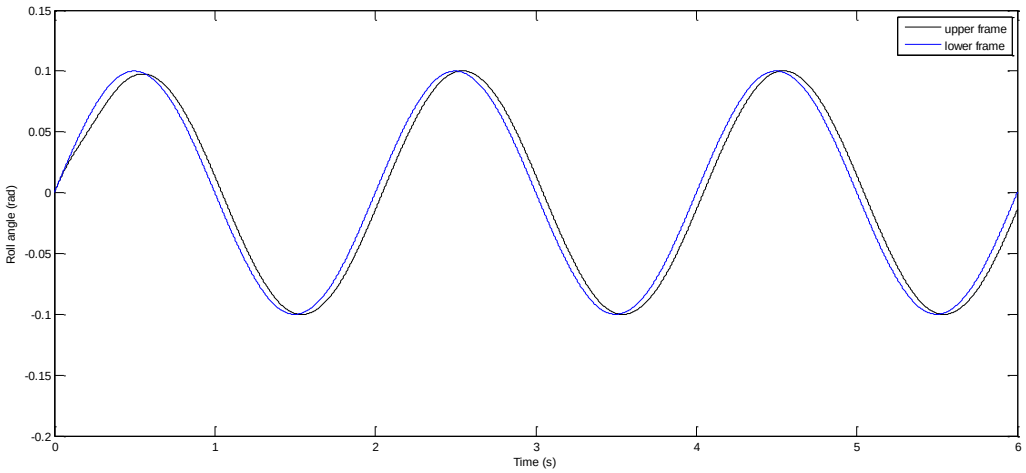

Figure 4.9 Response of roll movement at 0.5 Hz

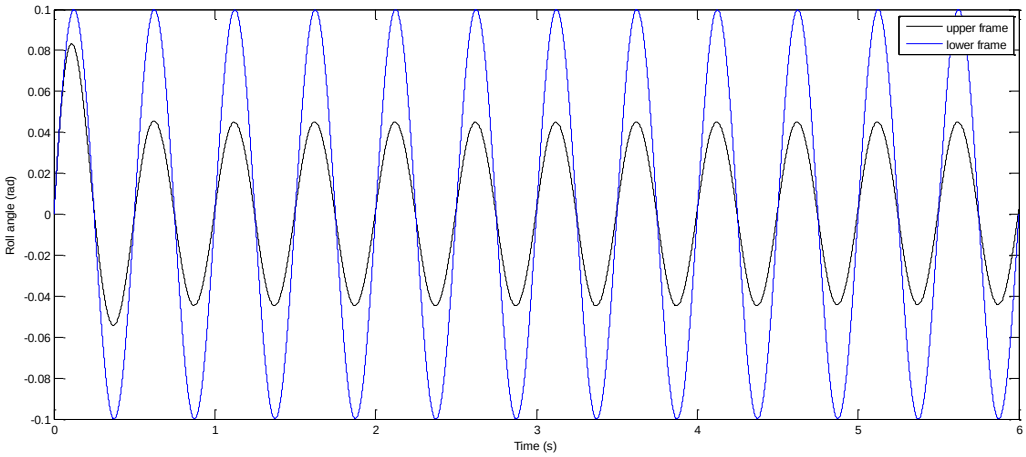

Figure 4.10 Response of roll movement at 2 Hz

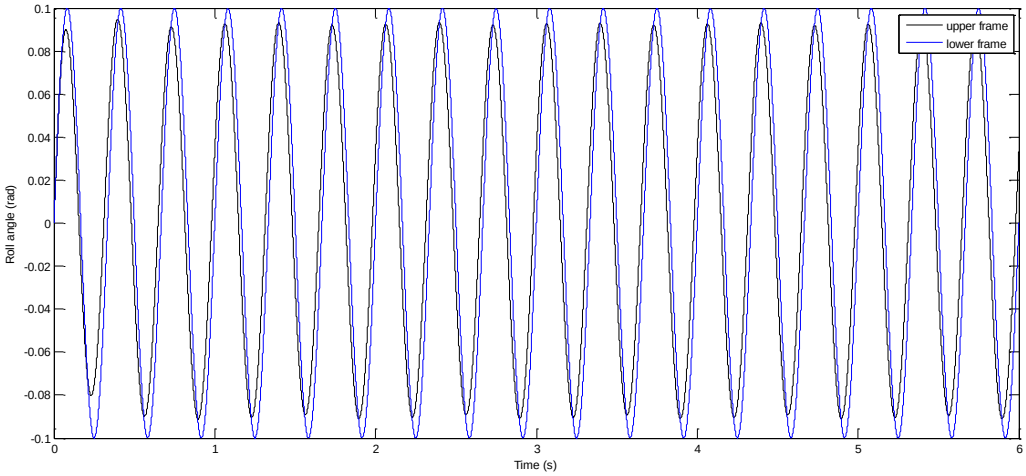

Figure 4.11 Response of roll movement at 3 Hz

4.3 Heave controller

Attenuating the vibration in heave direction is also an important goal for this thesis. However there is no suitable sensor which can detect the height in the inertial earth frame for this application. The sensors like sonar and infrared sensors could detect the distance between objects; in this case the only reference they can take is the ground, but the shape of ground is also a major source of vibration. Accordingly there are two options for this case

(1) Selecting sensors like sonar or infrared sensors to detect the height with regard to the ground, in this case the active suspension could only deal with the vibration introduced by the roughness of ground;
(2) Control the height between two frames using the average of cylinder length as a measurement. In order to reduce the vibration, the velocity is used to generate the reference which has the opposite direction towards to vibration;

In this work the second method is chosen in this thesis. The reason is that for off-road vehicle, handling the vibration imposed the fluctuation of ground is more important than dealing with vibration introduced by the roughness of ground. Also with a suitable PID value and well-tuned reference signal, the controller could achieve satisfactory performance.

The model in body-fixed reference frame (only considering the distance and velocity comparing to the lower frame) is

$$G_p = \frac{1}{ms^2} \tag{4.15}$$

The bandwidth, sampling time and other controller index choice are similar to the cases before. Besides the nonlinearity and system coupling which introduced by the dynamic of cabin should be compensated here. The controller parameter is showed in the table below.

Rise time	0.14 second
Settling time	2 second
Overshoot	4.56 %
Peak	1.05
Gain margin	18 at 82.8
Phase margin	75 at 11.4
Closed-loop stability	stable

Table 4.3 Index of PID controller for heave movement

Then reference signal should be generated based on the velocity of cabin. In this case an accelerometer is used to estimate velocity, so a band-pass filter should be implemented to filter out the slow component which created by error accumulations, as well as very high frequency which the controller is not fast enough to make proper reaction. The figure below shows the response of heave controller when the vibration is $0.5Hz$, $2Hz$ and $4Hz$.

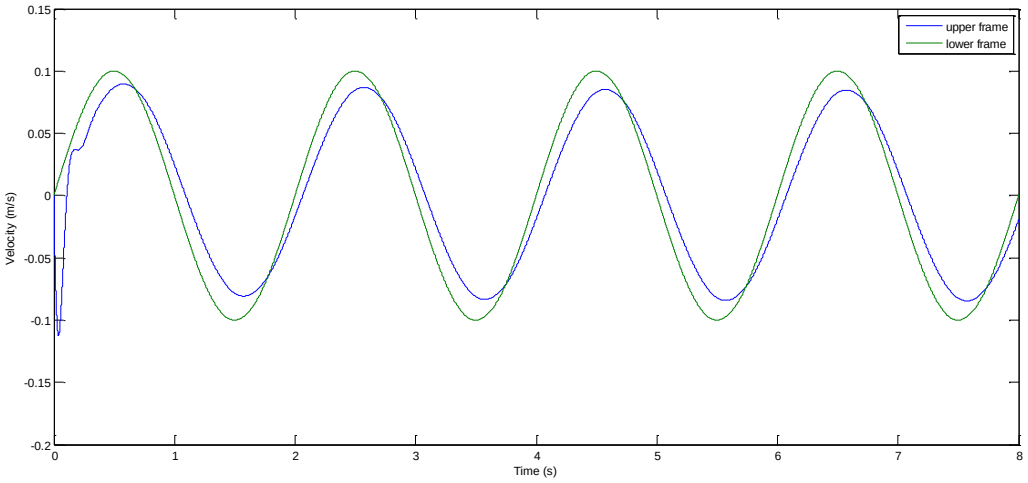

Figure 4.11 Heave response at 0.5 Hz

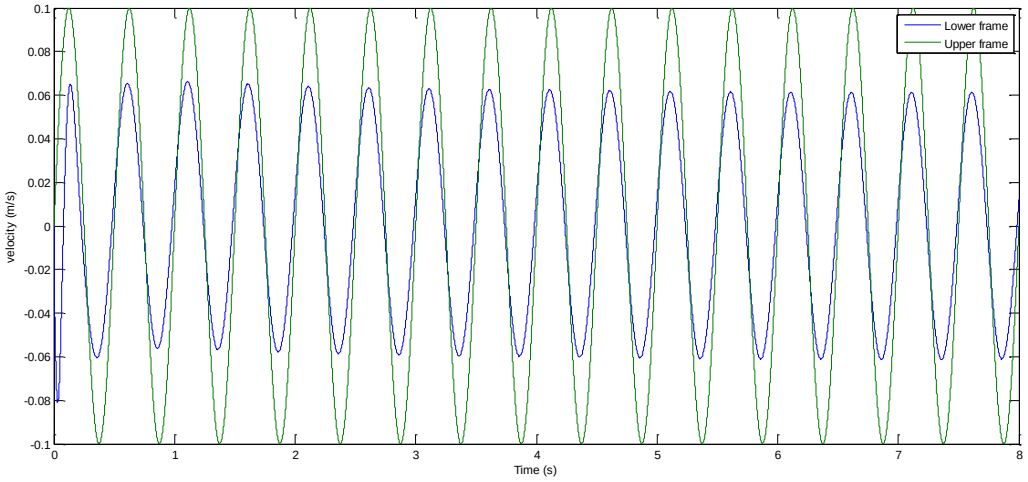

Figure 4.12 Heave response at 2 Hz

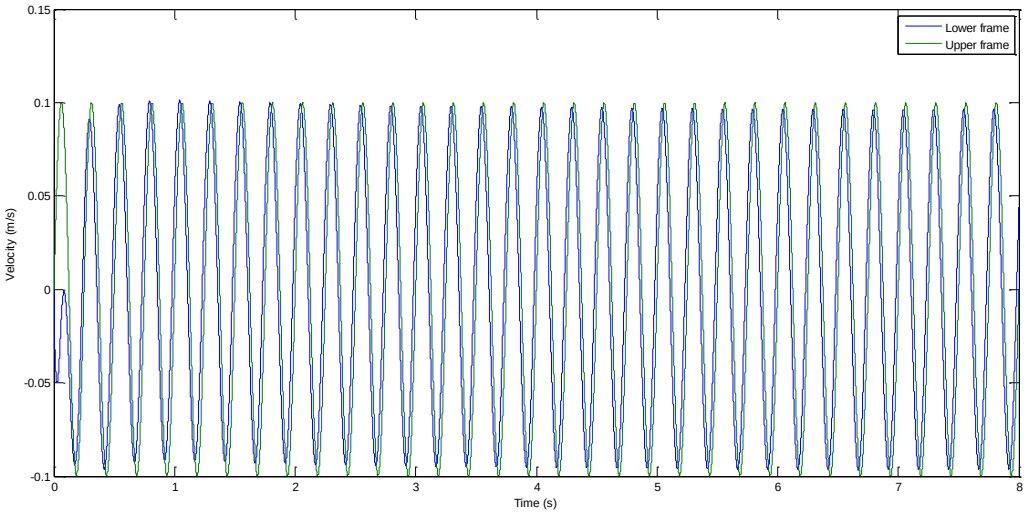

Figure 4.13 Heave response at 4 Hz

5. MODELLING, SIMULATION & CONTROL OF HYDRAULIC SYSTEM

This chapter explains the mathematical modeling, simulation and control development for the hydraulic system. The mathematical modeling includes the development of nonlinear, simplified and the linearized model of the system. The simulation results of the derived model are then compared with the SimHydraulics model and the system properties are deduced. Finally an Internal Mode Force Controller is developed to achieve the desired goal of force reference tracking.

As mentioned above a nonlinear, a simplified and a linearized model are developed in this chapter. The nonlinear model is developed to study the dynamic behavior of system and to study the effect of nonlinearity in them. The nonlinear model is then simplified because the nonlinear model developed is detailed and complex for control and diagnostic purpose. So a simplified model is developed by retaining all the dominant dynamics of the real plant. The linearized model is developed from the simplified plant model in order to develop the linear force controller.

5.1 Model development

Model Development, is a step-by-step approach for designing and developing a real time system being instrumental in studying the system and understand the effects of different components serving to predict the system behavior under different conditions.

The system is modeled with the following purposes:

1. Match the system dynamics with real system
2. Evaluate the performance of controller

The evaluation is done by simulating the nonlinear system model with the linearized controller and by assessing the performance of the closed loop system to meet the required specification.

To follow the derivations in the chapter, a naming convention and a nomenclature list has been made in the beginning of the first chapter.

5.2 Mathematical modelling

The hydraulic system consists of an asymmetric cylinder, a 4/3-way proportional valve, a tank and a variable displacement pump. The valve forms the heart of the hydraulic system that directs the flow of a liquid medium. The mathematical model is developed for a proportional valve and a asymmetric cylinder, and this valve-actuator combination is most widely used because of its compactness. In this section, the flow through the hydraulic valve and the force from the cylinder is modeled with flow equation and pressure built up equation respectively. The mathematical model is developed for the hydraulic system with the following assumptions

1. P_t and P_s are constant.
2. P_t is the tank pressure and the lowest pressure in the system and hence the flow Q_t is always positive.
3. P_s is the highest pressure in the system and hence the flow Q_s is never negative.

4. Flow through the valve ports $Q_B \; and \; Q_A$ is turbulent, so the orifice equation can be used assuming the coefficient of discharge C_D to be constant.
5. Leakage flow from valve is included.
6. Friction with in the cylinder and the mechanical system is neglected.

5.2.1Derivation

The pressure built -up in a cylinder can be expressed using the continuity equation

$$\dot{P}_A = \frac{\beta}{(V_{A0} + A_A x_{cyl})} \; (Q_A - \; \dot{x}_{cyl} A_A - Q_C) \qquad 5.1$$

$$\dot{P}_B = \frac{\beta}{(V_{B0} - A_B x_{cyl})} \; (-Q_B + \; \dot{x}_{cyl} A_B + Q_C)$$

Conferring to the principle of conservation of energy, Bernoulli found that when a liquid flows through an orifice, the square of its velocity is directly proportional to pressure differential and inversely proportional to the specific gravity of the fluid. With the existence of above proportionality, and the flow being turbulent, flow can be expressed using the orifice equation. The usage of a zero lapped spool eliminates the inclusion of leakage between the ports and deadband in the equation.

$$Q_A = C_D K_{va} \; x_v \sqrt{\frac{2}{\varrho}} \; (\sqrt{P_s - P_A}) \qquad for \; x_v \geq 0$$

$$Q_B = C_D K_{vb} x_v \sqrt{\frac{2}{\varrho}} \; (\sqrt{P_B - P_t}) \qquad 5.2$$

$$Q_A = C_D K_{va} x_v \sqrt{\frac{2}{\varrho}} \; (\sqrt{P_A - P_t}) \qquad for \; x_v < 0$$

$$Q_B = C_D K_{vb} x_v \sqrt{\frac{2}{\varrho}} \; (\sqrt{P_s - P_B})$$

$$Q_C = C_L \; (\sqrt{P_s - P_B})$$

Introducing a constant such that:

$$R_{va} = C_D K_{va} \sqrt{\frac{2}{\varrho}}$$

$$R_{vb} = C_D K_{vb} \sqrt{\frac{2}{\varrho}} \qquad 5.3$$

Substituting the above equations in the pressure build up equation, we obtain the following equations:

$$\dot{P}_A = \frac{\beta}{(V_{A0} + A_A x_{cyl})} \left(R_{va} x_v(\sqrt{P_s - P_A}) - \dot{x}_{cyl} A_A - C_L \left(\sqrt{P_A - P_B}\right)\right) \quad for\ x_v \geq 0$$

$$\dot{P}_B = \frac{\beta}{(V_{B0} - A_B x_{cyl})} \left(-R_{vb} x_v\left(\sqrt{P_B - P_t}\right) + \dot{x}_{cyl} A_B + C_L \left(\sqrt{P_A - P_B}\right)\right) \quad 5.4$$

Similarly the pressure build-up equation can be derived for $x_v < 0$.

The hydraulic pressure from the above equation is linked to the mechanical system through the force exerted by the cylinder on the mass to be displaced and is given by

$$m\,\dot{x}_{cyl} = P_A A_A - P_B A_B - f_f - f_e \quad 5.5$$

5.2.2 Valve model

Installation drawing of the valve is given in Figure 5.1 is taken from the valve data sheet. It is a two stage open centered double solenoid direction control valve.

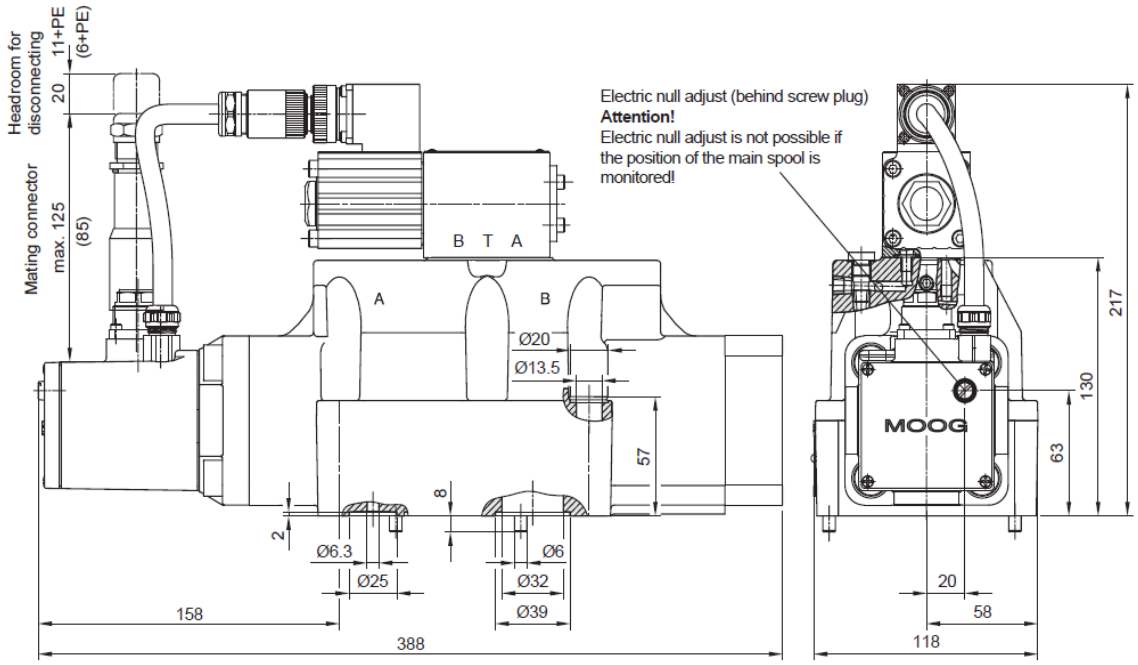

Figure 5.1 Valve installation drawing

In practice, a hydraulic valve is modeled as a first order system or as a second order system. It can also be modeled as higher order systems but the model becomes too complex and the will include more complicated dynamics. In general simple order valve system can be expressed as a first order system with a time constant t and a DC-gain K or as a second order system exhibiting oscillations and overshoot by specifying their natural frequency ω_v and damping ratio ζ as shown in 5.6.

$$\dot{x_v} = \frac{K}{t} * U - \frac{1}{t} * x_v \qquad 5.6$$

$$\ddot{x_v} = K\omega_v^2 U - 2\zeta\omega_v \dot{x_v} - \omega_v^2 x_v$$

Figure 5.2, shows the frequency response of the valve as given by the manufacturer. The plot shows the response of the valve for a frequency from 5-200Hz. In order to be able to represent the valve dynamics over a wide frequency range, a second order system model in 5.6 is considered.

There are a few parameters to be approximated from Bode plot, to get a linear model of the valve. From Figure 5.2, it is clear that there is no peak in the amplitude response, so the damping ratio could be considered to be $\zeta \leqslant 1$.

Generally in proportional valves, the cut-off frequency varies with the valve spool position, which is a non-linear characteristic, for which a nominal working region has to be chosen to decide on the frequency in such a way that the phase plot does not show steep characteristics.

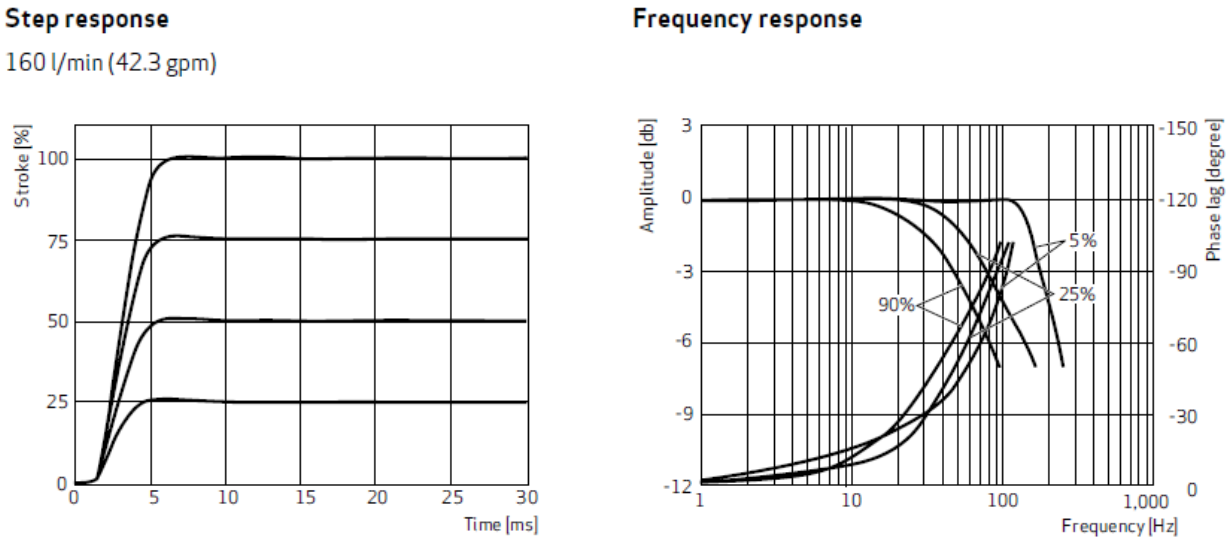

Figure 5.2 Response of valve from manufacturer

With $\omega_v = 70Hz\ \left(439.60\frac{rad}{sec}\right) and\ \zeta = 1$, the time constant of a critically damped system, can be calculated as defined in [Philips and Harbor, 2000, p.125eq.4-27],

$$t = 1/\ \zeta\ \omega_v = 0.00318 \text{ s}$$

The value for gain cannot be determined directly from Figure 5.2. Instead, the value can be approximated as a ratio of maximum spool displacement (x_v) to the maximum applied voltage (u). Both the values are taken from the valve datasheet of MOOG D672 valve.

$$K = \frac{x_{vmax}}{U_{max}} = 8.3333e - 004\ m/V$$

The second order frequency response of the valve with dc-gain "one" is as in Figure 5.3.

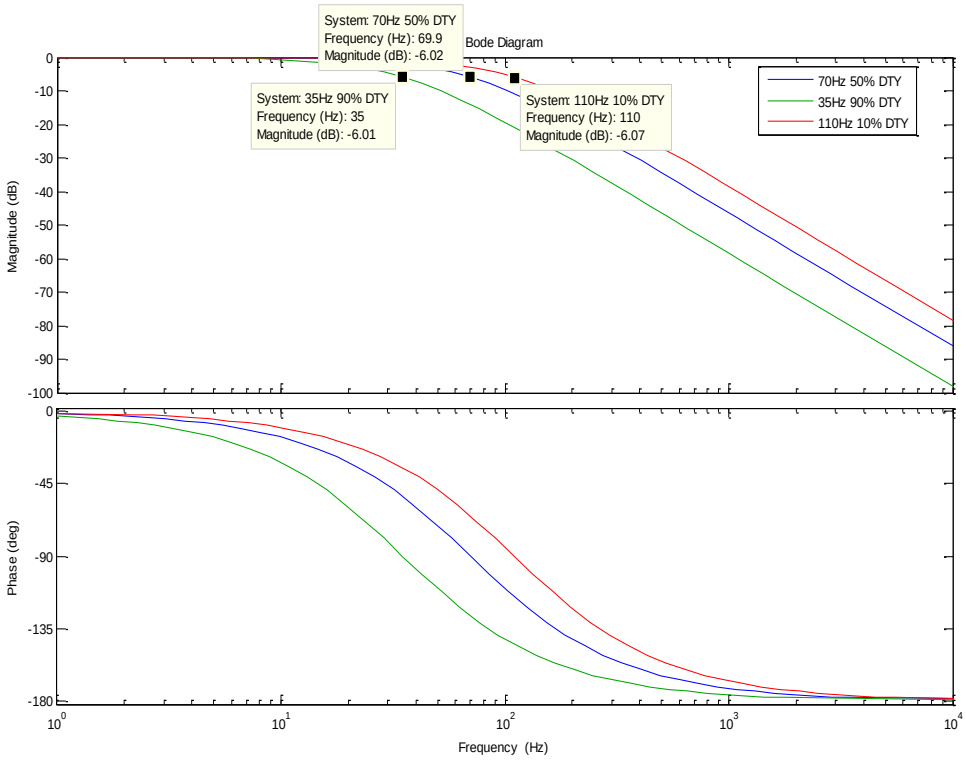

Figure 5.3Bode plot of Valve with unity gain

5.3 Nonlinear model simulation and results

This section explains the implementation of previously derived equations as Simulink block diagram. The results from the simulation are also added along with the models. The model of the hydraulic system can be created in two ways:

Case I: Considering that the volume in cylinder chamber changes along with the displacement of the cylinder rod and the equations that contribute to the combined dynamics of the system are given in 5.4 and are repeated below:

$$\dot{P}_A = \frac{\beta}{(V_{A0} + A_A x_{cyl})} \left(R_{va} x_v \left(\sqrt{P_s - P_A}\right) - \dot{x}_{cyl} A_A - C_L \left(\sqrt{P_A - P_B}\right)\right)$$

$$for\ x_v \geq 0$$

$$\dot{P}_B = \frac{\beta}{(V_{B0} - A_B x_{cyl})} \left(-R_{vb} x_v \left(\sqrt{P_B - P_t}\right) + \dot{x}_{cyl} A_B + C_L \left(\sqrt{P_A - P_B}\right)\right) \qquad 5.7$$

Similarly the pressure build-up equation can be derived for $x_v < 0$.

Case II: The two volumes are calculated to be a constant with x_{cyl} in the fully retracted and extended position respectively, in order to make the model simple.

$$\dot{P}_A = \frac{\beta}{(V_{01})}\left(R_{va}x_v(\sqrt{P_s - P_A}) - \dot{x}_{cyl}A_A - C_L\left(\sqrt{P_A - P_B}\right)\right) \quad for\ x_v \geq 0$$

$$\dot{P}_B = \frac{\beta}{(V_{02})}\left(R_{vb}x_v\left(\sqrt{P_B - P_t}\right) - \dot{x}_{cyl}A_B - C_L\left(\sqrt{P_A - P_B}\right)\right) \quad 5.8$$

Similarly the pressure build-up equation can be derived for $x_v < 0$.

The second sets of equations are adopted here for creating the model. In the equations derived in previous section, the pressure terms and the cylinder position are the states and can be obtained with the aid of sensors. Since the valve used is a proportional direction control valve, spool position is proportional to the applied voltage. The remaining unknown parameters shown in Table 5.1 are to be determined.

Parameters	***Symbol***	***Unit***
Discharge coefficient A	R_{va}	$m^2/s\sqrt{Pa}$
Discharge coefficient B	R_{vb}	$m^2/s\sqrt{Pa}$
Initial Volume in Cylinder Chamber A	V_{A0}	m^3
Volume in Cylinder Chamber B	V_{B0}	m^3
Bulk Modulus	β	Pa
Volume in Cylinder Chamber A	V_{01}	m^3
Volume in Cylinder Chamber B	V_{02}	m^3
Coefficient of leakage	C_L	$m^3/s\sqrt{Pa}$

Table 5.1

5.3.1 Area

The cylinder piston areas are determined from the cylinder drawings and are as follows A_A=0.0013 m^2: A_B = 7.6576 e-004 m^2 .

5.3.2 Initial volumes VA0 and VB0

The initial volumes (V_{A0}, V_{B0}) takes up a minimum and maximum value during extension and retraction. They are determined quite accurately with the assumption that the stroke is off by 1mm from the start and off by 5 mm in the end position from a total stroke of 200 mm. Spool

thickness is considered while calculating the offset for the end position. Volume of fluid entrapped inside the pipes and hoses connecting the hydraulic parts of the system are neglected.

$$V_{Amin} = 1.2566e-06\ m^3 \qquad V_{Amax} = 2.4504e-04\ m^3$$
$$V_{Bmin} = 7.6576e-07\ m^3 \qquad V_{Bmax} = 1.4932e-04\ m^3$$

The total volume in chamber V_{01}, V_{02}would take up the value of $V_{Amax}\ and\ V_{Bmax}$ as they represent the fully extended or retracted position.

5.3.3 Bulk modulus

Bulk modulus of the fluid changes with pressure and the amount by which it changes is dependent on the dissolved air in the fluid. For the purpose of simulation the value is assumed to be 1E9, obtained directly assuming that VG32 mineral based oil is being used in the system.

5.3.4 Discharge coefficient

The discharge coefficient of a proportional valve can be found from their pressure drop vs. flow relationship graph in Figure 5.4. An important detail to be noticed is that the value of discharge coefficient varies over its stroke. Hence the final value can be an average calculated at various pressure drops (in each spool landing) and their corresponding flow values. The orifice equation expressed in 5.2 forms the base to obtain the value of discharge coefficient and is given as

$$R_{va} = R_{vb} = Q/(x_{vmax}\sqrt{0.5\,\Delta P}) \approx 6.9488\text{e}-05$$

Here the value of discharge coefficient is same for both the working ports as they have the same geometry.

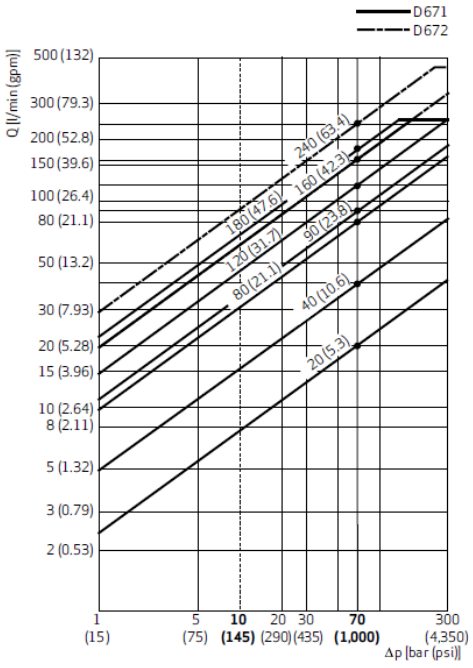

Figure 5.4 Pressure drop Vs. Flow rate

5.3.5 Nonlinear simulation model

The simulation model in Figure 5.5 consists of three parts valve dynamics, valve system and the mechanical system. The valve dynamics and the valve system are modeled as in equation 5.6 &

5.8. In order to simplify the process, the mechanical system is not the actual suspension frame but is considered to be a mass whose weight is evenly distributed among the four cylinders.

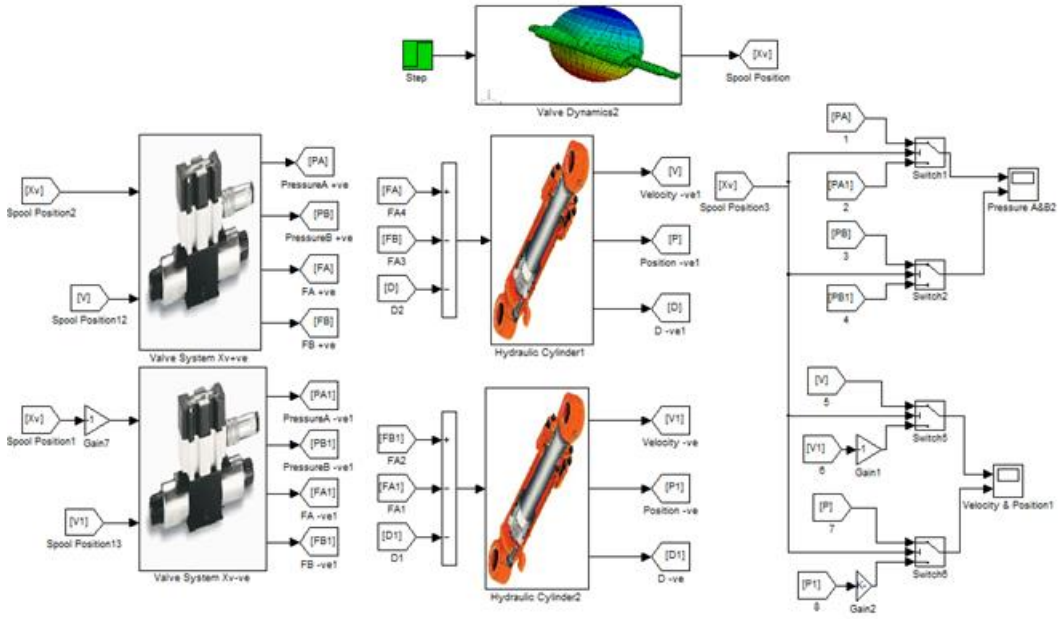

Figure 5.5 Nonlinear simulink model

In actuality, the cylinder position and velocity are limited. Similar kind of saturation cannot be taken into account by utilizing double integrator with saturation limits in the model. In simulation models, when the position reaches its upper saturation, the velocity will be internally integrated. In order to avoid this, a circuit as shown in Figure 5.6 is designed to ensure that velocity is immediately set to zero as the cylinder stroke reaches its maximum or minimum limit. The simulation results in Figure 5.7 & Figure 5.8 show the output of both the normal case and with a limit in velocity as mentioned above. From the graph, it is quite evident that the inclusion of logic circuit has made the velocity to zero as the piston reaches its maximum stroke or minimum stroke

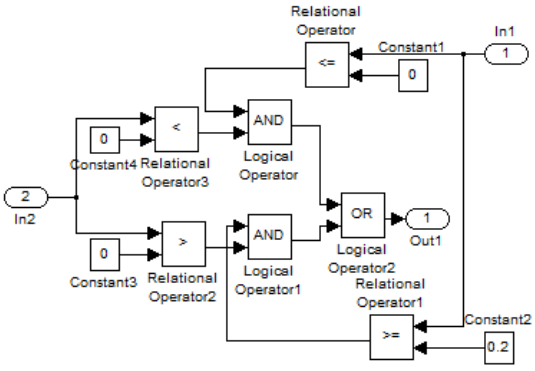

Figure 5.6 Logic circuit to limit velocity

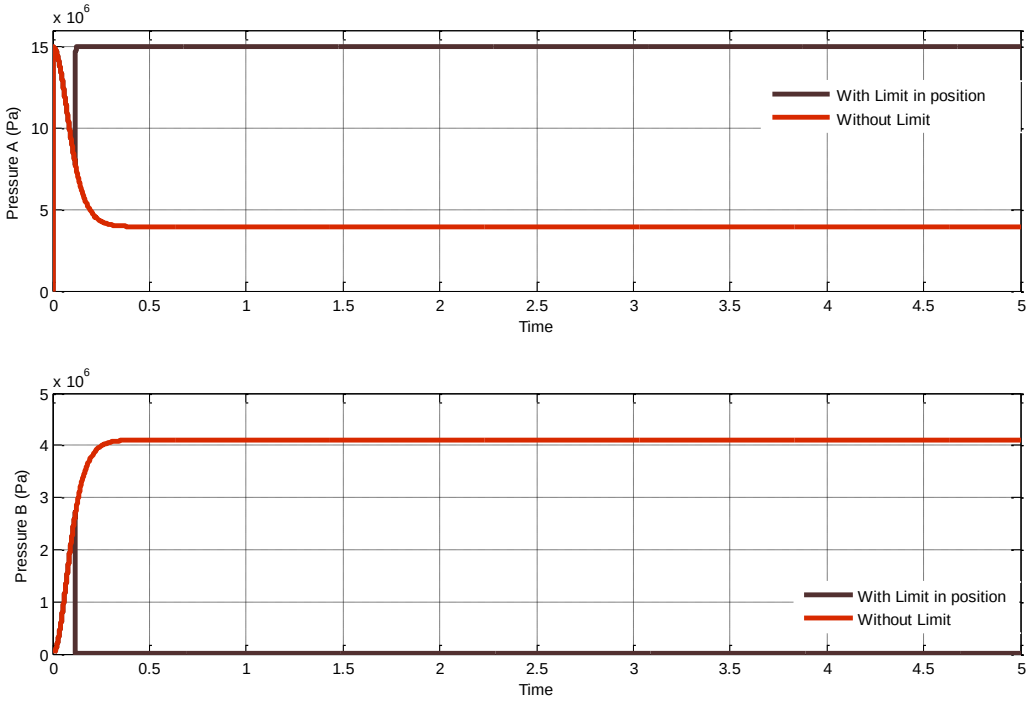

Figure 5.7Step response of nonlinear model

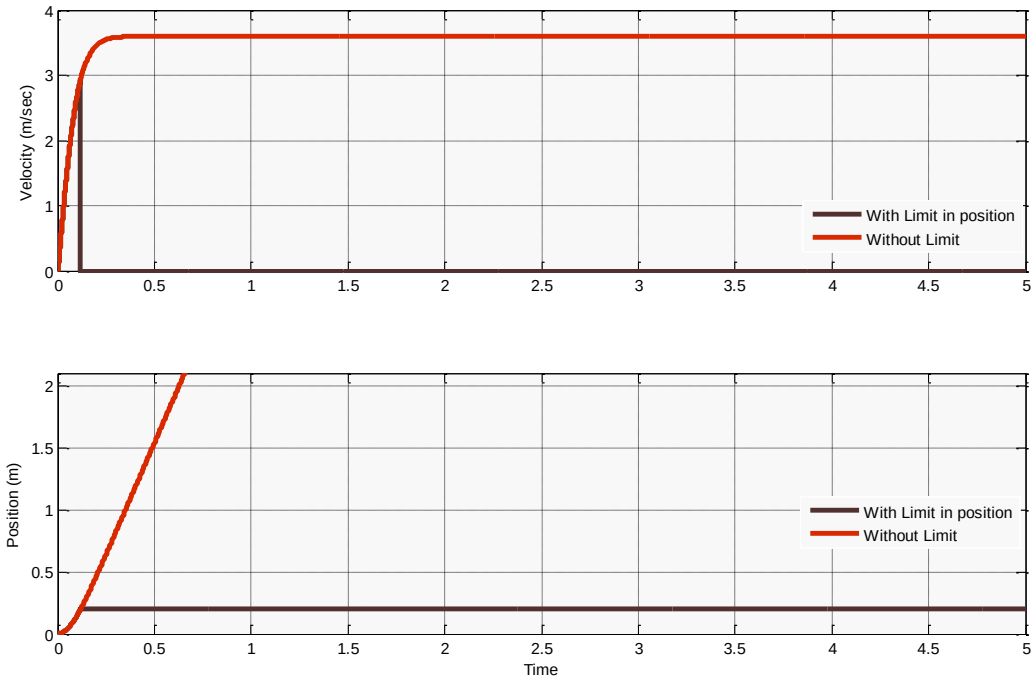

Figure 5.8Step response of nonlinear model with limit in position

5.4 Model simplification and linearization

The Simplified Model and a Linearized Model is developed in this chapter. The two models are developed to design the controller for the nonlinear model.

Simplified Model: Simplified model is comparable to the simulation model with the exception of neglected valve dynamics and a steady state simplification of flow in the hydraulic system model by ignoring the compression flow in both chambers.

In reality when there is a large pressure change, the entrapped fluid in the cylinder is compressed and the bulk modulus of the fluid changes. Amount of air, in the form of bubbles entrapped in the system strongly influences the bulk modulus. In reality the bulk modulus and the entrained air contribute to a "spring effect" in the hydraulic system. The negative effect of this is that,

1. Effective stiffness is reduced.

2. It affects the dynamic behavior: since there is a mass to be accelerated and the interaction of mass with the stiffness results in natural resonant frequency, creating noise, vibration and also could lead to system failure.

Linearized Model: This is a linearized version of the simplified model and the equations are linearized using a first-order Taylor expansion.

5.4.1 Simplified model

This section explains the derivation of a reduced order model. The hydraulic part is simplified and the valve dynamics is neglected. Since a proportional valve is used, the spool position is assumed to have a linear relation with the voltage related by DC-Gain K as in second order valve model represented in equation 5.6.

$$x_v = KU \tag{5.9}$$

The hydraulic system is simplified with the same assumptions as in the derivation of simulation model along with the following steady state assumption

$$\dot{x}_{cyl} = \frac{Q_A}{A_A} = -\frac{Q_B}{A_B} \tag{5.10}$$

The above assumption clearly ignores the compression flow in both chambers and introduces a steady state condition. The flow Q_A into chamber A is proportional to a cylinder velocity $\dot{x}_{cyl}$ and a flow in Q_B.

In order to make the expression 5.10 simpler, new terms α and σ are introduced to represent *cylinder area ratio* and *valve flow ratio* respectively.

$$\alpha = A_B/A_A \tag{5.11}$$

$$\sigma = R_{vb}/R_{va} \tag{5.12}$$

Using this we can rewrite 5.10 as

$$\alpha Q_A = -Q_B \quad 5.13$$

5.4.1.1 Positive spool displacement

The simplified model derivation for positive spool displacement i.e. for $x_v \geq 0$, and the corresponding flow is given by

$$Q_A = R_{va} x_v (\sqrt{P_s - P_A}) \quad 5.14$$

$$Q_B = -\sigma R_{va} x_v (\sqrt{P_B - P_T})$$

Substituting the flows from 5.14 into 5.13

$$\alpha R_{va} x_v (\sqrt{P_s - P_A}) = -\sigma R_{va} x_v (\sqrt{P_B - P_T} \quad 5.15$$

Now deriving equations for P_A & P_B from above,

$$P_A = P_s - (\sigma^2 (P_B - P_T)/\alpha^2)$$
$$P_B = P_T - (\alpha^2 (P_A - P_s)/\sigma^2) \quad 5.16$$

Net force acting on the system is given by,

$$F_L = P_A A_A - P_B A_B \quad 5.17$$

With the above relation the virtual load pressure can be obtained by dividing it with A_A,

$$P_L = F_L/A_A = P_A - \alpha P_B \quad 5.18$$

The pressure in the individual chambers can be expressed as a function of virtual load pressure by substituting 5.16 in 5.18

$$P_L = P_A - \alpha(P_T - (\alpha^2 (P_A - P_s)/\sigma^2)) \quad 5.19$$

$$P_L = P_s - (\sigma^2 (P_B - P_T)/\alpha^2 - \alpha P_B \quad 5.20$$

Now deriving equations for P_A & P_B from 5.19 and 5.20,

$$P_A = (\alpha^3 P_s + \alpha\sigma^2 P_T + \sigma^2 P_T)/\alpha^3 + \sigma^2 \quad 5.21$$

$$P_B = (\alpha^2 P_s + \sigma^2 P_T + \alpha^2 P_T)/\alpha^3 + \sigma^2 \quad 5.22$$

Due to the steady state assumption, the individual chamber pressures are defined as a function of load pressure which does not happen in general due to the effect of compressible flow in each

chamber. Substituting the above equations in 5.14 and simplifying it further yields the simplified flow equation

$$Q_A = \sigma\, R_{va} x_v \left(\sqrt{(P_s - \alpha P_T - P_L)/\alpha^3 + \sigma^2}\right) \qquad 5.23$$

$$Q_B = -\alpha\, \sigma\, R_{va} x_v \left(\sqrt{(P_s - \alpha P_T - P_L)/\alpha^3 + \sigma^2}\right)$$

From the derived flow equation it could be seen that the equation corresponds to 5.13.

5.4.1.2 Negative spool displacement

The derivation is similar to positive spool displacement but for $x_v < 0$ and a slight modification in the flow equation unlike 5.14.

$$Q_A = R_{va} x_v \left(\sqrt{P_A - P_T}\right)$$
$$Q_B = -\sigma R_{va} x_v \left(\sqrt{P_S - P_B}\right) \qquad 5.24$$

Rest of the derivation is carried out in a similar way and the final simplified flow equation is given as

$$Q_A = \sigma\, R_{va} x_v \left(\sqrt{(P_L + \alpha P_S - P_T)/\alpha^3 + \sigma^2}\right) \qquad 5.25$$

$$Q_B = -\alpha\, \sigma\, R_{va} x_v \left(\sqrt{(P_L + \alpha P_S - P_T)/\alpha^3 + \sigma^2}\right)$$

The equations contributing flow in both positive and negative spool displacement can be further reduced by introducing a term collecting all the constants and by introducing the linear relation between spool position and applied voltage.

$$K_L = \sigma\, R_{va} \mathrm{K}/\left(\sqrt{\alpha^3 + \sigma^2}\right) \qquad 5.26$$

Hence the simplified flow equation is given by

For positive spool displacement:

$$Q_A = K_L \mathrm{U}\left(\sqrt{(P_s - \alpha P_T - P_L)}\right) \qquad 5.27$$

$$Q_B = -\alpha K_L \mathrm{U}\left(\sqrt{(P_s - \alpha P_T - P_L)}\right)$$

For negative spool displacement:

$$Q_A = K_L \mathrm{U}\left(\sqrt{(P_L + \alpha P_S - P_T)}\right) \qquad 5.28$$

$$Q_B = -\alpha K_L \mathrm{U}\left(\sqrt{(P_L + \alpha P_S - P_T)}\right)$$

The load pressure built up equation can be obatained by differentiating 5.18 and expressed in terms of chamber pressures $\dot{P}_A$ & $\dot{P}_B$

$$\dot{P}_L = \frac{\beta}{(V_{A0} + A_A x_{cyl})} \left(Q_A - \dot{x}_{cyl} A_A - Q_C\right) - \frac{\beta\alpha}{(V_{B0} - A_B x_{cyl})} \left(-\alpha Q_A + \dot{x}_{cyl} A_B + Q_C\right) \qquad 5.29$$

In order to make the expressions simple, the following functions are introduced

$$V_{A1} = V_{A0} + A_A x_{cyl}$$
$$V_{B1} = V_{B0} - A_B x_{cyl} \qquad 5.30$$
$$\Gamma = V_{B1}/V_{A1}$$

Introducing the above functions in 5.29 and further simplifying it yields the final load pressure built up equation,

$$\dot{P}_L = \frac{\beta}{(V_{A1}\Gamma)} \left[(\Gamma + \alpha^2)Q_A - (\Gamma + \alpha)C_L P_L - (\Gamma + \alpha^2)\, \dot{x}_{cyl} A_A\right) \qquad 5.31$$

This is the finalised load pressure equation of the simplified model.

5.4.2 Linearized model

The pressure built up equation 5.31 and flow equations 5.27 and 5.28 for positive and negative spool displacements are nonlinear and they are linearized about an operating point using the Taylors expansion series:

A nonlinear model $\dot{x} = f(x,u)$, $y = g(x,u)$ can be linearized around an operating point (x_q, u_q) by considering a neighborhood around the operating point and approximating the nonlinear model with a truncated Taylor series:

$$\dot{x} \simeq f(x_q, u_q) + \frac{\partial \mathrm{f}}{\partial \mathrm{x}}\, \Delta x + \frac{\partial \mathrm{f}}{\partial \mathrm{u}} \Delta u \;||\; \mathrm{x}=x_q, u = u_q$$
$$y \simeq g(x_q, u_q) + \frac{\partial \mathrm{g}}{\partial \mathrm{x}}\, \Delta x + \frac{\partial \mathrm{f}}{\partial \mathrm{u}}\, \Delta u \;||\; \mathrm{x}=x_q, u = u_q \qquad 5.32$$

And on adopting the general form mentioned in 5.32 to the flow equation 5.27 and 5.28 gives

$$Q_A(U, P_L) = Q_A(U_q, P_{Lq}) + \frac{\partial Q_A}{\partial \mathrm{U}}\, \Delta U + \frac{\partial Q_A}{\partial P_L} \Delta P_L \;||\; \mathrm{U}=U_q, P_L = P_{Lq} \qquad 5.33$$

The term Δ refers to the change in value of the variable from its operating point. With the assumption that $\frac{\partial Q_A}{\partial \mathrm{U}} = K_U$ and $\frac{\partial Q_A}{\partial P_L} = K_P$, equation 5.33 can be written in a generalized form as

$$\Delta Q_A = K_U\, \Delta U + K_P \Delta P_L \qquad 5.34$$

The equation would be the same for both positive and negative control signal for the coefficients K_P, K_U changes. To indicate the equation for positive and negative signal, a suffix P and N are added respectively.

$$\Delta Q_A = K_{UP}\, \Delta U + K_{PP}\, \Delta P_L \quad \text{for U}\geq 0$$
$$\Delta Q_A = K_{UN}\, \Delta U + K_{PN}\, \Delta P_L \quad \text{for U}<0 \qquad 5.35$$

Taking the partial derivatives of the flow equation 5.27 and 5.28 gives the value of the coefficients

$$K_{UP} = K_L(\sqrt{(P_s - \alpha P_T - P_{Lq})} : K_{UN} = K_L(\sqrt{(P_{Lq} + \alpha P_S - P_T)} \quad 5.36$$

$$K_{PP} = K_L U_q/(2\sqrt{(P_s - \alpha P_T - P_{Lq})} : K_{PN} = K_L U_q/(\sqrt{(P_{Lq} + \alpha P_S - P_T)}$$

These equations substituted in the pressure built up equation 5.31 to obtain the final linearized model.

5.4.3 Operating point

In order to design a controller for the nonlinear system, the system should be linearized about an operating point. The parameters of the hydraulic system vary over time and these variations are not considered while modeling the system. Hence an idea over the parameter variation should be obtained before selecting the operating point as they are most critical with respect to design specification, for the same controller being able to operate in all situations.

Other than the load pressure and spool position few of the other parameters that varies and that are critical are Volume in chamber (V_{A1}, V_{B1}), Bulk Modulus (β), Leakage coefficient (C_L), Discharge coefficient (R_{vb}, R_{va}). The parameters mentioned are all temperature dependent, but their variation is neglected with the assumption that temperature does not vary much from the normal operating condition.
The effect of variation in system dynamics of the heavily damped system for two different values of bulk modulus (β) is shown in the bode plots in Figure 5. 9. Bode plot for different values of bulk modulus clearly indicate that it greatly affects the resonant frequency of the system. Since the suspension system has higher rate of change of acceleration i.e. effect of compressibility is high and the requirements on the bandwidth helped to choose $\beta = 1E9\ Pa$. The other factors also has an effect on the system dynamics but not as dominant as β.

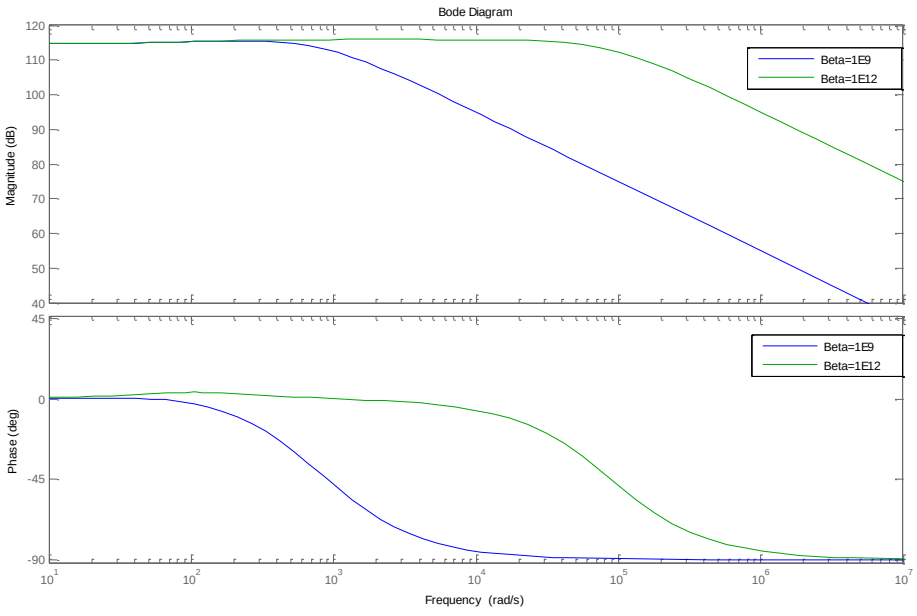

Figure 5. 9 Bode plot for $\beta = 1E9\ Pa$ & $\beta = 1E12\ Pa$

Finally the state space form of the system about the operating point $U_q = 0V$ & $P_{Lq} = -(\alpha P_S)\ Pa$ can be found by substituting the values in the state vector and input vector given below respectively,

$$\begin{pmatrix} \dot{P}_L \\ \dot{v} \end{pmatrix} = \begin{pmatrix} -\frac{d}{m} & \frac{A_A}{m} \\ C1\,C4 & C1\,C2 + C1\,C3 \end{pmatrix} \qquad 5.37$$

$$(U) = \begin{pmatrix} 0 \\ C1\,C5 \end{pmatrix}$$

Where

$$C1 = \frac{\beta}{(V_{A1}\Gamma)}, C2 = -(\Gamma + \alpha^2)K_{PP}, C3 = -(\Gamma + \alpha)C_L$$
$$C4 = -(\Gamma + \alpha^2)A_A, C5 = K_{UP}(\Gamma + \alpha^2) \qquad 5.38$$

5.4.4 Simulation of simple model and linearized model

The section explains the block diagram modeling and simulation of the simplified mathematical model derived in the earlier section. As in Figure 5.10 the system is modeled with a steady state flow condition and the output is in terms of load pressure. Simulation results of the nonlinear simplified model and the linearized model are compared to check for the model accuracy within the operating region.

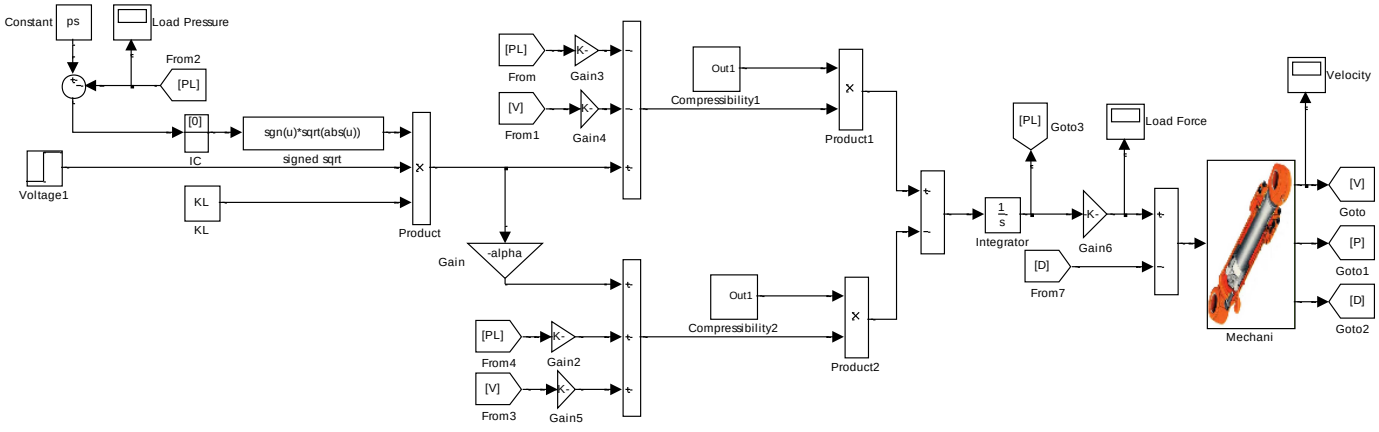

Figure 5.10 Simplified Simulink model

5.4.5 Comparison of simplified and linear model

The verification of linearized model is done by comparing the velocity and load pressure response of the linear and nonlinear model to a step input of 0.001 V.A small step is applied to check if the linearized model is able to describe the dynamics of the real system around the operating point and the result is shown in Figure 5.11 & Figure 5.12 is found to be quite satisfactory.

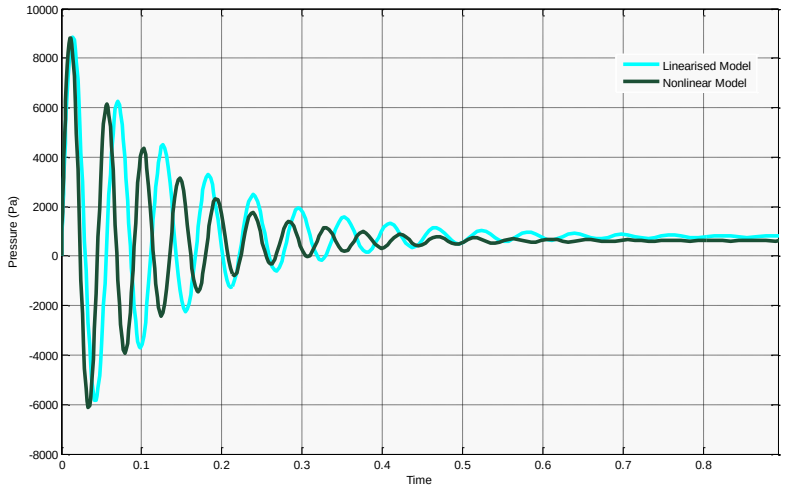

Figure 5.11 Pressure response of simplified vs. linearized model for 0.001V

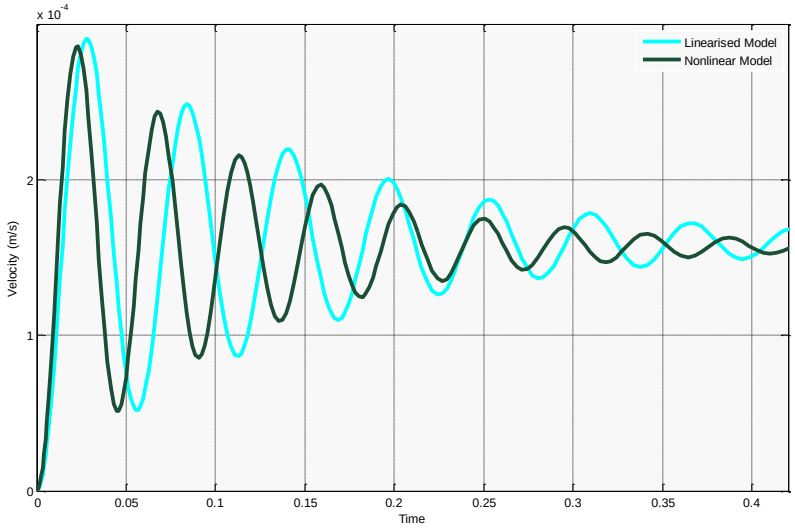

Figure 5.12 Velocity response of simplified vs. linearized model for 0.001V

A larger step input of 0.5 V is given to both the systems and the results are as in Figure 5.13 & Figure 5.14. By comparing the velocity plots for the different step responses, it is quite evident that the system response of the linearized system is same but the amplitude of the output is scaled by a factor of ratio of two step inputs and hence is 500 times larger. But the nonlinear model has changed its behavior with time as it gets away from the operating point. Hence it can be concluded that the linearized model is able to describe the characteristics with in the region of parameters selected.

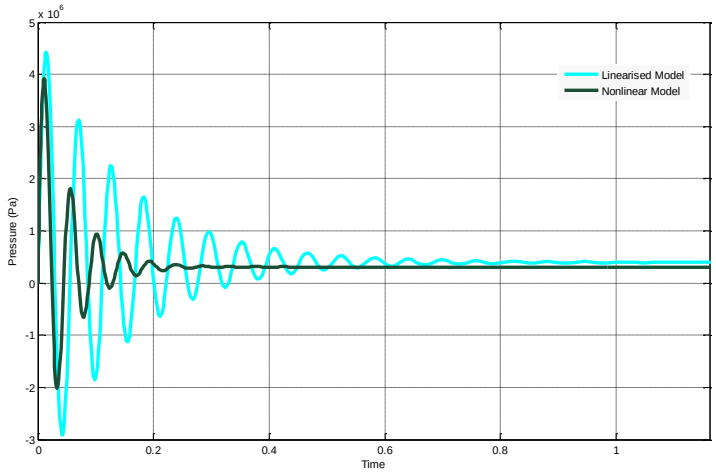

Figure 5.13 Pressure response of simplified vs. linearized model for 0.05V

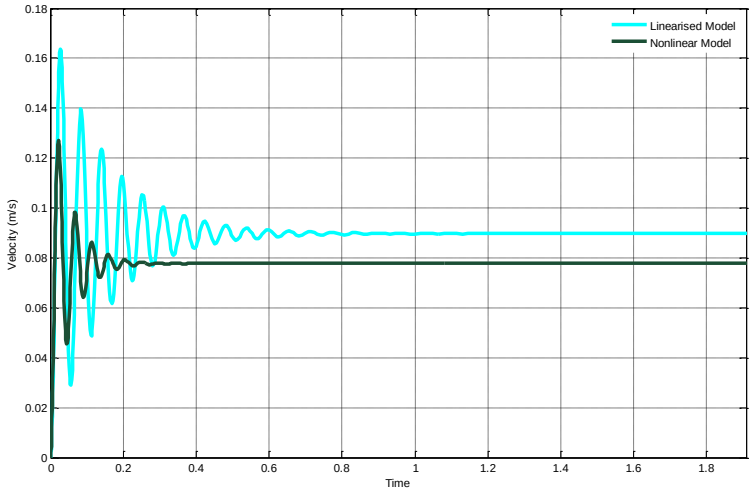

Figure 5.14 Velocity response of simplified vs. linearized model for 0.05V

5.5 SimHydraulics simulation

This section explains the simulation of hydraulic system in Simhydraulics thus providing an opportunity to simulate and analyze the system in a so called "near to reality" basis. Creating a model that captures the relevant dynamics and simulates quickly can be challenging with mathematical modeling.

5.5.1 Valve characteristic matching

The first step performed, was to match the valve flow characteristics. Creating an accurate model of a directional valve requires proper interpretation of data sheets provided by the manufacturer. Since the manufacturers do not follow a common standard this process generally turns out to be a bit difficult. There are 3 ways in Simhydraulics, with which a valve can be characterized.

1. Parameterization of Valves Characterized by Maximum Area and Opening.
2. Parameterization of Valves Characterized by Area vs. Opening Table
3. Using Experimental Data for Valve Parameterization

The proportional direction control valve is characterized by maximum area vs. valve opening method mentioned above. The value for discharge coefficient was calculated from the data sheet as mentioned in Figure 5.4. From the data sheet, a vague idea on the maximum opening and maximum stroke was obtained and the circuit Figure 5.15 was simulated by varying these values within that specified region to get the desired result. The purpose of utilizing a second pressure source in Figure 5.15 is to give a pressure drop of 35 bars in each spool landing and match the flow output as provided by the manufacturer in Figure 5.16. Final value of maximum spool opening and opening area is found to be 0.020 m and 0.000314m^2 respectievely. The final tuned valve opening vs. flow rate response of the valve is as in Figure 5.17.

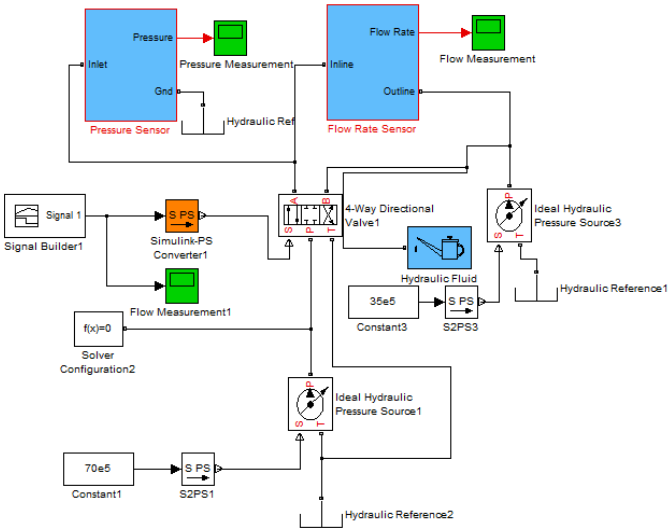

Figure 5.15 Valve flow calibration model

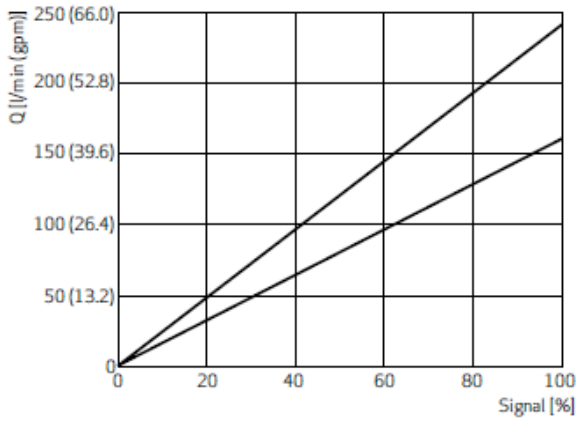

Figure 5.16 Flow characteristics of valve by manufacturer

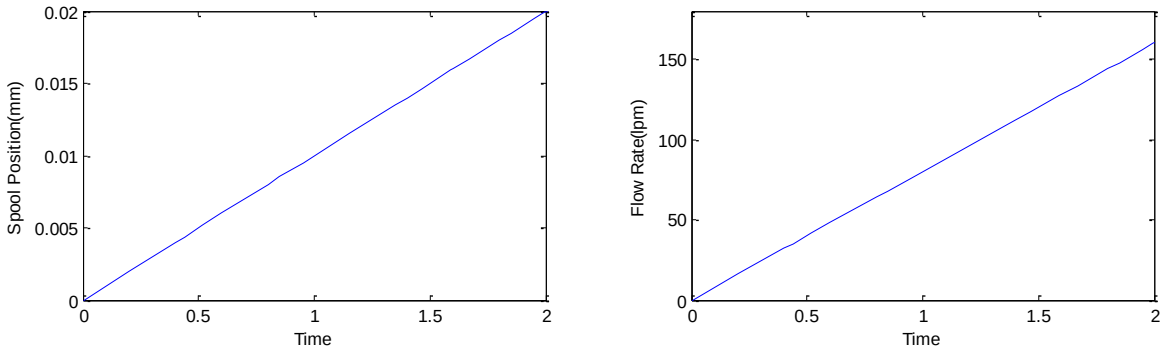

Figure 5.17 Tuned valve response

5.5.2 One cylinder simulation

This section explains the open loop, closed loop velocity and force control of one cylinder with the calibrated valve. The results from this are used to verify the Simulink model and understand the requirements of the system to match the specifications.

With the valve being calibrated, a Simhydraulics circuit was designed as in Figure 5.18 with one cylinder and a constant pressure source to verify the open loop dynamics of the nonlinear simulink model. The results on their pressure dynamics for a sine input is shown in Figure 5.20 and it could be noted that there exists transient peak in the pressure response of the SimHydraulics model as a result of the leakage flow existing in the valve. The velocity and position response of the two models shown in Figure 5.20 are quite similar.

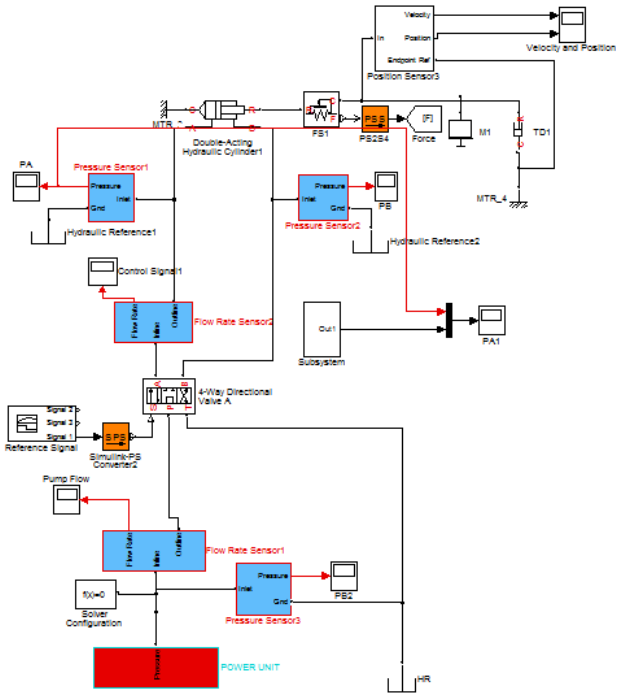

Figure 5.18 Open loop simulation of one cylinder

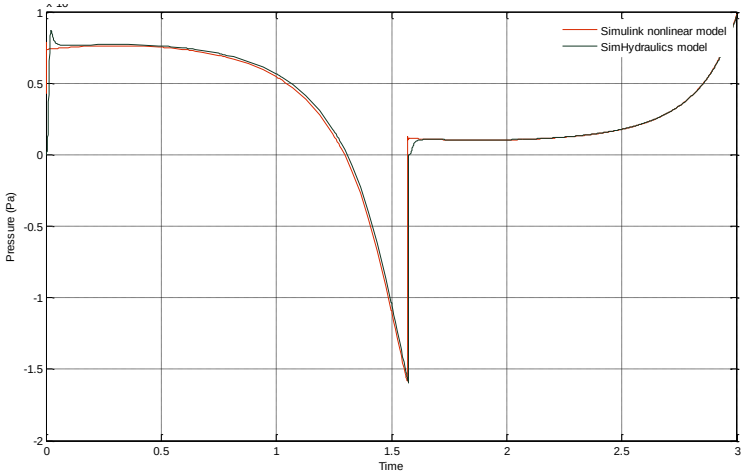

Figure 5.19 Pressure response of Simulink and SimHydraulics model

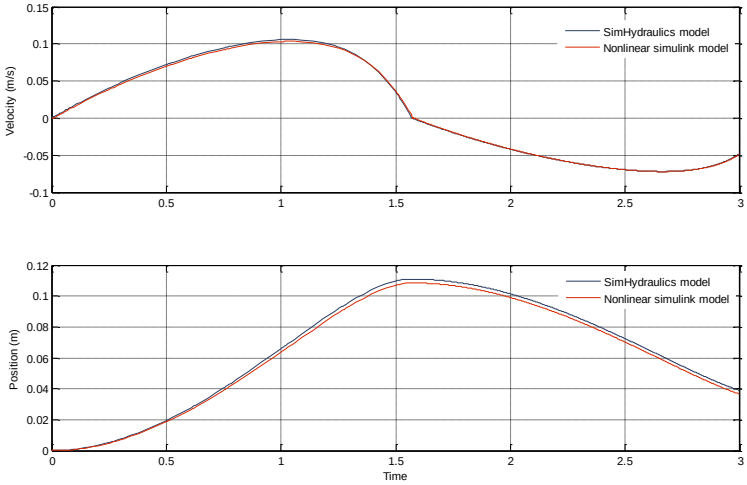

Figure 5.20 Velocity and Position of Simulink and SimHydraulics model

5.5.3 Closed loop simulation

The desired task of developing an active suspension system is achieved by means of a closed loop force controller. The system modeled in 5.5.2 does not give an insight in to the system flow and velocity characteristics as the state variable being controlled is pressure. Hence a closed loop force control circuit is designed in Simhydraulics, which in turn would help in determining the flow requirement of the system at different amplitude/frequency reference obtained from the outer loop controller. The controller used here is a basic P-controller to deduce the flow requirement of the system which in turn will also help in determining the valve working frequency range. Results obtained from this simulation would give an understanding in confirming the nominal cut-off frequency of the valve to design the inner loop controller for the simplified linearized model. The detailed controller design is explained in the next section.

Simhydraulics, demands assigning very high values for the contact stiffness and contact damping in the hard stop properties of the cylinder for it to limit the stroke to 0.2 m. This in turn limits the possibility of simulating the model for a continuous cycle. Hence the values of flow and velocity shown in Figure 5.21 are interpreted as the maximum demand at the peak force amplitude of the sine wave at different frequencies for one cycle. The usage of constant pressure source helps in maintaining the system pressure to the set value and simultaneously meeting the flow demand of the system.

The reference signal is given taking in to consideration of the worst case force demand per cylinder at different frequencies. The real forwarder machine works at low frequency, high amplitude and vice versa but in simulation the amplitude is considered to be the same to know the maximum flow demanded by the system.

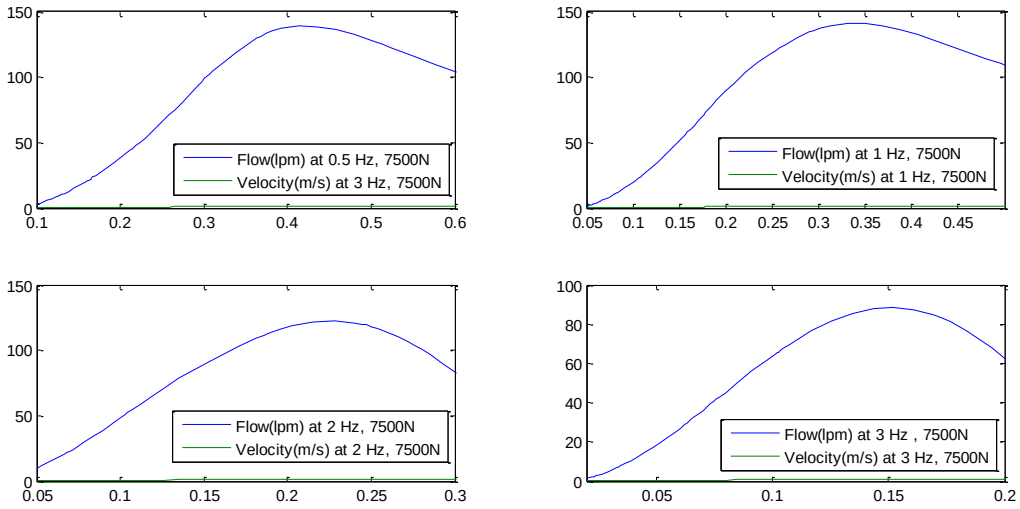

Figure 5.21 Flow of closed loop system at different frequency & 7500 N

From the graph it could be inferred that the maximum flow required by each cylinder during extension stroke to compensate for external vibration is around 150 l/min. Cylinder's flow demand during extension is more in contrast to retraction, for the cylinder has lesser volume displace due to reduction in area. The above result helps to conclude that the entire system with all the four cylinders would approximately require 600 l/min to achieve the velocity required to accelerate the upper frame.

5.6 Control design

The controller is developed based on the Internal Mode Control (IMC) algorithm with the help of MatlabR2012a SISO toolbox. This method is based on zero-pole cancellation and hence is quite intuitive and easy to design. But this method could make the closed loop system to have a poor response to load disturbance if it cancels out the slowest pole. The reason for choosing this control strategy is because IMC can explicitly take into considerations of model uncertainty and hence allows having a trade-off between control performance and robustness. IMC also takes integral action implicitly. The pz-map shown in Figure 5.21 shows that the controller does not cancel out the slower poles and therefore is insensitive to external load disturbances. As per rule of thumb, the outer loop is designed 5 times slower than the valve frequency as a result the controller is expected to have a cut-off frequency of 15Hz.

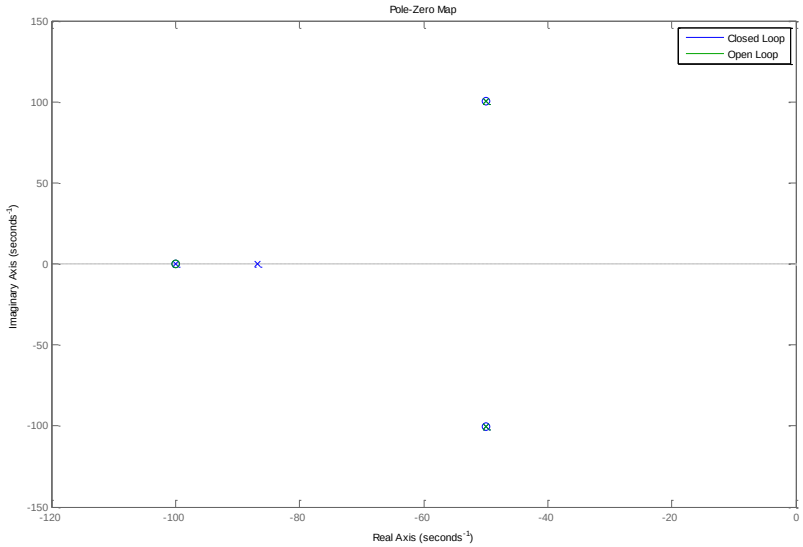

Figure 5.22 pz-map of open loop and closed loop system

The linearized model in 5.37 is used as the process model to develop the controller. Since the linearized model is derived from the simplified model, there would be a mismatch between the process model and the linearized model. Since the controller being developed is expected to have good performance in low frequency range, inconsistencies existing between the process and linear model at high frequencies can be neglected. The absence of non-invertible components in the linearized model made it easier to tune the controller. The generalized controller transfer function and the control law for the IMC is given below

$$Gc = (Gp)^{-1} * Gf$$

$$U = (R - f) * Gc/(1 + [Gprocess - Gp] * Gc)$$

Where $Gc, Gp, Gprocess$ & Gf represents the transfer function for the controller, process model, actual process and filter respectively. R and f signifies the reference signal and error feedback signals in that order. The selection of the filter order, n, is done in order to make the controller transfer function proper. The filter time constant determines the dynamics of the system as it represents the characteristics of the slowest pole in the system. By considering the requirement on cut-off frequency, the closed loop time constant was given a value of 0.012 and order of the filter was chosen to be three. The closed loop bode plot of the system is as shown in Figure 5.23.

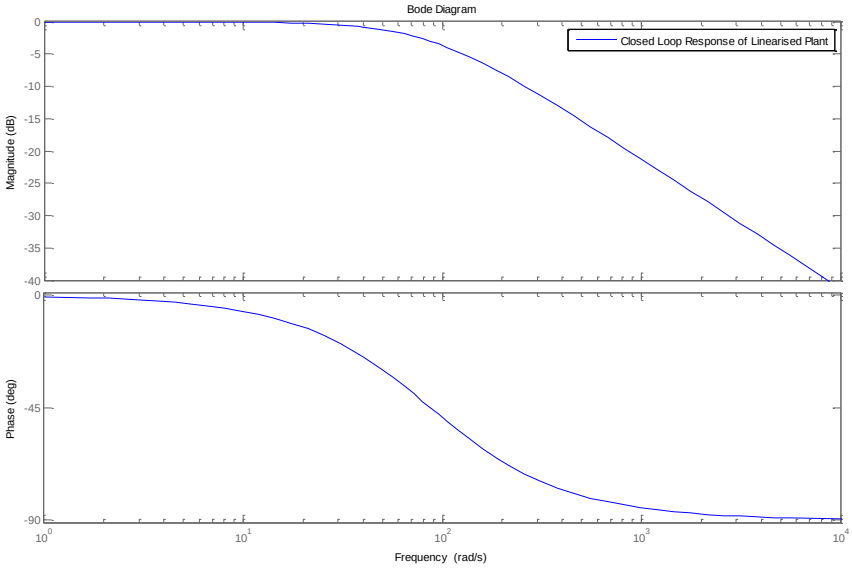

Figure 5.23 Closed loop bode plot of the hydraulic system

The controller developed for the linearized model was implemented in the nonlinear model in Figure 5.5 and the system's output response to a sine wave of two frequencies 1 Hz & 2 Hz is as in Figure 5.23 and Figure 5.26 respectively. The output result shows a good tracking performance with in the target frequency range and the voltage control signal for different input frequencies do not saturate and are within limits as seen in Figure 5. 25 and Figure 5.27. It can also be observed that the valve's input voltage requirement increases at low frequency due to the increased flow demand during the operation. As the frequency increases the tracking performance of the controller is getting reduced and a slim effect can be observed in Figure 5.26.

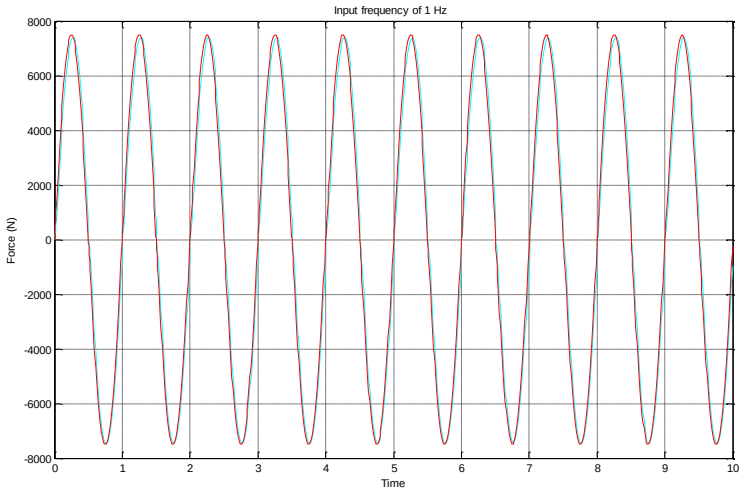

Figure 5.24 Output response of closed loop system at 1 Hz

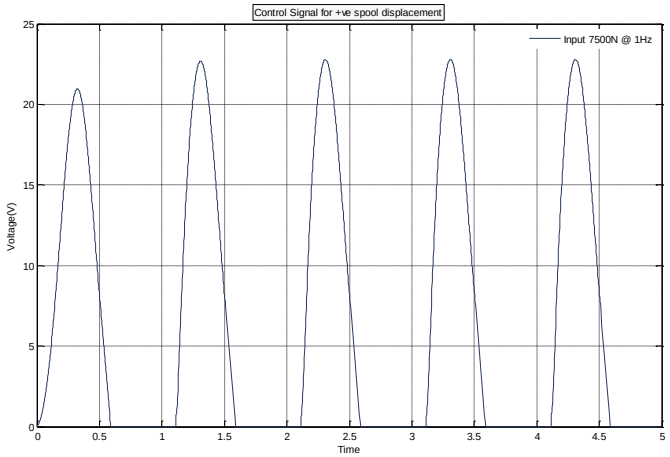

Figure 5. 25 Voltage control signal at 1 Hz

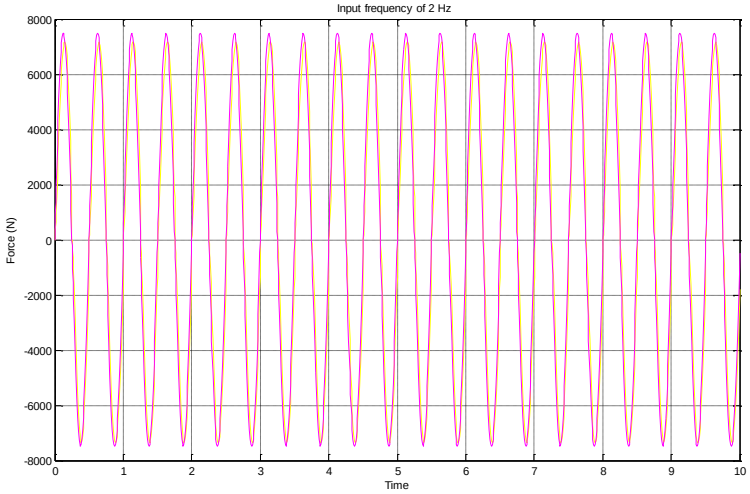

Figure 5.26 Output response of closed loop system at 2 Hz

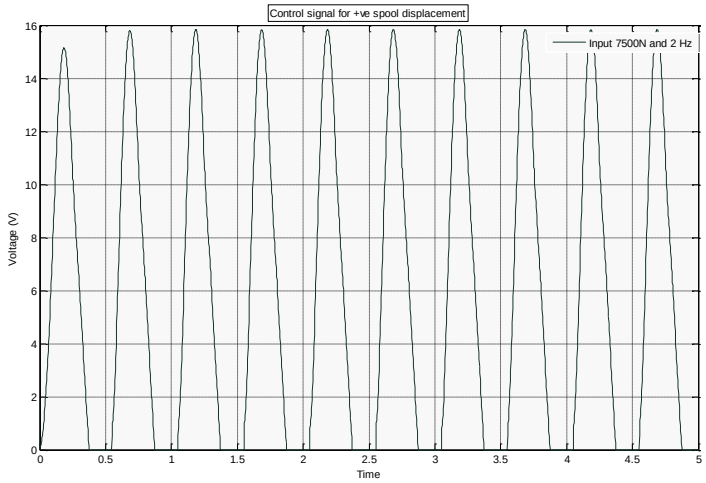

Figure 5.27 Voltage control signal at 2 Hz

This concludes the chapter with the inner loop system model and internal model force controller being developed for integration with the mechanical system, which forms the outer loop of the system.

6 OVERALL SYSTEM SIMULATION

In this chapter the inner-loop and outer-loop controllers are integrated to simulate the overall system. The vibration input is from forest research institution Skogforsk. The overall system response to the data measured in the working environment is analyzed, and the functionality of system is validated.

6.1 Heave controller

In this simulation, the heave vibration data in acceleration is fed into the SimMechanics model, Figure 6.1 shows the same performance as expected in previous analysis. At the beginning of simulation, there is a spike in acceleration due to the initialization of the controller. It could be seen that the controller have the capability to reduce the magnitude of vibration around 2Hz. Please note that this vibration signal not only consist of heave vibration data, but also includes the coupling of roll and pitch motion.

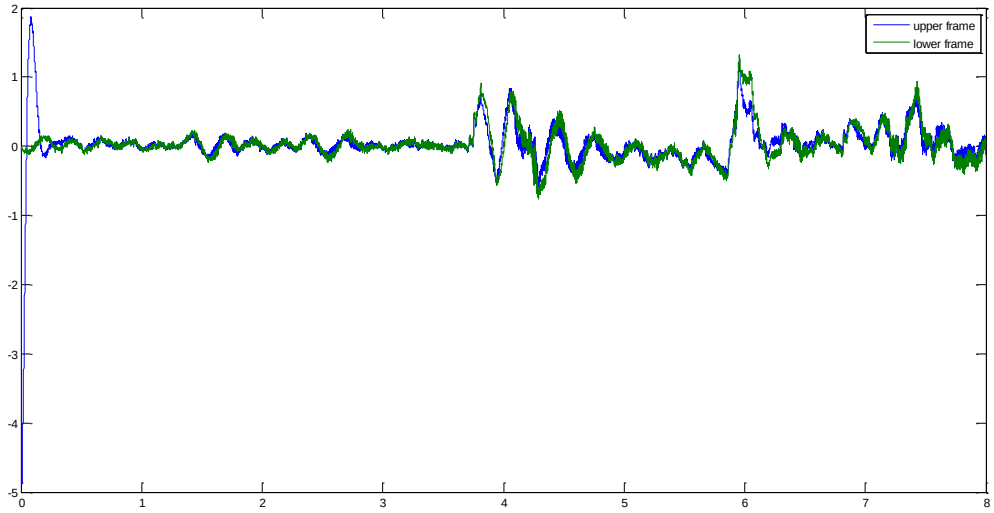

Figure 6.1Performance of heave controller

6.2 Roll and pitch controller

In chapter of mechanical system control design, the roll and pitch controller is designed to reduce the vibration between $1Hz$ to $3Hz$ and follow the movement of lower frame at the frequency lower than $0.5\ Hz$. The vibration data obtained from the forest industry is in angular velocity; in the simulation they are integrated to angular displacement and fed into SimMechanics file.

The Figure 6.2 shows the response of roll movement towards to vibration data. It could be seen that the controller cannot reduce the vibration in very high frequency, but shows desired performance in low frequency domain. The Figure 6.3 is the response data filtered by a low-pass filter with the bandwidth of $3Hz$. The upper frame follows the very slow vibration and reduce the vibration in the target frequecy region.

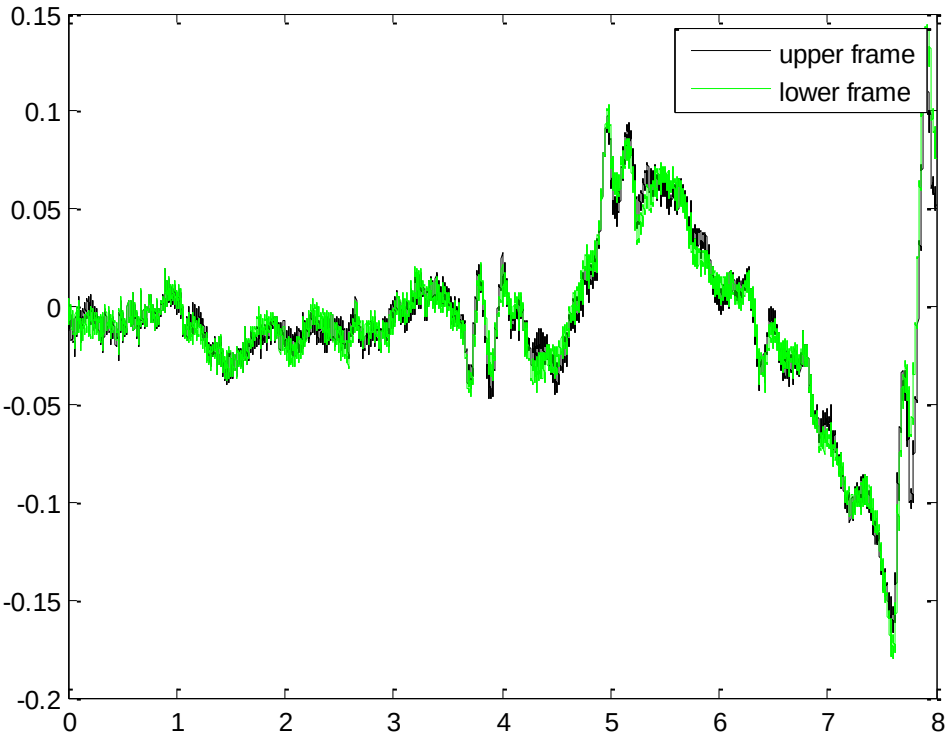

Figure 6.2 Vibration of roll movement

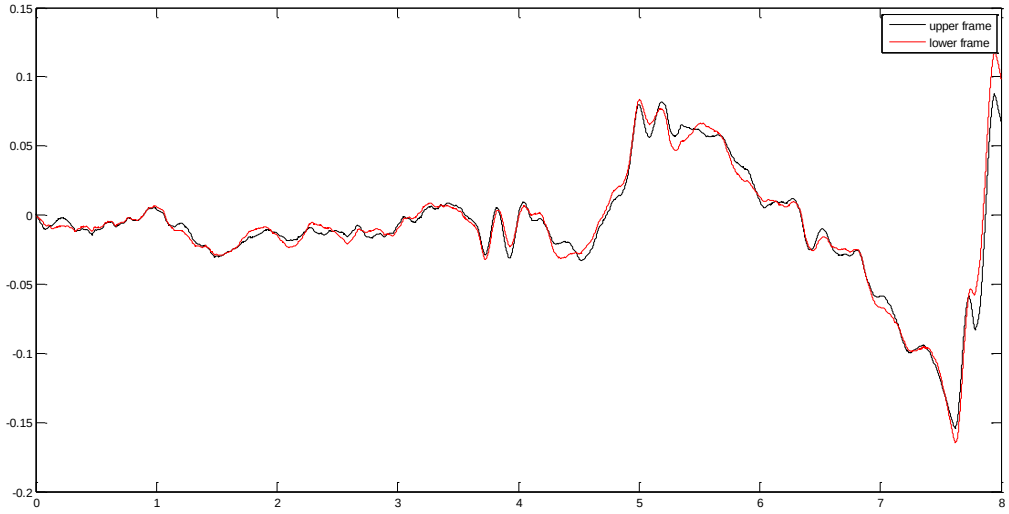

Figure 6.3 Low frequency vibration component of roll movement

6.3 Stroke utilization

With the limitation of stroke of cylinder, efficiently utilizing the stroke within the limit to achieve the desired performance is major task in this work. Figure 6.4, shows the utilization of stroke. It shows that 35 mm of the stroke is used which is less than the limitaion of $\pm$ 100 mm.

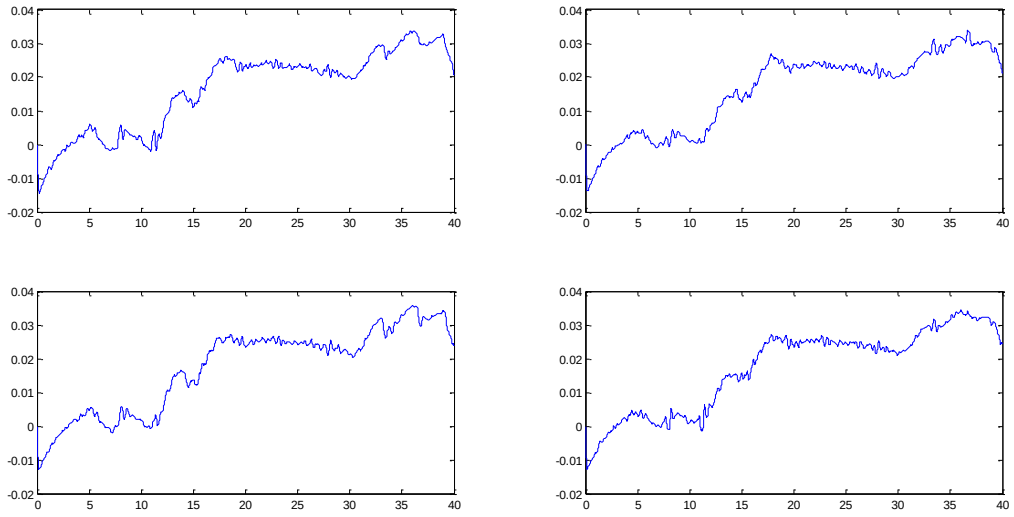

Figure 6.4 Stroke utilization of cylinders

6.4 Force tracking and Flow rate

The inner loop controller designed in Chapter Five to provide force tracking within a bandwidth of 15 Hz, confirms the performance as expected for relatively large vibration frequency. The output response from the cylinder is shown in Figure 6.5.

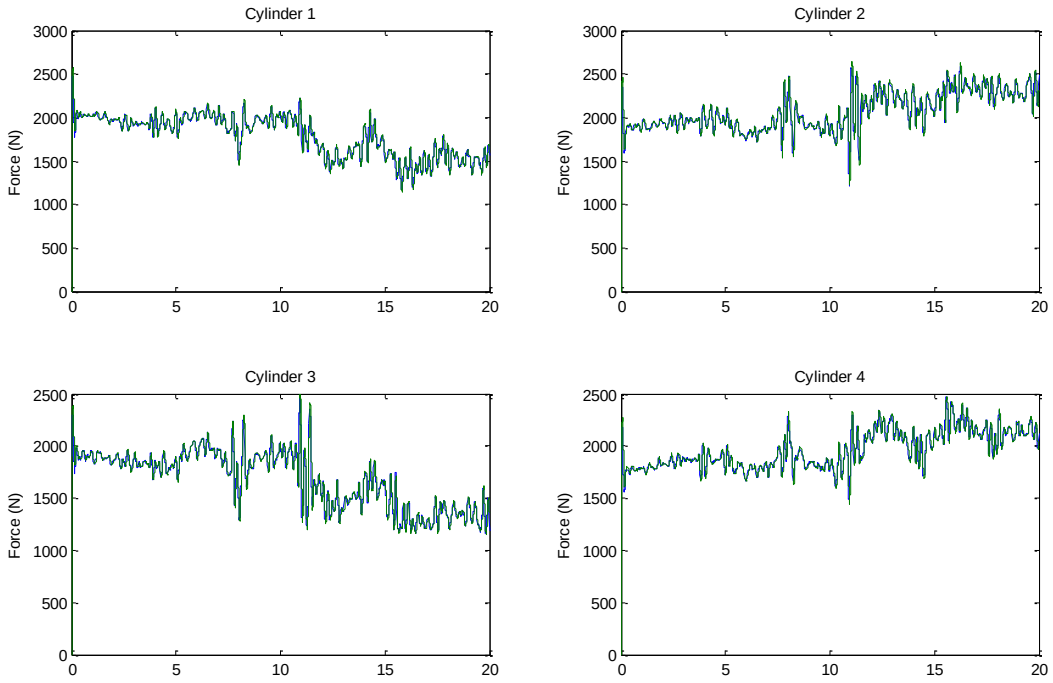

Figure 6.5 Cylinder force tracking

The flow required by each cylinder to achieve the desired force is given in Figure 6.6. It could be seen that the flow demand in Cylinder 1 and Cylinder 3 are reducing with time. The reason for such behaviour is because of the change of ground level. When the ground plane changes, Cylinder's 2 and 4 puts extra effort to compensate for the induced vibration as a result the reference force computed by the control allocation module also increases and can be seen in Figure 6.5. When compared to flow demand calculation performed in Chapter 5.5.3, the average

flow demanded by the entire system with the test track data as input is approximately 188.88 l/min. The low amplitude, high frequency test data has created a huge difference in flow demand midst the two results.

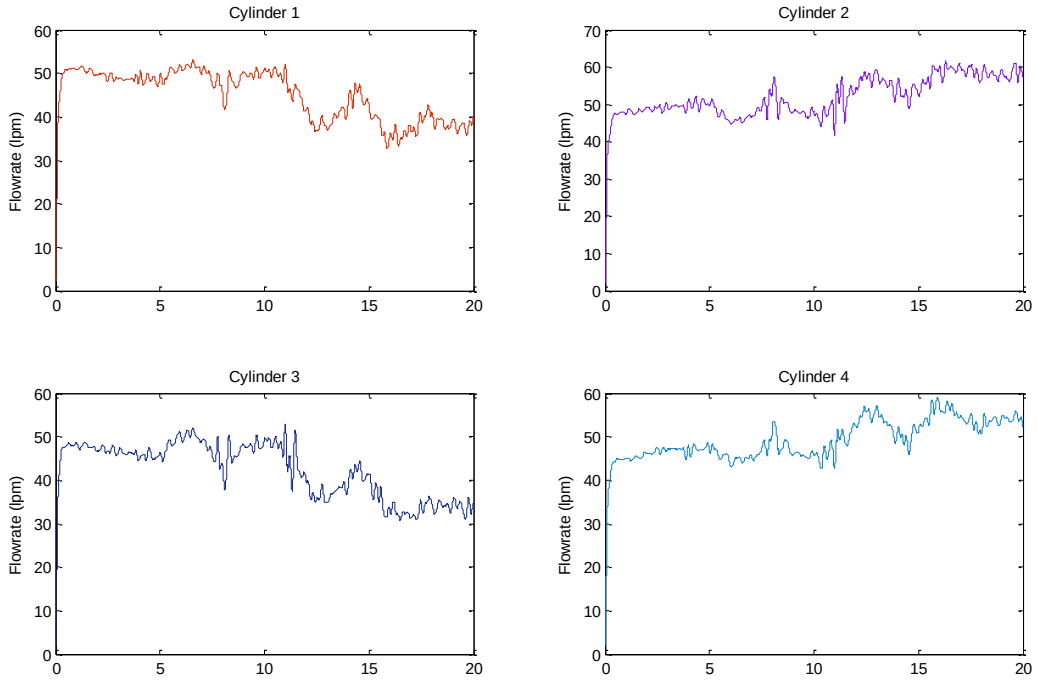

Figure 6.6 Flow rate in to four cylinders

7 SENSOR SELECTION

In this chapter the sensor selection for the active suspension system is discussed. Because this work is the initiate of the project, the system is over-sensed. According to previous simulation the information of angular position, angular velocity and acceleration of upper frame, distance between lower and upper frame, as well as the inclination of lower frame is required. In order to detect the angular velocity and the acceleration, inertial sensors are selected. Based on the measurement from inertial sensor the angular position in earth inertia frame could be estimated. Besides, the inclinometers and pressure sensors are also selected to measure the inclination and pressure at working ports during the phase of control prototype.

7.1 Inertial sensor

In this work the inertial sensors are selected to measure the accelerations and angular velocity. Most of advanced inertial sensors have faster response and equip with digital output. Comparing to inclinometers the inertial sensor can provide cleaner and faster angular velocity feedback. To reduce the trouble from sensors, the control prototype will use the velocity signal from gyro as feedback. Also the axes of gyroscope in inertial sensor have a tight orthogonality; with a Kalman filter the gyroscope can also output angles in the earth frame of reference. For this implementation the bandwidth of inertial sensor should larger than $200Hz$ and an accuracy of $0.1°/s$. The inertial sensor from Analog Devices ADIS 16362 is selected.

ADIS 16362 is comprised of a tri-axis digital gyroscope and a tri-axis digital accelerometer and a temperature sensor. This inertial sensor has the bandwidth of $330\ Hz$. The gyroscope has an orthogonal alignment which less than $0.05°$. The sensor has a quick start time of $180\ ms$ and sleep mode recovery time $4\ ms$. ADIS has a factory calibrated sensitivity, bias, and axial alignment with the temperature $-20℃\ to + 70℃$. ADIS 16362 use SPI as communication port which directly output digital signal of angular velocity, acceleration and temperature. Figure 7.1, shows the functional block of ADIS 16362.

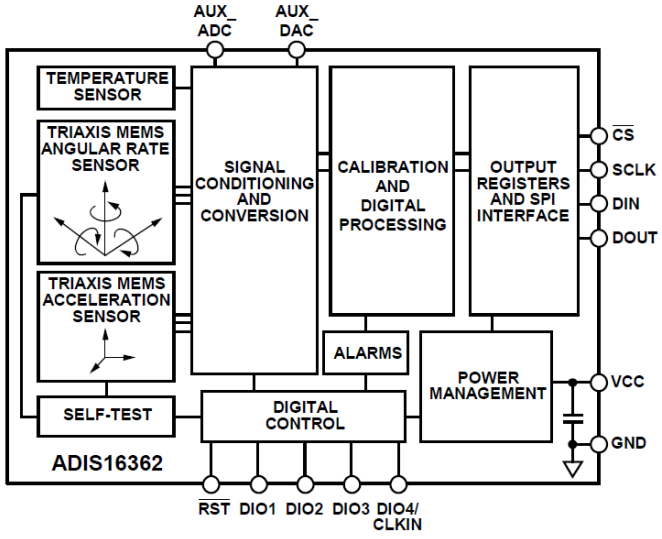

Figure 7.1 Function block diagram of ADIS16362

7.2 Inclinometer

In order to measure the angular position of upper and lower frame inclinometer are selected in this work. Inclinometer (inclination sensor) is the sensor which measures the inclination of an

object. In this thesis the sensor IS2A 33P18 from GEMAC is selected. IS2A 33P18 is a 2-dimensional inclination sensor with the measurement of range of $\pm 33°$ and its operation temperature range is $-40℃\ to + 80℃$. IS2A 33P18 use current output with the range of $4\ mA$ to $20\ mA$. Comparing to other inclination sensors IS2A 33P18 has a relatively wide bandwidth of 18Hz, also the accuracy of $\pm 0.125°$ is satisfactory in this implementation. Figure 7.2, is a picture of IS2A 33P18.

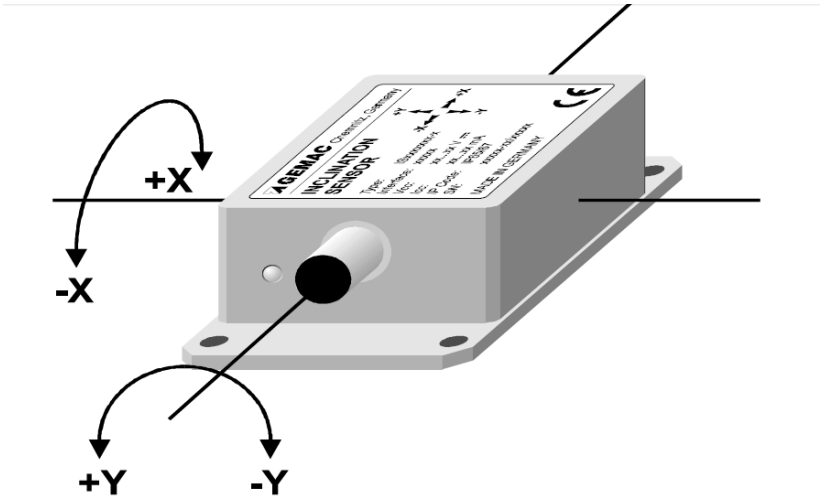

Figure 7.2 Inclinometer IS2A 33P18

7.3 Pressure sensor

The need for selecting a pressure sensor aroused as the existing cylinder is not equipped with an inbuilt pressure sensor. In the control structure, the pressure at the cylinder ports and the velocity of the cylinder are the states hence they should be obtained to describe the system dynamics. Two major aspects while selecting the sensor was the pressure range, and the output type. The custom made pressure sensor recommended by the company fits the requirement and hence is selected. The specification of the sensor is as follows

Normal working pressure: $0 - 400$ bars

Output Signal Type: $0 - 10$ V DC (3 wire)

Burst pressure: 1700 bars

8 HYDRAULIC HARDWARE SELECTION

This chapter explains the selection of vital components required for real time implementation of active suspension system in the forwarders. The components are selected based on analysis of the simulations done in the earlier chapters. Few simulations results are added in this chapter to support the selection.

8.1 Hardware

Two major hydraulic components direction control valve and accumulator are selected in this chapter and the reason why they play an important role in the system performance is also explained.

8.2 Valve selection

Valves form the heart of the hydraulic system. Performance of a hydraulic system depends mainly on the valve that is being used in the system. In real world, mobile hydraulic vehicles utilises load sensing pumps as their pressure source for efficient utilization of energy. The load sensing pump demands the use of load sensing valve to get the feedback on the load pressure and this system would prove very useful for mobile vehicles. But in this work a constant pressure pump is used, for which an open centred valve is used. If not an open centred valve, the pressure port will be blocked in neutral position and the pump pressure would build up and become very high. But with proper pump unloading circuit, a closed centre valve of the same type can be used to utilize the pump efficiently.

The valve selection is done based on two criteria

1. Requirement on the Frequency response
2. Requirement on the pressure-flow characteristics

8.2.1 Requirement on the Frequency response

The vibration attenuation frequency region of interest is in between 0.5-3Hz. Since the hydraulic system forms the inner most loop, as per rule of thumb the valve should have ten times the outer loop frequency i.e. 300Hz to have a robust performance. In general direction control valve do not have this frequency response. The system is designed assuming the inner cascaded structure to be 5 times faster and hence a valve with a frequency within 70Hz has to be selected. An interesting point to be noted about the valve is the frequency response: as they don't remain constant for entire range of operation. The response tends to change with the spool displacement. It is always recommended to use 20-80% of spool stroke for good performance. This is another motivation behind choosing a constant pressure pump as load sensing valve do not have faster frequency response when compared to proportional directional control valves.

8.2.2 Requirement on the pressure-flow characteristics

In section 5.5.3, the flow demand by one cylinder for different frequencies was simulated and found to be approximately 150l/min. The flow requirement on the valve is based on the results from the simulation. But for the flow requirement, the valve's pressure drop characteristic is

taken in to account before making the final decision. It was taken care that the selected valve does not have high pressure drop to provide the required flow.

Based on the above requirements, MOOG D672 double solenoid proportional direction control valve is recommended. The valve is capable of supplementing flow up to 300l/min but at the cost of pressure and reduced frequency response. The frequency response and the pressure-flow characteristics are shown in figure 5.2 and 5.4.

8.3 Accumulator Selection:

Accumulators are pressure storage device which hold the fluid under pressure with the aid of an external source like spring, gas etc. The need for accumulator in this system can be derived from the simulation results obtained in section 5.5.3. From the simulations it is quite intuitive that the overall flow demand in the system to actuate four cylinders is approximately around 600 l/min. Existing pump source in the forwarder vehicle is capable of providing a flow of 220-280 l/min which in turn results in a shortage of 320 l/min. The pump pressure drops to a very low value when there is an excessive flow demand than the pump's capacity as a result, the load pressure will fluctuate to a great extent and system becomes unstable. One way to overcome this problem would be to supplement the pump flow with an auxiliary pump but this option turns out to be very expensive for mass production. Including accumulators in the system is the best and practical method to overcome the problem.

The minimum pressure in the system plays an important role in the proper functioning of accumulator. The suspension frame with the cabin approximately weighs around 2000Kg. Hence the cylinders should be capable of providing a minimum of 20000N to hold the cabin in position. Which would approximately be 50bar in each cylinder over which the pressure drop across the valve is considered and accounts to 130bar. The maximum system pressure is considered to be 240bar. Taking in to consideration of the response time of the system, a bladder accumulator is chosen over piston type.
The calculations on accumulator sizing, shown below are performed with the help sizing manual from Stauff (Ref).

1. Precharge pressure is usually considered to be 90% of the minimum working pressure which is equal to$0.9 * 130 = 117\ bar$.
2. The maximum flow demand is while extending i.e. the accumulator has to supplement the pump with approximately 400l/min Hence volume of liquid required per second is V= $Q * t/60$=0.352 gallons (1.33 liters).

Therefore the Precharge pressure would be $0.9 * 150 = 135$ bar

Maximum demand of flow is when extending i.e. the accumulator has to supply around 400 l/min (actual value being 380 l/min). Hence volume of liquid required per second is given by

V= $Q * t/60$=0.352 gallons (1.33 liters).

Here the t represents the time in which the volume has to be displaced. From law of motion it is interpreted that to when a body is accelerated over the stroke length of piston, the time taken to achieve it is 0.2 sec.

With the values above, the volume of accumulator can be found with the formula below

Volume of the accumulator $Va = Vw * \frac{E}{f}$ and $E = 1.24$ to $supplement$ $pump$ $flow$

$$f = 1 - \left(\frac{1}{a}\right)^{\frac{1}{n}} : a = \frac{\text{MaxPressure}}{\text{MinPressure}} : \text{n from graph based on avgerage pressure}$$

$$\text{f computed to be } 0.2629$$

The values for a and n are taken from the accumulator sizing data provided by Stauff and in the selection the process is considered to be adiabatic due to the faster work cycles.

By substituting the values, volume of accumulator required to supplement the flow is 1.663 gallons i.e. 6.3 liter. Design rule is to have it 20% higher than calculated hence $Va = 7.5$ $liter$.

This concludes the hydraulic hardware selection chapter.

9 CONCLUSION AND FUTURE WORK

9.1 Conclusion

The main goal of this thesis was to develop a complete simulation model of an active suspension system for a forwarder vehicle. Development of a simulation model would deliver an insight in to the system behavior, requirements, limitations and feasibility for real time implementation. The conduit to achieve the final goal of vibration suppression included several important tasks

1. Modeling and simulation of previously designed suspension mechanism
2. Overcoming the problem of over actuation and control allocation
3. Hydraulic system modeling, control and requirement analysis
4. System integration and performance

Modeling and simulation of the passive suspension mechanism

A Newton-Euler model is derived based on kinematic and dynamic analysis. In order to model the system dynamic earth inertia frame and body-fixed frame are selected as frame of reference, both nonlinear and linear model is derived.

Overcoming the problem of over-actuation and control allocation

An effective linear quadratic algorithm is developed to compute the optimal solution; compare to the universal solution the computation load is also reduced.

Hydraulic system modeling, control and requirement analysis

Hydraulic system models were developed with the aim of developing the force controller and for deducing the flow requirements of the complete system under the normal operating conditions. The developed force controller showed satisfactory performance with in the designed frequency bandwidth and the data's collected from several simulations has helped in deducing the flow requirements and has helped in selecting suitable hardware's required for real time implementation.

System integration and performance

The developed SimMechanics mechanical system and Simulink hydraulic system were integrated together to achieve the final goal of simulating an "active suspension system". The results from the simulation, within the designed target input, clearly implies that the system does function the way as expected thereby providing an active suspension to the forwarder cabin. When system was given an input from the data measured from the test track, model showed acceptable performance in the low frequency domain. Based on the information from simulation, hydraulic and electronics hardware is selected.

The results indicates that at theoretical and simulation level, the desired goal of developing an active suspension system to eliminate the significant vibration induced in the operator cabin is feasible and realized.

9.2 Future Work

1. Velocity of the cylinder is considered to be a state variable in the hydraulic controller design. The velocity of the cylinder can be calculated by numerical differentiation of the position signal obtained from the inbuilt position sensor in the cylinder. But the measurement data is subjected to noise and hence a proper filtering technique has to be chosen to get unadulterated data.

2. System identification needs to be performed before implementation of the control design. First the dynamics of hydraulic system needs to be identified to make sure the force control is working properly, and then parameters of mechanical model, e.g. inertia, need to be identified to guarantee the performance of outer loop controllers.

3. Attentions need to be paid to computation time of real-time implementation. Since the inner loop controller will be running at 500Hz and the computation load of outer loop controller is high, so the computational time delay might be an issue in this case. Simplified method should be taken if such problem happens.

4. The height controller could be tuned to compensate the vertical motion introduced by roll and pitch motion.

5. The cylinder used in this work is asymmetric and supply pressure is constant which demands installation of proper pressure reducing accessories at the cylinder working ports.

6. The concept of force control is adapted in this work because of which the load pressure will be varying. Taking this in to consideration, Load-sensing system would prove beneficial but the desired frequency response of the valve, to satisfy the requirement is not possible with such system.

1. Chris M. NELSON and Paul F. BRERETON, The European Vibration Directive
2. Hrovat, D. (1997). Survey of advanced suspension developments and related optimal control applications. Automatica, 33(10), 1781–1817.
3. K. J. Åström, Control System Design, 2002
4. Model Predictive Control Allocation for Overactuated Systems Stability and Performance
5. Paul A. Jensen and Jonathan F. Bard, Operations Research Models and Methods
6. Cheng Cheng, Modeling of the Ride Comfort of a Forwarder
7. LIU Chunsheng and JIANG Bin, Novel Adaptive Control Allocation in Overactuated System Using Quadratic Programming